DEVELOPMENT OF IONIC LIQUIDS MEDIATED NOVEL FOOD PRESERVATION SYSTEM BY ENHANCING SOLUBILITY OF FLAVONOIDS

エムディー, シムル, イスラム

DEVELOPMENT OF IONIC LIQUIDS MEDIATED NOVEL FOOD PRESERVATION SYSTEM BY ENHANCING SOLUBILITY OF FLAVONOIDS

九州大学

A Thesis Submitted to Kyushu University for the degree of Doctor of Philosophy

BY

MD. SHIMUL ISLAM

Department of Chemical Systems & Engineering

Graduate School of Engineering

Faculty of Engineering

Kyushu University

Japan

December 2022

TABLE OF CONTENTS

CHARPER-1: IONIC LIQUIDS ASSISTED FOOD PRESERVATION SYSTEM: CHALLENGES AND OPPORTUNITIES

CHAPTER-3: CHOLINE OLEATE BASED MICELLAR SYSTEM AS A NEW APPROACH FOR LUTEOLIN FORMULATION

CHAPTER-4: FORMULATION AND CHARACTERIZATION OF CHOLINE OLEATE BASED MICELLES FOR CO-DELIVERY OF LUTEOLIN, NARINGENIN, AND QUERCETIN

ABSTRACT

The reduction of food waste and ensuring food safety are seen as an important dynamic for diminishing hunger and foodborne diseases in the world. The tendency of consumers to natural preservatives is increasing day-by-day due to the adverse side effects of chemical preservatives. Many of the plant derived compounds known as flavonoids have potential chemical and biological properties, but their applications are limited due to its low solubility. In the pharmaceutical and biomedical fields, ionic liquids (ILs) are used as stabilizer agents for biomolecules, as solvents, or as part of drug carrier systems for poorly soluble drugs. Utilization of ILs as solubilizing agents or carrier materials for flavonoids are limited and their application as food preservatives are scare in the literature. A study was designed to screen and synthesize low toxic ILs from natural compounds amino acids and phenolic acids as a potent green solvent for dissolving Luteolin (LUT). Twenty cations (standard amino acid ethyl esters) and nine anions (phenolic acids) were assessed for dissolution of LUT via COSMO-RS. To address poor aqueous solubility of flavonoids, we synthesized and characterized four novel proline ethyl ester-based phenolic acids ILs (PEEP-ILs). The PEEP-ILs (60% IL in water) increased aqueous LUT solubility through multiple hydrogen bonding, π–π, and cation–π interactions between the LUT and the ILs. The relatively harmless PEEP-ILs retained better organoleptic properties of red apple piece. Nanoencapsulation of flavonoids by a carrier material can shield them from the damaging effects of pH, oxygen, and light. The LUT-loaded micellar formulation (LUT-MF) developed by choline oleate ([Cho][Ole]) formed spherical micelles with a mean particle size of approximately 73 nm. Enhanced aqueous solubility, release rate, *in vitro* antioxidant and antimicrobial activity revealed that treating strawberries with LUT-MF effectively preserved color and prevented decay over 8 days storage at 10°C. To utilize synergistic properties of flavonoids, choline oleate assisted micellar formulations of luteolin, quercetin and naringenin were developed to increase their solubility and bioactivity. Better antioxidant and antimicrobial activity prevented the coagulation of milk from microbial metabolism. ILs derived from cations and anions of natural sources could replace conventional solvents and/ or carrier materials for the delivery of poorly water-soluble flavonoids and potentially be used as natural preservative alternative to chemical preservatives in the food industry. However, we should concentrate more on the optimization of the formulations for better performance and their safety on foods as well as on human and animal.

CHARPER-1: IONIC LIQUIDS ASSISTED FOOD PRESERVATION SYSTEM: CHALLENGES AND OPPORTUNITIES

1.1. Food Preservation

Food preservation is the procedure or technique used to keep food from spoiling and lengthen its shelf life. Foods from plant or animal sources are consumed for their nutritional value. They are composed of moisture, protein, lipids, carbohydrates, minerals, and other organic compounds. To retain food quality at the required level for the greatest possible health benefits and nutritional value, food preservation entails a variety of food processing techniques. Foods can be grown, harvested, processed, packaged, and distributed using various food preservation techniques to provide value-added goods, combat improper agricultural planning, and offer dietary variety [1]. Currently, food preservation techniques play a significant part in waste reduction by promoting safe food consumption while decreasing food loss [2]. With the advancement of civilization, the demand for more processed food in bigger quantities and of higher quality grew and grew.

1.1.1 Importance of food preservation

Many cutting-edge food preservation technologies are required to prevent the massive amount of food wastage every single day and to feed millions of people worldwide. Maintaining an accurate and precise balance between technology and design is crucial for diet diversity, value added foods, and seasonality in agricultural output [3]. People enjoy consuming a variety of foods with a range of tastes, flavors, nutritional benefits, dietetic requirements, and other characteristics. Unfortunately, it has been estimated that up to 2 billion people may not have enough to eat, and that up to 40000 people may die every day from illnesses resulting from inadequate diets, which may lack certain nutrients like calories, protein, or minerals.

The population of the globe, which stood at 7.3 billion people in 2015, is anticipated to grow to more than eight billion within 2030 and around ten billion within 2050 [4]. Food production must be boosted by 70% to supply enough food for the rising population. Worldwide, more than 30% of the food was lost or wasted. When converted into calories, this significant amount of FLW would equal 28% of all agricultural land used globally for agricultural production and an economic cost of nearly USD 750 billion [5]. Food waste reduction using sustainable food preservation techniques must be developed to provide food for an expanding global population.

1.2 Spoilage of food

Food spoilage is the term for any sensory changes (tactile, visual, smell, or flavor) that make food unsuitable or unpleasant for human ingestion [6,7]. Food spoilage can occur at any steps in the food chain. Color, smell, flavor, texture, or the food itself can be used to identify the early stages of food spoilage. Food spoilage can may result from microbial infections, physical injury, insect damage, or native enzymatic action in food itself.

1.2.1 Physical causes of food spoilage

Physical spoilage is considered as food that has undergone physical alteration or instability. Examples of physical spoilage include moisture alteration, moisture movement between distinct components, and isolation of constituents. Moisture content, temperature, glass transient temperature, crystal development, and crystallization are the main elements influencing physical spoilage [1].

Water is one of the most crucial elements influencing how quickly food deteriorates due to microbial or nonmicrobial effects. The alteration in the water content of food items is a common reason for their deterioration. It could take the shape of water gain, water loss, or water movement. The water activity (a_w) of a food item directly influences moisture transfer in food. Most fresh food items have a_w levels above 0.99. Bacteria need higher water activity than yeasts and molds and more water is needed by gram negative bacteria than gram positive bacteria. The minimal a_w demands are typically found in molds, with intermediary requirements in yeasts. The a_w of food can be decreased using many thermal and non-thermal techniques. The growth of microbial cells and spores, toxin production, and enzymatic activity of food are all inhibited by the reduction of a_w in food [8].

The most important element influencing fruit and vegetable deterioration is temperature. There is a temperature range where delayed ripening and post-harvest life are both maximized. Additionally, ideal relative humidity and ideal air flow around fruit and vegetables are needed for slow ripening. The survival and growth of microorganisms are strongly influenced by temperature. Avoiding temperature abuse along the entire supply chain of produce processing is essential to maintaining the quality, sensory, and nutritional shelf life of products. The growth of many microorganisms has inhibited while others have their growth delayed by storage at low temperatures. Foods that are prone to freeze damage may suffer unfavorable effects because of low temperatures. Most tropical fruits and

vegetables are vulnerable to damage from chilling. This often happens between 5 and 15°C prior to the food product beginning to freeze [9].

The glass transition temperature affects how long food goods may be stored. Food products' solid constituents might be either crystalline or amorphous in nature. This phenomenon is influenced by the temperature, relative humidity, and solids composition. The amorphous matrix can take the form of a rubber that is more liquid-like or a highly viscous glass. The shift from a glassy to a rubbery state takes place at the glass transition temperature. The glass transition temperature and food physical stability are connected. The proportion of water and other plasticizers greatly influences the glass transition temperature. Due to the glass transition phenomenon, dry food products change state when stored in extremely humid environments [1].

Food deterioration can also be a result of freezing. Foods that are slowly frozen or frozen several times suffer greatly because of crystal development. They have significant extracellular ice accumulation. These foods are more stable than processed meals with gradual freezing because rapid freezing creates ice inside food cells. Emulsifiers can be applied during freezing to reduce the formation of big ice crystals. Foods having a high sugar content can crystallize sugar because of moisture buildup or temperature rise. The result is a gray or white look as sugar rises to the surface [1].

1.2.2 Microbial causes of food spoilage

Food deterioration that results from the action of microorganisms is known as microbial spoilage. This is the start of a complicated recycle process of elements into the environment. Different microbes frequently damage perishable foods. The shelf life of natural foods is typically very low. Examples of perishable commodities with a short shelf life include fish, meat, and bread. Other food can be kept fresh much longer, but it eventually spoils. Food that has been heavily infected by bacteria often looks normal and does not smell bad, making it extremely dangerous. The presence of extremely dangerous poisons and bacterial spores is sometimes not identified until the laboratory testing is done.

Bacteria have a cell wall and can be found in a variety of sizes and forms. Bacteria can alter food in several ways, many of which may not be desired. The alterations include the generation of pigments, the breakdown of food components, the creation of noxious-smelling compounds, and the poisons development. Some bacteria can develop spores that can survive in challenging conditions [10]. The two most prevalent foodborne bacteria

linked to foodborne illnesses are Staphylococcus aureus and Listeria monocytogenes. Gram-positive S. aureus bacteria are responsible for a variety of acute and chronic illnesses, including abscesses, septicemia, arthritis, and endocarditis [11]. In nature, microorganisms are everywhere. Fresh produce is frequently contaminated with food-borne diseases such *E. coli O157:H7, Staphylococcus aureus, Salmonella, and Listeria monocytogenes*, which can have negative effects on public health. These microorganisms have long been known to be harmful pathogens that can cause several food-borne illnesses [12].

Yeasts are larger and proliferate more slowly than bacterial cells. High water activity (a_w) and moderate acidity are favorable condition for the most of yeasts. Fruit juices and other packaged, low-pH foods are more likely to support the growth of yeast. The proliferation of yeast may lead the foodstuffs to smell, feel, and appear turbid. Even though molds can come in a variety of colors, they often look and feel like cotton. They are dispersed as microscopic spores that sprout anywhere in presence of nutrients. Mold spore can withstand a wide range of pH and temperature. Molds can flourish at moderate pH, low temperature, and high a_w, but can survive at adverse conditions. In fact, they can overrun bacteria and yeasts in low a_w environments. Adjusting temperature, water activity, pH, and adding preservatives, and selecting the right packaging materials may all slow or stop the growth of most microbes [7].

1.2.3 Chemical causes of food spoilage

Foods inherently undergo chemical and biological processes, which provide unappealing sensory outcomes in food. They may have fundamental quality variations depending on- (a) pH changes by metabolism and microbial growth, (b) toxin production, and (c) oxidation of fatty compounds and pigments.

The basic spoiling reaction in chilled fresh meat and seafood turns amino acids into ammonia and organic acids at the presence of oxygen [1]. The process of oxidizing lipids, in which unsaturated fats (lipids) react with oxygen, is referred to as "rancidification". The results in food products include color change, flavor loss, and the creation of hazardous chemicals. Metal oxides can function as a catalyst for rancidification, and light exposure speeds up the process. Following this process, carbonyl molecules are created that give food its rancid flavor.

The hydrolysis of peptide bonds in a protein molecule by protease enzymes constitutes proteolysis, a common and irreversible post-translational alteration. This reaction occurs commonly with foods that include nitrogen molecules. After undergoing proteolysis, proteins are eventually transformed into amino acids or small peptides. The taste of many of these peptides is unpleasant and can be either bitter or sour. In a putrefaction process, amino acids divert to a combination of foul-smelling sulfur compounds, amines, and organic acids. Protein putrefaction also produces indole, phenols, and ammonia in addition to amino acids. Most of these compounds have unpleasant smells. At temperatures higher than 15°C, putrefaction is prevalent in meats and other protein-rich meals [1]. As a result of lipolytic enzyme activity, hydrolytic rancidity degrades lipids. The presence of water in this reaction causes the cleavage of free fatty acids from triglyceride molecules. Rancid tastes or odors are present in these free fatty acids. Hydrolytic rancidity in fats, such as butter, is obvious because the liberated volatile fatty acids have a strong foul odor and taste [1,13].

The Maillard reaction, browning process in absent of enzyme, is another major reason why food spoils. The amino group of proteins or the amino acids found in foods experience this process. The typical effects of the Maillard reaction include color darkening, a decrease in the solubility of proteins, the development of bitter flavors, and a decrease in the nutritional availability of certain amino acids. This reaction happens when dry milk, dry whole eggs, and breakfast cereals are stored [14].

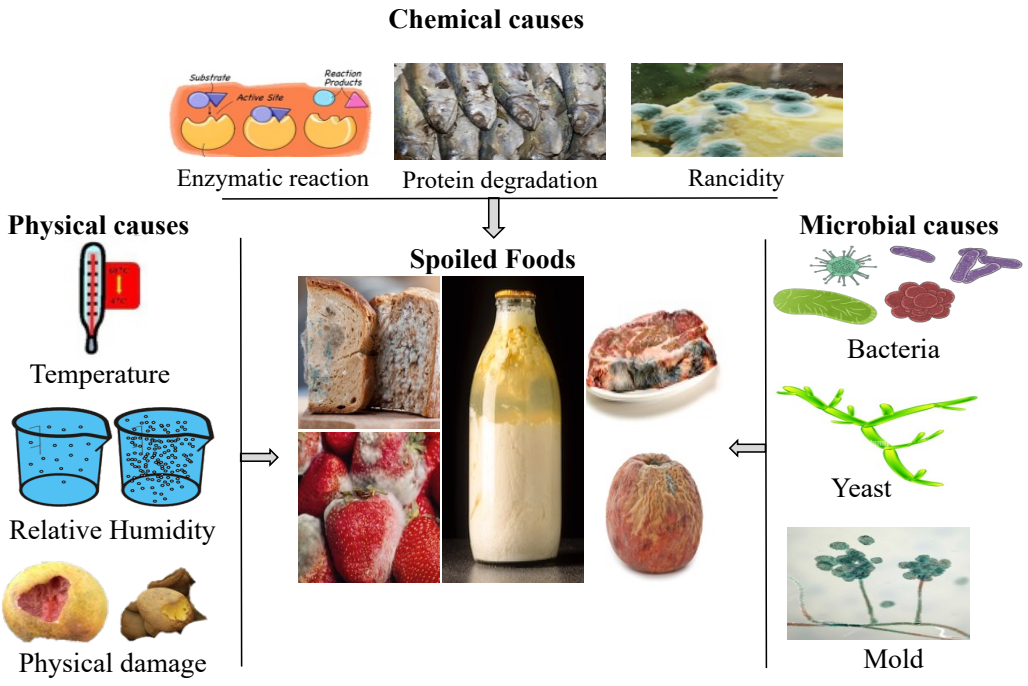

Fig. 1.1. Multiple causes of food spoilage

1.3. Conventional food preservation techniques

Physical, biological, and chemical processing alone or in combination are used to preserve foods in terms of waste reduction and human health maintenance.

1.3.1 Thermal treatment

One of the cutting-edge methods for food preservation is heat or thermal treatment. Thermal energy as a hot fluid is used for a specified time and temperature to optimize the quality of foods. The method has long been successfully used in a variety of food industries, including those of bread, dairy, fruits and vegetables[3,15,16]. A physical preservation method called pasteurization involves heating food to a specified temperature to kill the enzymes and microorganisms that cause deterioration. This method eliminates almost all pathogenic bacteria, yeasts, and molds. It is a gentler thermal treatment that is typically used to increase food's shelf life at low temperatures, usually at 4°C. Thermal sterilization completely destroys all the viable microorganisms and spore formers resulting in a longer period of shelf life. This is an intense heat treatment used to inactivate microorganisms at temperatures above 100°C (often 115°C to 130°C). Food matrix degradation, taste alterations, nutritional losses, browning, and gelatinization reactions are the detrimental effects of heat treatment [3].

Advanced freezing and cooling techniques have been widely used for food preservation. Freezing slows down physiological, biochemical, and chemical reactions by creating ice from water below freezing temperatures. Around -18°C storage temperature is required to achieve the freezing conditions. Cooling is the process of maintaining foods at temperatures above freezing and below 15°C at the liquid state of the water [3]. Cooling process between -1 to 8°C is used to slow down biochemical and microbial activities and to increase the shelf life of both fresh and processed foods. Foods that are properly packaged and kept at a cool temperature always prevent the introduction of germs and ensure food safety. Although cooling and freezing are successful, there are several worrying difficulties with chilling time, uneven ice crystal formation speed, storage costs, and specialized conditions. Evaporation of water from foods to produce solid foods with low water activity is the goal of drying process. With this technique, the moisture content is decreased to the point where these microbes' activity is suppressed. Most microbes can grow when the water activity is

above 0.95. Bacteria remain dormant at water activities lower than 0.9. At water activity levels below 0.88, most bacteria cannot grow.

1.3.2 Non-thermal treatment

A specific dose of ionizing radiation, sound waves of high frequency and intensity and a single oxygen or nascent oxygen from ozone are applied to grains, fruits, and vegetables for disinfestation, improvement of shelf life by preventing their rates of maturation and senescence, elimination of foodborne pathogens. Even at large doses, IR has no effect on the nutritional components including lipids, carbs, proteins, minerals, and most vitamins. When IR is administered in large doses, some micronutrients, especially the vitamins A, B_1, C, and E, may be lost [1,3].

1.3.3 Chemical preservatives

Food additives are a variety of organic substances that are intentionally or unintentionally added to foods during production or processing and are not typically intended to be consumed as foods. Preservatives are food additives that can prevent, delay, or stop the growth of unwanted microorganisms or any other damages by their involvement for the extension of shelf life and maintenance of organoleptic attributes of foods. More than 100,000 chemical agents are currently in use, and this figure is growing yearly. The major goals of using food preservatives are to increase and maintain nutritive value, improve quality, decrease waste, increase customer acceptability, make food more accessible, and expedite the supply of foods [10]. There are two categories of preservatives: Class I (naturals preservatives like salt and honey) and Class II (synthetics preservatives such as sodium, potassium and calcium salts of benzoate, propionate, nitrite, sulphites etc.). The most widely used preservatives in the global food industry are sodium nitrite, sorbates, benzoates, propionates, and sulfites among these compounds. The dose and selectivity of chemical reagents depend on the types and number of microorganisms, and the physicochemical characteristics of foods.

1.3.4 Limitations of conventional food preservation techniques

- The negative impacts of heat treatment include food matrix disintegration, flavor changes, nutritional losses, browning, and gelatinization actions.
- Cooling and freezing produce uneven ice crystal formation, freeze damage and sugar crystallization in foods and alter their taste.

- Dry food products change state when stored in extremely humid environments.
- Some micronutrients, particularly the vitamins A, B_1, C, and E, may be lost when ionizing radiation is applied in excessive dosages.
- Recently chemical preservatives are declining world-wide acceptance by consumers for their presumed hostile effects on health.
- Chemical preservatives, such as sodium and potassium nitrites and nitrates, the various benzoates, sulphites, diphenyl, hexamethylenetetramine, and orthophenylphenol demonstrate adverse consequences such as skin rashes and itching, breathing difficulty, sneezing, gastrointestinal upsets, toxicity, and potent carcinogenic nature.
- Exposure to high concentrations of nitrate or nitrite may make it more common for children to develop nose and throat tumors, leukemia, and brain tumors.
- Allergies, diarrhea, and internal bleeding are the negative effects of benzoic acid in experimental animals.
- In experimental animals, sulphur dioxide gas and its salts may have side effects such as polyuric inflammation, visceral organ atrophy, and irritation of the bronchial passages.

Therefore, the inclination of consumers to alternative preservatives is growing day-after-day. The use of nitrates and nitrites as additives is debatable. The usage of these substances may enhance the development of carcinogenic nitrosamines, particularly in acidic environments. In addition to being carcinogens, nitrosamines can also have mutagenesis consequences. In those who are exposed to high levels of nitrate, nitrate alters the structure of hemoglobin by adhering to it, resulting in a shift in the so-called methaemoglobin that causes the skin to turn blue [10].

1.4 Alternatives to conventional food preservation techniques

Natural preservatives have been created to lessen the use of chemical preservatives because of their negative impact on the organo-leptic and sensory qualities of foods. Bio-preservatives are organic substances derived from animals, microbes and plants that extend the shelf life and maintain the quality of foods. Many of these substances function as antimicrobials and antioxidants agents that disintegrate microbial cell, and obstruct the routes of microorganisms that synthesize bioactive molecules [17,18].

1.4.1 Animal and microbial products as natural preservatives

The most prevalent naturally occurring antibacterial substances in animals are proteins and enzymes such as lysozyme, lactoferrin, and lactoperoxidase. Due to their antibacterial capabilities, they provide defense against predators. They kill gram-positive bacteria and gram-negative bacteria by destroying the cell membranes of microorganisms. Chitosan, partial deacetylation product of chitin, is consisted of polymers of glucosamine and N-acetyl glucosamine. They are non-toxic, biodegradable, and compatible, and their effectiveness as an antibacterial and natural food preservative has grown to inhibit a variety of microorganisms, including molds, yeasts, and bacteria [19]. Lysozymes from animal sources are effective against food spoilage microorganisms. They can be directly incorporated into a food matrix and are thought to be Generally Recognized As Safe (GRAS). Due to their stability across a wide pH range (2–10) and wide temperature range (4-95°C), lysozymes have drawn particular attention. Lysozymes have been shown to have a significant potency against *Bacillus stearothermophilus, Listeria monocytogenes, Clostridium tyrobutyricum* and *Micrococcus spp.,* Lysozyme's ability to damage the peptidoglycan layer of bacterial cell walls has been attributed to its antibacterial activity. Another animal-based antibacterial is lactoperoxidase (LPS), an enzyme that is abundant in cow's milk and is released by the epithelial cells of the mammary gland. Bacteria such as *Shigella, Salmonellae*, *Coliforms,* and *Pseudomonas* can be effectively inhibited and destroyed by lactoperoxidase [17].

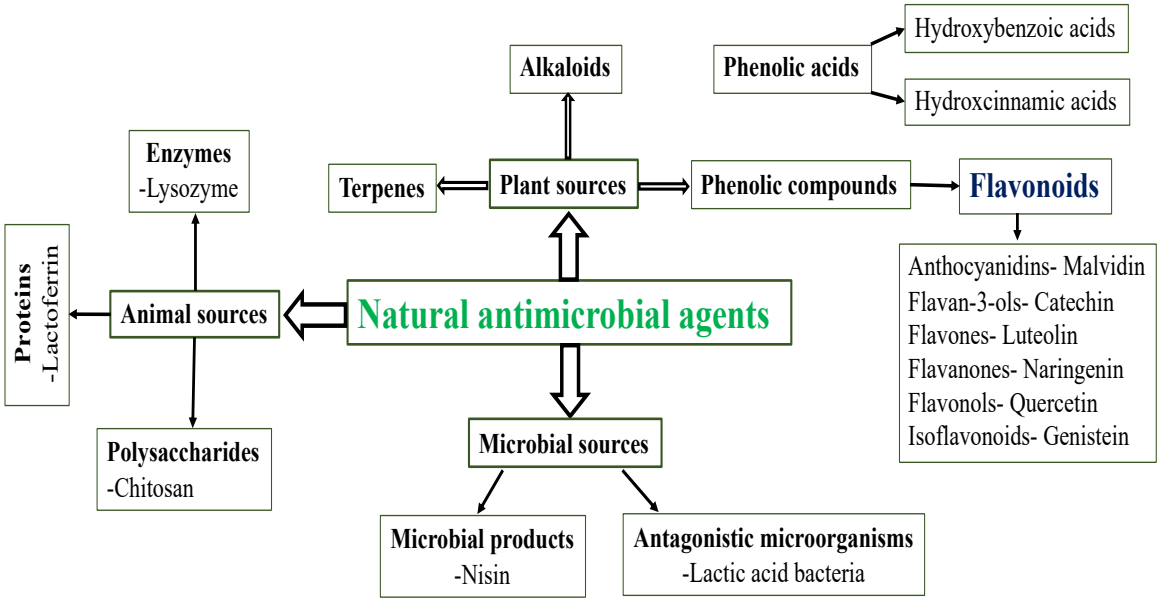

Fig. 1.2. Alternatives to chemical preservatives.

Some bacteria and their derivatives have the capacity to prevent the growth of food spoilage microorganisms. When they are used in foods, the shelf life, quality and safety improve significantly. The process of preserving food by using these antagonistic bacteria and their metabolites is called biopreservation. The Lactic Acid Bacteria (LAB) are well-known antagonistic bacteria that have found extensive use in food systems [17]. LAB have the primary ability to produce lactic acid as a byproduct of the fermentation of glucose[20]. The most significant LAB genera for food applications are *Lactobacillus, Lactococcus, Pediococcus, Leuconostoc, and Streptococcus*. Additionally, LAB are employed in the production of fermented foods and is often regarded as safe for ingestion. Due to their capacity to produce a wide range of antimicrobial by-products, such as organic acids, acetaldehyde, H_2O_2, small non-protein compounds, and bacteriocins, LAB also have a preservative effect on foods. Bacteriocins are a viable alternative and an efficient way to control pathogens particularly in minimally processed food products, such as fruits and vegetable products. They might, however, work better when combined with other food preservation techniques [19,21].

1.4.2. Plant products as natural preservatives

Bioactive substances of plants are being used by humans as foods and medicines for thousands of years. They can be categorized into three major groups: terpenes, alkaloids, and phenolic compounds. Terpenes are isoprenes with five carbons $(C_5H_8)_n$ that can have a simple or polymerized molecular structure. Terpenoids, which contain oxygen atoms, have several chemical activities. Alkaloids are nitrogen containing cyclic chemical molecules made from amino acids. An aromatic ring with one or more hydroxyl groups, in a simple molecular structure or with a high polymerization grade, represents the chemical structure of phenolic compounds. This group consists of phenolic acid (hydroxybenzoic acids, and hydroxycinnamic acids) and flavonoids. The strongest antibacterial properties are identified in phenolic compounds, which are extensively distributed in nature [19]. Essential oils (EOs) are secondary oily, fragrant volatile mixtures made up of 20–60 different ingredients that are all present in varying amounts. Physiologically active substances of EOs have antimicrobial and antioxidant properties on foodborne pathogens and lipid oxidation. As EOs are hydrophobic, their actions cause structural and functional damage to bacterial cell membranes, altering their structure and fluidity [17,22].

1.5. Flavonoids

Flavonoids, from latin word 'flavous' means clear pure yell, are the byproduct of plant secondary metabolism. Several thousand of flavonoids are substances having a phenylchromanone structure with various hydroxyl groups [18,23]. Despite being found in many different parts of plants in nature, flavonoids are mostly extracted from the colored parts of plants, such as flowers, fruits, vegetables, grains, nuts, and seeds [24,25]. According to their hydroxylation pattern and the substituents attached to the C ring, flavonoids can be divided into several categories: (i) anthocyanidins such as malvidin; (ii) flavan-3-ols such as catechins; (iii) flavones such as luteolin; (iv) flavanones such as naringenin; (v) flavonols such as quercetin; and (vi) isoflavonoids such as genistein. The pattern of substituents on the A and B rings varies between different compounds within each family [23].

1.5.1. Functional activities of flavonoids

Flavonoids are linked to a wide range of human health-promoting benefits as well as plant defensive mechanisms. Flavonoids produce color, aroma, and flavor in plants which attract pollinators, insects, birds, and mammals. Most significantly, flavonoids and other phenylpropanoids protect plants from numerous biotic and abiotic stresses, give them immunity to fight against diverse diseases, and function as potent antimicrobials or immune boosters for plants.

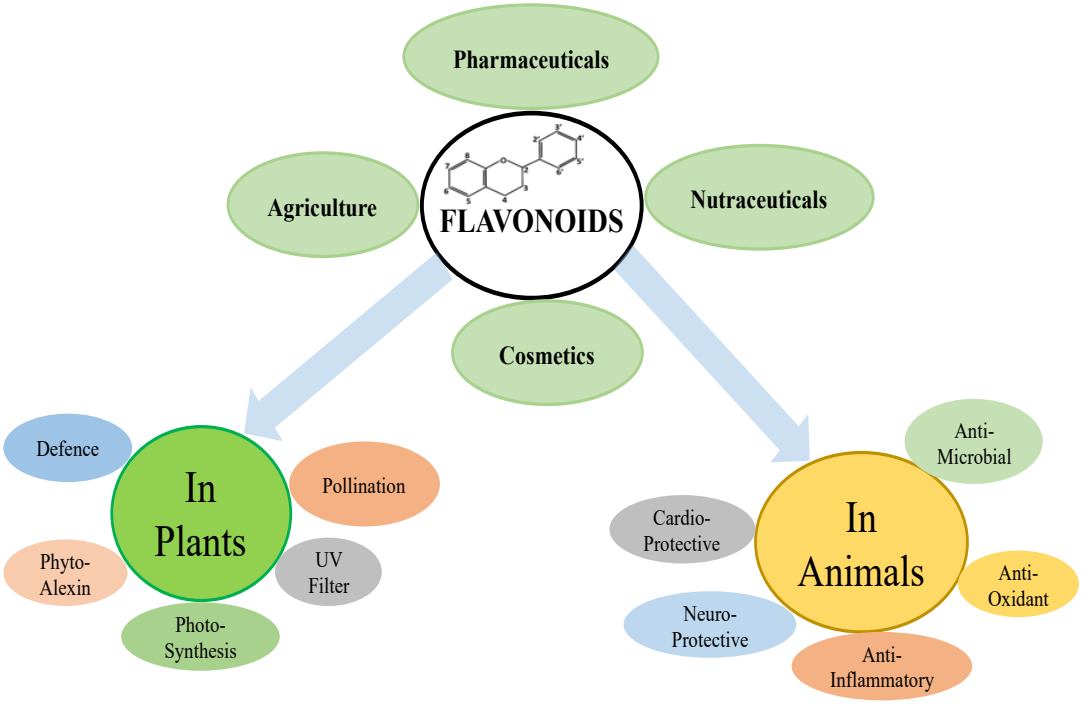

Fig. 1.3. Diverse roles of flavonoids. Adapted from [30]

The medical benefits of flavonoids, which are present in the human diet, include anti-inflammatory, anti-allergic, antioxidant, hepatoprotective, antiproliferative, and anticarcinogenic characteristics [24,25]. The enormous beneficial roles of flavonoids have drawn the researchers' attention to explore those roles of flavonoids in pharmaceutical and food industries [24]. Thus, flavonoids are promising contestants for further investigation for their probable role in food preservation. Luteolin, quercetin, naringenin and other flavonoids show hepatoprotective, neuroprotective, anticancer, antioxidant, antimicrobial, anti-inflammatory activities [26–29].

1.5.2 Antimicrobial activities of flavonoids

Plant-derived flavonoids exhibit antibacterial action through pathways distinct from those of traditional antibiotics. Osmoregulation, respiration, transport, peptidoglycan production and cross-linking, and lipid biosynthesis are all carried out by the bacterial plasma membrane. The membrane integrity is a need for carrying out all these tasks, and its disturbance may directly or indirectly result in the metabolic failure and, ultimately, bacterial mortality [25,31]. The peptidoglycan is a crucial part of the bacterial cell walls, and flavonoids and traditional antibacterial medications frequently work by inhibiting the development of this substance. Phenolic substances interact with the cell walls of bacteria, causing the cell wall to break down and the release of the contents of the cells [32]. However, the mechanism underlying the interaction between flavonoids and membranes has not been yet fully known, and the literature to date is still debatable [33]. Bacteria have been subjected to extensive research on flavonoids, particularly catechins. Catechins are frequently associated with interactions with cell membranes and antimicrobial properties. By attaching to the lipid bilayer and binding to the production of internal and extracellular enzymes, catechins were shown to break the bacterial membrane, in contrast to the protective actions of flavonoids on membranes [34].

The most ubiquitous plant flavone- luteolin, flavonol- quercetin and flavanone- naringenin is mainly found in various fruits, vegetables, beverages as well as in flowers, leaves, seeds, etc [28,29,35]. MIC and MBC of luteolin dissolved in dimethyl sulfoxide (DMSO) against *L. monocytogenes* were 32–64 and 64–128 μg/mL and 16–32 and 32–64 μg/mL for *S. aureus*. Moreover, LUT revealed robust inhibitory characteristics on the biofilm formation, better antibiotics spreading within biofilms and eradicated efficiently mono- and dual-species biofilm cells [11]. It has been demonstrated that quercetin prevents the growth of

several bacteria, fungi, and viruses. With a MIC range from 1 to 8 mg/mL, quercetin inhibited the growth of *Streptococcus mutans, Streptococcus sobrinus, Lactobacillus acidophilus, Streptococcus sanguis, Actinobacillus actinomycetemocomitans, and Prevotella intermedia*. *Staphylococcus aureus and Pseudomonas aeruginosa* were both inhibited by quercetin at MIC levels of 20 µg/mL. Inhibiting the synthesis of nucleic acids and proteins, reducing the expression of virulence factors, damaging cell membranes, altering membrane permeability, inhibiting the expression of virulence factors, and preventing the formation of biofilms are some of the mechanisms by which it exerts the antimicrobial action [28]. Naringenin has a broad range of antimicrobial properties, particularly antibacterial and antifungal activities. It has been reported that naringenin has a strong antibacterial action towards resistant isolates of *Helicobacter pylori* and methicillin-resistant *Staphylococcus aureus*. The antibacterial effect of naringenin is demonstrated by its inhibition of the autoinducer-mediated cell signaling pathway [29]. Investigation of antibacterial potential of individual phenolic compounds against *B. cereus*, *S. aureus, E. coli*, *S. Infantis* disclosed that luteolin and rutin were the most effective, with the lowest MIC value[36].

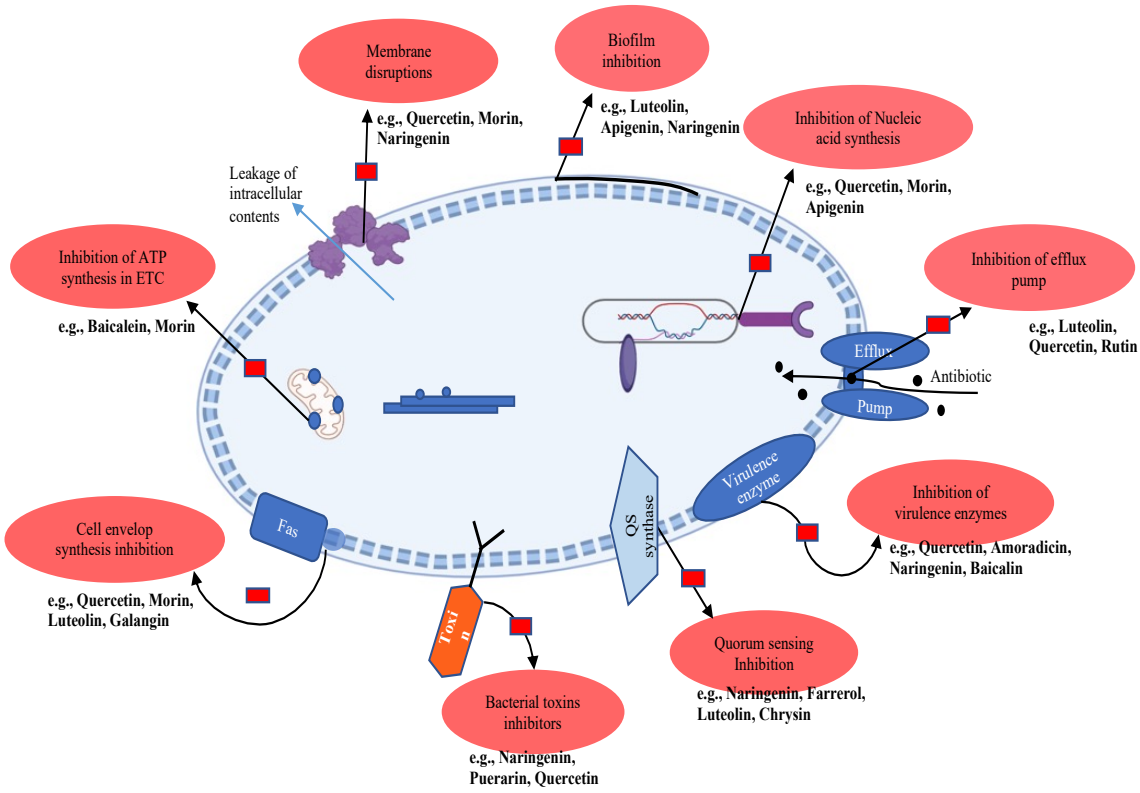

Fig.1.4. Antimicrobial action mechanism of flavonoids. Reproduced from [24].

1.5.3 Antioxidant activities of flavonoids

Numerous phenolic substances exhibited antioxidant properties resembling those of the well-established dietary antioxidant α-tocopherol. The most powerful antioxidant was the phenolic substance having an ortho-diphenolic structure, such as catechins, quercetin, and hydroxycinnamic derivatives. Kaempferol, caffeic acid, gallic acid, chlorogenic acid, quercetin, luteolin, and rutin function as chain breakers in oxidation reactions. Naringenin, apigenin, thymol, carvacrol, *p*-coumaric acid, vanillic acid, and *p*-hydroxybenzoic acid act as retarders and ferulic acid, protocatechuic acid, and eugenol, show intermediate behavior. Chain breakers delay the oxidation of lipidic substrates until the antioxidant has been completely consumed. Retarders must be used at higher doses to protect linoleic acid from oxidation since they slow down peroxidation without causing a clear lag phase. In fact, all of the phenolic compounds that function as retarders had an $EC_{1h} > 8$ mol/L value that indicated a decreased antioxidant capacity [36].

1.5.4 Limitations of flavonoids

The effectiveness of flavonoids is closely related to their bioavailability, permeability, and solubility. Lower solubility causes slower rates of absorption and dissolution. As a result, greater doses are needed to achieve a therapeutic effect. Flavonoids are a class of phytochemicals that have drawn much attention due to their multiple health advantages. The limited bioavailability of flavonoids is due to intestinal first-pass metabolism and phase 2 metabolism; however, it raises questions for therapeutic development. Additionally, flavonoids typically have low water solubility because of their high lipophilicity, which is a result of the flavone structural structure. These qualities make flavonoids class IV drugs (low solubility–low permeability) under the Biopharmaceutics Classification System (BCS) [37].

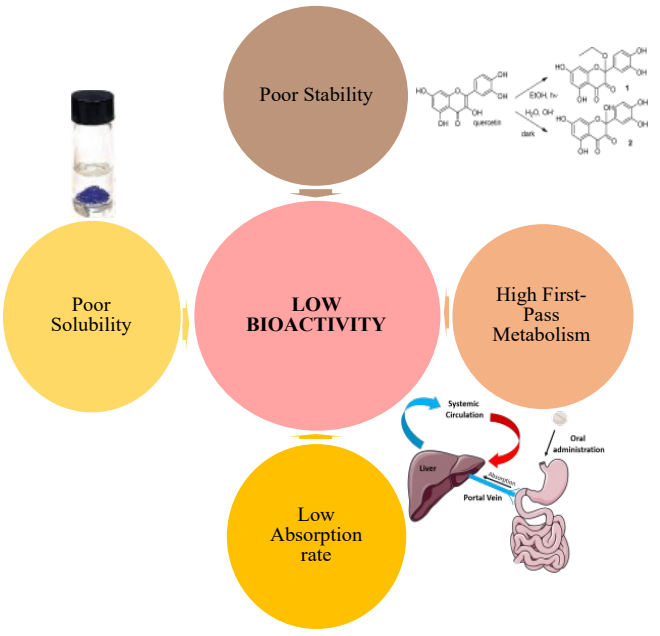

Fig. 1.5. Drawbacks of flavonoids

Oral administration of 5, 7, 3′, 4′-tetramethoxyflavone, a derivative of luteolin, at 50 mg/kg body weight showed the highest absorption (0.79 μg/ml) and bioavailability (14.3%) of luteolin [38]. Luteolin has been regarded as a sparingly soluble bioactive in diverse pure solvents such as water, ethanol, methanol, isopropanol, and dimethyl sulfoxide etc. The solubility of luteolin (mole fraction) was found utmost in polyethylene glycol-400 (0.127) followed by dimethyl sulfoxide (0.0715), 2-butanol (0.00553), 1-butanol (0.00536), ethyl acetate (0.00511), isopropanol (0.00414), ethanol (0.00308), ethylene glycol (0.00238), methanol (0.000816) and water (0.00000417) at 318.2 K [39]. Naringenin has an extremely low affinity for water, with a water solubility of just around 46 μg/ mL, resulting in a 5.81% maximum oral bioavailability. It has a low plasma bioavailability due to fast hepatic first-pass metabolism and conversion into glucuronide intermediate metabolites [29]. The aqueous solubility of anhydrous quercetin is 2.15 μg/mL at 25 °C [40]. Thus, the bioactivities of flavonoids are restricted by its low solubility and bioavailability [41]. Hence it is essential to improve the solubility and stability of flavonoids.

1.6. Novel techniques for flavonoids delivery

Bioactive substances are entrapped in nanostructures to be delivered to different body locations. The capsules' small size guarantees the delivery of the bioactives to the intended spot. The stability, solubility, and encapsulation effectiveness of nano-capsules are superior to those of microcapsules. Precision targeting of bioactive chemicals can be accomplished with nano-capsules smaller than 1000 nm much more easily than with microcapsules [10,18,21]. European Commission defines nanoparticles as a natural, incidental, or manufactured materials containing particles, in an unbound state or as an agglomerate or as an aggregate and where, for 50% or more of the particles in the number size distribution, one or more external dimensions is in the size range 1-100 nm [10]. The physicochemical characteristics, stability, solubility, and bioavailability of phenolic compounds can be greatly impacted by their incorporation in foods. Encapsulation can stop the decomposition of phenolic compounds against the damaging effects of light, oxygen, and pH. Additionally, encapsulation can stop the interaction of polyphenols with other food ingredients. Polyphenol-loaded nanoparticles can be utilized to create novel functional foods, which can effectively deter a variety of diseases. Bioactive compounds are covered with a carrier material or captured within carriers in nanoencapsulation technique which can protect against the adverse effect of pH, oxygen, and light during processing, storage, and transport.

Nanoencapsulation can also minimize contact between bioactive compounds and other food components with a sustained release [42]. The carrier materials for the nanoencapsulation play an imperative role in presenting the biological activities of the encapsulated compounds.

There are many methods for enhancing flavonoid formulations, and the process is frequently revised. The use of alternative solvents and cosolvents, controlled crystallization methods, comminution to reduce particle size, preparation of hydrates and solvates, cocrystallization, micellization or dispersion are all examples of delivery techniques. To increase the stability and bioavailability of bioactive chemicals, a variety of nanoscale delivery systems, including as emulsifiers, gels, and liposomes, have been extensively used in recent years for their small size, high surface-to-volume ratio and good dispersibility. Different state-of-the-art approaches such as inclusion complex [43], nanoemulsion [44], nanoparticle formulation [45], solid dispersion [46] are being exercised to overcome the low aqueous solubility, poor efficacy, and low oxidation stability of flavonoids with excellent encapsulating capacity, high penetration of biological barrier, and good controlled release property [45]. All the modern delivery systems are not flawless. They also have limitations. Some of them can't deliver flavonoids at required doses. Some of them required higher amount of carrier materials. So, alternative delivery strategies are required to improve the solubility and stability of flavonoids.

1.7. Ionic Liquids

Ionic liquids (ILs) are stable salts that are entirely consisted of organic cations and inorganic anions and have melting temperatures below 100°C. The availability of a wide variety of cation and anion combinations encourages the development of ILs. ILs are preferred over conventional solvents and/or catalysts in many chemical and physical processes, frequently displaying "green" and "designer" features to a useful scale [47] [48][49] The widely used structural head groups of ionic liquids are primarily imidazolium, pyridinium and quaternary ammonium bases. However. these head groups are not environmental-friendly and non-biodegradable. Anions and/or cations obtained from natural sources mainly include amino acids, non-nutritive sweeteners, glucose, carboxylic acids, and choline derivatives that show both a lower environmental impact and toxicity. The use of the cholinium cation instead of the methylimidazolium cation leads to a drastic decrease in toxicity. In the pharmaceutical and biomedical fields, Bio-ILs are used as stabilizer agents for biomolecules,

as solvents, or as part of drug carrier systems for poorly soluble drugs, such as in API-IL systems [48].

1.7.1 Applications of Ionic Liquids in different fields

Because of their tailored made properties, ILs have continued to be used in several fields throughout the past few decades. Below is a list of some application fields for ILs, but not all of them, including-

- ILs have been used as liquid lubricants in a variety of systems, and it has been discovered that these materials can exhibit amazing wear protection and greatly reduce friction in the clean conditions.
- ILs are used in analytical chemistry for sample preparation, and detection using chromatography or capillary electrophoresis (CE).
- ILs as electrolytes or IL-based polymer electrolytes in lithium batteries and capacitors.
- Deconstruction of lignocellulosic biomass, extraction, and separation of bioactive compounds from plants using ILs as a green solvent.
- ILs as novel reaction media and in heavy metal extraction

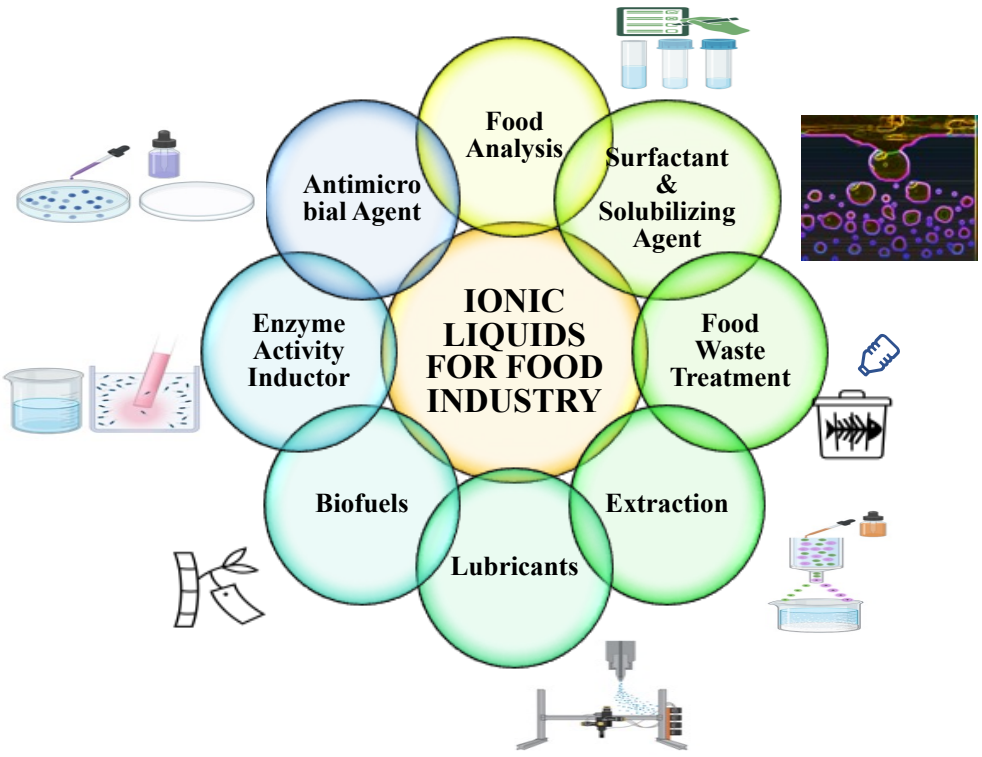

Fig. 1.6. Applications of ionic liquids for food industries. Adapted from [50]

1.7.2 Applications of ILs in food and agricultural industries.

Ionic liquids can generally be utilized as antimicrobial and antioxidant agents as well as to deliver crystalline solids as (1) cosolvents, (2) emulsifiers, (3) copolymers, and (4) solvents or antisolvents. Much interest is being paid to the IL-based vesicles, micelles, and microemulsions as possible drug delivery systems.

1.7.2.1 Ionic Liquids as antimicrobial agents

Antimicrobial properties of ILs have attained great interest of researchers rapidly. The pharmaceutical and industrial prospects of ILs became apparent when it was discovered that many different types of ILs prevented the growth of various microbial species. Pathogenic and nonpathogenic bacteria, fungi, and other microorganisms have been demonstrated to be inhibited by imidazolium, pyridinium, pyrrolidinium, piperidinium, ammonium, and other ILs. As a result, it may have an useful property in medicine [49]. Ionic liquids are believed to have antimicrobial effects by their attachment to the cell membranes, the deactivation of membrane proteins and phospholipids, disruption and disintegration of the phospholipid bilayer and the release of intracellular cytoplasm, and the cell lysis. Additionally, ionic liquids may change the ability of trans-membrane proteins to transport lipids, water, and nutrients by interacting with them [51]. Ionic liquids created by combining the ascorbate anion with the alkyltrimethylammonium, dialkyldimethylammonium, and alkylmethylbis(2-hydroxyethyl) ammonium cations showed excellent antibacterial and antifungal characteristics when used to treat various microorganisms, including pathogens. The most effective product, dimethyldioctylammonium and didecyldimethylammonium, have two lengthy alkyl substituents in the cation. These compounds produced the best performance against *Micrococcaceae, Pseudomonadaceae, Lactobacillaceae, and Bacillaceae*, as well as fungi from the genera *Botrytis, Alternaria, Fusarium, and Cladosporium* [52]. Novel chitosan-based transparent films prepared with cholinium hexanoate and cholinium citrate ionic liquids showed antibacterial activity against *Staphylococcus aureus* and *Klebsiella pneumoniae* [53].

1.7.2.2 Ionic Liquids as antioxidant agents

Antioxidants are substances that either greatly or entirely stop other molecules from oxidizing. Typically, these compounds guard against the action of free radicals and the

harmful effects of reactive oxygen species (ROS). The fundamental cause of the decline in food quality is free radicals. The antioxidant activity of ILs made from L-carnitine as a cation and phenolic acids and L-ascorbic acid as anions was evaluated. The ILs made from gallic acid, gentisic acid, and caffeic acid were found to have the high efficacy in the neutralization of radicals. Their antioxidant activity was noticeably higher than those of ascorbic acid/vitamin C, a common natural antioxidant [54]. In comparison to equivalent hydroxycinnamic acids, cholinium-based ionic liquids from hydroxycinnamic acids showed a greater free-radical scavenging activity [55]. Protic ionic ILs based on 3-Dimethylamino-1-propanol ferulate and 3-Diethylamino-1-propanol ferulate were determined to exhibit significant antioxidant activity, with EC_{50} values of 12.93 ± 0.05 and 14.09 ± 0.10 μM, respectively [56]. The antioxidant capacities of several new cholinium-based ILs, including dicholinium ellagate and cholinium caffeate, syringate, vanillate, gallate, and salicylate, were examined. These ILs showed antioxidant activities that were not only comparable to but even higher than those of their acidic predecessors [57].

1.7.3 Applications of ILs for flavonoids and drugs

1.7.3.1 ILs as solubility enhancer

A variety of low aqueous soluble molecules have been effectively solubilized using ionic liquids, mostly due to their capacity to interact with the solute and, if present, co-solvent, breaking preexisting bonds and encouraging solute integration. Early investigations on the solubility of IL drugs mainly concentrated on measuring the solubility of small drugs in pure and aqueous IL composition [58]. For low water-soluble bio-compounds such essential oils, vitamins, flavors, and colors, ILs have been revealed as a solubility enhancer. ILs based on imidazolium, ammonium, and phosphonium as well as [Cho]Cl were used to test the solubility of gallic acid and vanillin in water using more than 20 hydrotropes. In comparison to popular Na-based hydrotropes including sodium benzoate, sodium citrate, and sodium thiocyanate, the solubility was increased up to 46 times for [C4mim]Cl at 303 K [50]. Ammonium and phosphonium chlorides demonstrated 60–120 times greater solubilization of ibuprofen than water solution alone, and imidazolium thiocyanate and dicyanamide demonstrated that both the cation and anion can work together to increase the overall solubility by facilitating interactions between the organic molecules and the aqueous solution [59]. Ionic liquids (ILs) as a designer solvent may be novel solvent to address the low solubility and bioavailability problem of luteolin. The solubility of nobiletin (flavonoid)

in choline and geranic acid (ionic liquid) was 7.2 mg/mL, whereas that of nobiletin in water was reported to be 0.016 mg/mL, indicating that the solubility of nobiletin was remarkably enhanced in choline and geranic acid ionic liquid by approximately 450 times compared with water [37]. Therefore, ionic liquids may be promising substitute for solubilizing luteolin.

1.7.3.2 ILs as building blocks

Ionic liquids can be utilized as building blocks to create nanoparticles by adding electric charges to increase the colloidal stability of the nanoparticles [51].

1.7.3.3 ILs as a surfactant

Surface active agents (surfactant) as carrier materials are generally used as promising vehicle for bioactive compound because of their long-term stability and high drug solubilization capacity. However, several common cationic and anionic surfactants, such as cetyltrimethylammonium bromide, benzalkonium chloride, sodium dodecyl sulfate, sodium dodecylbenzene sulfonate etc. are toxic and non-biodegradable for their higher concentration requirement to produce long lasting micelles [60]. Because IL-based surfactants have low CMC values, they are more effective at adjusting the system's interfacial tension. Additionally, its ionic profile may disrupt the equilibrium between the hydrophobic and electrostatic interaction, which could result in significant modifications to the micellar structure. Some ILs, including those with long chains exhibit amphiphilic properties that are pertinent to their categorization as a new class of surfactants. Natural anions and cations with surfactant capabilities and decreased cytotoxicity are the foundation for the potential to manufacture surface active IL (SAIL) surfactants that are acceptable to foodstuff [50].

There are few reports in which ILs are used for delivering hydrophobic phytochemicals/ drugs [60,61]. Formulations using IL have demonstrated remarkable promise for the transdermal drug delivery. Thus, it was demonstrated that lidocaine hydrochloride adsorbed on the surfaces of the aggregates created by the surface-active ionic liquids [C_{12}MIM][Cl] and [C_{14}MIM][Cl]. Different surfactant solutions of curcumin were micellized by the hydrophilic IL [C_4MIM][BF_4], and [C_4MIM]-[C_8SO_4] stabilized curcumin, perhaps through hydrogen bonding and potent hydrophobic interactions [49]. In an aqueous solution, the long-chain ILs based on imidazolium and pyridinium behave as conventional cationic surfactants and have higher surface activity. Its propensity to self-assemble intensifies as

the length of the alkyl chain linked to the polar headgroup increases. The CMC values for the amide-functionalized ILs are lower than those for the non-functionalized salts, indicating that the possible hydrogen-bonding between the amide groups and alkyl side chain [62]. Paclitaxel was solubilized and stabilized using cholinium amino acid ILs, which stopped the drug molecules from aggregating for three months [63]. The solubility of celecoxib, acyclovir, methotrexate, and dantrolene sodium was improved by more than 20 folds in water using the same choline oleic IL as microemulsions [61]. The aqueous solubility of curcumin rises from 30 nmol to around 22 mmol because of complexes formed between choline oleic acid and curcumin [60].

1.8 Application of ILs in food preservation

Compared to biopolymer-based films, the use of ILs in the development of packaging films is quite inadequate. Antimicrobial ionic liquids, for example, can be added to packaging materials to limit the microbial growth by lowering live counts of bacteria, leading to the creation of novel, inventive packaging materials with antimicrobial capabilities. Green antimicrobial composite films made of 1-allyl-3-methylimidazolium chloride and biopolymers such cellulose, starch, and lignin have been created as potential options for fresh food packaging [64]. The creation of gelatin-based ionogel films with improved antibacterial and antioxidant properties involved the use of a bioactive ionic liquid called choline salicylate. The ionic liquid did not undergo any chemical modifications during the manufacturing process and instead served as a plasticizer in the film's structure. When compared to films without ionic liquids, the gelatin/ionic liquid-based films demonstrated the good bacterial growth suppression. This might be due to the cholinium salicylate's effective antibacterial action against *Bacillus subtilis*. The gelatin-IL film was applied to a peeled red apple piece, while the control piece was left in the air. The two parts were examined visually for air-oxidation activity after 120 min. It is clear to see that wrapping the apple in film significantly reduced air oxidation, demonstrating the film's suitability for packaging edible foods with outstanding antioxidant, antibacterial, and UV protection capabilities [65].

1.9 Aim and outline of this thesis

It has been widely documented over the past few years that ILs are regarded as a superior solvent, outstanding surface active components due to their adjustable physical, chemical,

and biological properties. Additionally, the versatility of ILs can provide a rare opportunity to create a specific process that might potentially reduce the process costs and have a significant impact on environmental concerns. Because of their excellent drug solubilization capability and long-term stability, surface active agents (surfactants) are frequently exploited as prospective carriers for bioactive compounds. There are not many ILs used as solubilizing agents or carrier materials for applications in the food industry. We designed this study to examine the opportunities and difficulties of ILs applications in the food system. The overall objectives of this study are:

1. To screen, synthesize, and characterize the suitable, low toxic, and biocompatible ILs as a solubilizing agent for improving solubility and bio-functionality of a sparingly soluble flavonoid, luteolin.
2. To formulate and develop nano-sized micellar formulation of luteolin using the low amount of carrier material to enhance luteolin dissolution and bioactivity and to investigate their performance on a food model
3. To develop a co-delivery system for the encapsulation flavonoids (luteolin, naringenin and quercetin) and to investigate their in vitro synergistic effects.

For these purposes in Chapter-2, we devised to screen and synthesize bio-based phenolic acids bearing an amino acid ester ILs as a potent green solvent for dissolving Luteolin (Lut) for food processing applications. Twenty cations (typical amino acid ethyl esters) and nine anions (phenolic acids) were chosen, mixed, and used to create 180 ILs, which were subsequently evaluated using COSMO-RS for LUT dissolution. Then the potential ILs were synthesized and characterized using ^{1}H NMR, Fourier-transform infrared spectroscopy (FT-IR), elemental analysis, thermal gravimetric analysis (TGA), differential scanning calorimetry (DSC), and HPLC to explore how these properties alter with the corresponding anions. The solubility of LUT in ILs was evaluated by the manual shaking method and quantified through HPLC. COSMO-RS prediction of LUT solubility was validated by determining the experimental solubility. ^{1}H NMR studies and COSMO-RS predictions were performed to gain insight into the possible solubility mechanism of LUT in ILs. Finally, a food preservation test was performed to check the efficacy of LUT with ILs.

Encapsulation of flavonoids can be promising delivery system in food. Formulation based delivery has become a cutting-edge method due to their capacity for self-assembly, controlled release profile, and high drug encapsulation efficiency. In C**hapter-3**, we

concentrated on developing nano-sized micellar formulation of Luteolin using low amount of carrier material, choline oleate, to enhance LUT dissolution and bioactivity using the solid-in-water nanodispersion technique. LUT-loaded micellar formulations (LUT-MF) were optimized in terms of the organic phase component, concentration of [Cho][Ole], and mixing method, and the particle size and size distribution, morphology, the encapsulation efficiency, and maximum aqueous solubility were investigated. The dissolution rate, antioxidant activity, and *in vitro* antibacterial properties of the LUT-MF were also assessed to support their application in the food industry. Finally, LUT-MFs were used on strawberry fruits as a model food to evaluate their food preservation effects.

Synergism of phytochemical compounds of plants provide them a stronger defense mechanism against different diseases and serve as potent antimicrobials or immunological boosters. Different flavonoids exhibit their antimicrobial activity through various mechanisms. To utilize synergistic properties of flavonoids, we concentrated in **Chapter-4** to develop choline oleate assisted micellar formulations of luteolin, quercetin and naringenin in combinations to increase their solubility and bioactivity. Three formulations were selected by visual observation from the six prepared formulations. The selected formulations, naringenin loaded micellar formulation (Nar-MF), luteolin and naringenin loaded micellar formulation (LN-MF), and luteolin, naringenin and quercetin loaded micellar formulation (LNQ-MF), were characterized by using dynamic light scattering (DLS), XRD and TEM. The encapsulation efficiency, loading capacity and maximum aqueous dispersibility were measured. Finally, they were also evaluated for their in vitro release profile, antioxidant capacity, and antibacterial capability.

Finally, in **Chapter-5**, we summarized the findings of this research and briefly explored potential future research possibilities.

1.10 References

[1] S.K. Amit, M.M. Uddin, R. Rahman, S.M.R. Islam, M.S. Khan, A review on mechanisms and commercial aspects of food preservation and processing, Agric. Food Secur. 6 (2017) 1–22. https://doi.org/10.1186/s40066-017-0130-8.

[2] W. Martindale, W. Schiebel, The impact of food preservation on food waste, Br. Food J. 119 (2017) 2510–2518. https://doi.org/10.1108/BFJ-02-2017-0114.

[3] A. Sridhar, M. Ponnuchamy, P.S. Kumar, A. Kapoor, Food preservation techniques and nanotechnology for increased shelf life of fruits, vegetables, beverages and spices: a review, Environ. Chem. Lett. 19 (2021) 1715–1735. https://doi.org/10.1007/s10311-020-01126-2.

[4] S. Tavman, S. Otles, S. Glaue, N. Gogus, Food preservation technologies, in: Sav. Food, Elsevier, 2019: pp. 117–140. https://doi.org/10.1016/B978-0-12-815357-4.00004-3.

[5] L. Xue, G. Liu, Introduction to global food losses and food waste, in: Sav. Food, Elsevier, 2019: pp. 1–31. https://doi.org/10.1016/B978-0-12-815357-4.00001-8.

[6] D.E. Burkepile, J.D. Parker, C.B. Woodson, H.J. Mills, P.A. Sobecky, M.E. Hay, E. Hay, J. Mills, Chemically Mediated Competition between Microbes and Animals : Microbes as Consumers in Food Webs Published by : Ecological Society of America Stable URL : http://www.jstor.org/stable/20069301 Your use of the JSTOR archive indicates your acceptance of JST, 87 (2009) 2821–2831.

[7] A. Lianou, E.Z. Panagou, G.J.E. Nychas, Microbiological spoilage of foods and beverages, in: Stab. Shelf Life Food, Woodhead Publishing, Duxford, UK, 2016: pp. 3–42. https://doi.org/10.1016/B978-0-08-100435-7.00001-0.

[8] F.T. Bozoglu, O. Erkmen, Food Preservation by Reducing Water Activity, in: Food Microbiol. Princ. into Pract., Wiley, 2016: pp. 44–58. https://doi.org/10.1002/9781119237860.ch30.

[9] O. Alegbeleye, O.A. Odeyemi, M. Strateva, D. Stratev, Microbial spoilage of vegetables, fruits and cereals, Appl. Food Res. 2 (2022) 100122. https://doi.org/10.1016/j.afres.2022.100122.

[10] A. Malik, Z. Erginkaya, H. Erten, Health and Safety Aspects of Food Processing Technologies, Springer International Publishing, Cham, 2019: pp. 1–672. https://doi.org/10.1007/978-3-030-24903-8.

[11] W. Qian, M. Liu, Y. Fu, J. Zhang, W. Liu, J. Li, X. Li, Y. Li, T. Wang, Antimicrobial mechanism of luteolin against Staphylococcus aureus and Listeria monocytogenes and its antibiofilm properties, Microb. Pathog. 142 (2020) 104056.

https://doi.org/10.1016/j.micpath.2020.104056.

[12] O.S. Qadri, B. Yousuf, A.K. Srivastava, Fresh-cut fruits and vegetables: Critical factors influencing microbiology and novel approaches to prevent microbial risks—A review, Cogent Food Agric. 1 (2015) 1121606. https://doi.org/10.1080/23311932.2015.1121606.

[13] F. Kong, R.P. Singh, Chemical deterioration and physical instability of foods and beverages, in: Stab. Shelf Life Food, Woodhead Publishing, Duxford, UK, 2016: pp. 43–76. https://doi.org/10.1016/B978-0-08-100435-7.00002-2.

[14] M.N. Lund, C.A. Ray, Control of Maillard Reactions in Foods: Strategies and Chemical Mechanisms, J. Agric. Food Chem. 65 (2017) 4537–4552. https://doi.org/10.1021/acs.jafc.7b00882.

[15] N.J. Wurlitzer, A.P. Dionísio, J.R. Lima, D. dos S. Garruti, I.M. da Silva Araújo, R.F.J. da Rocha, J.L. Maia, Tropical fruit juice: effect of thermal treatment and storage time on sensory and functional properties, J. Food Sci. Technol. 56 (2019) 5184–5193. https://doi.org/10.1007/s13197-019-03987-0.

[16] V. Prieto-Santiago, M.M. Cavia, S.R. Alonso-Torre, C. Carrillo, Relationship between color and betalain content in different thermally treated beetroot products, J. Food Sci. Technol. 57 (2020) 3305–3313. https://doi.org/10.1007/s13197-020-04363-z.

[17] G. El-Saber Batiha, D.E. Hussein, A.M. Algammal, T.T. George, P. Jeandet, A.E. Al-Snafi, A. Tiwari, J.P. Pagnossa, C.M. Lima, N.D. Thorat, M. Zahoor, M. El-Esawi, A. Dey, S. Alghamdi, H.F. Hetta, N. Cruz-Martins, Application of natural antimicrobials in food preservation: Recent views, Food Control. 126 (2021) 108066. https://doi.org/10.1016/j.foodcont.2021.108066.

[18] P. Martinengo, K. Arunachalam, C. Shi, Polyphenolic Antibacterials for Food Preservation: Review, Challenges, and Current Applications, Foods. 10 (2021) 2469. https://doi.org/10.3390/foods10102469.

[19] R.C. Baptista, C.N. Horita, A.S. Sant'Ana, Natural products with preservative properties for enhancing the microbiological safety and extending the shelf-life of

seafood: A review, Food Res. Int. 127 (2020) 108762. https://doi.org/10.1016/j.foodres.2019.108762.

[20] L. Axelsson, Lactic acid bacteria: classification and physiology, in: Lact. Acid Bact. Microbiol. Funct. Asp. Third Ed. Revis. Expand., 2004: pp. 1–66.

[21] J. Castro-Rosas, C.R. Ferreira-Grosso, C.A. Gómez-Aldapa, E. Rangel-Vargas, M.L. Rodríguez-Marín, F.A. Guzmán-Ortiz, R.N. Falfan-Cortes, Recent advances in microencapsulation of natural sources of antimicrobial compounds used in food - A review, Food Res. Int. 102 (2017) 575–587. https://doi.org/10.1016/j.foodres.2017.09.054.

[22] A.K. Pandey, M.L. Chávez-González, A.S. Silva, P. Singh, Essential oils from the genus Thymus as antimicrobial food preservatives: Progress in their use as nanoemulsions-a new paradigm, Trends Food Sci. Technol. 111 (2021) 426–441. https://doi.org/10.1016/j.tifs.2021.02.076.

[23] I. Gutiérrez-del-Río, J. Fernández, F. Lombó, Plant nutraceuticals as antimicrobial agents in food preservation: terpenoids, polyphenols and thiols, Int. J. Antimicrob. Agents. 52 (2018) 309–315. https://doi.org/10.1016/j.ijantimicag.2018.04.024.

[24] A. Biharee, A. Sharma, A. Kumar, V. Jaitak, Antimicrobial flavonoids as a potential substitute for overcoming antimicrobial resistance, Fitoterapia. 146 (2020) 104720. https://doi.org/10.1016/j.fitote.2020.104720.

[25] I. Górniak, R. Bartoszewski, J. Króliczewski, Comprehensive review of antimicrobial activities of plant flavonoids, Phytochem. Rev. 18 (2019) 241–272. https://doi.org/10.1007/s11101-018-9591-z.

[26] A.A. Moeiniafshari, A. Zarrabi, A.K. Bordbar, Exploring the interaction of naringenin with bovine beta-casein nanoparticles using spectroscopy, Food Hydrocoll. 51 (2015) 1–6. https://doi.org/10.1016/j.foodhyd.2015.04.036.

[27] D. Aluani, V. Tzankova, M. Kondeva-Burdina, Y. Yordanov, E. Nikolova, F. Odzhakov, A. Apostolov, T. Markova, K. Yoncheva, Evaluation of Biocompatibility and Antioxidant Efficiency of Chitosan-Alginate Nanoparticles Loaded With Quercetin, Int. J. Biol. Macromol. 103 (2017) 771–782.

https://doi.org/10.1016/j.ijbiomac.2017.05.062.

[28] A. Faridi Esfanjani, S.M. Jafari, Biopolymer nano-particles and natural nano-carriers for nano-encapsulation of phenolic compounds, Colloids Surfaces B Biointerfaces. 146 (2016) 532–543. https://doi.org/10.1016/j.colsurfb.2016.06.053.

[29] A. Arafah, M.U. Rehman, T.M. Mir, A.F. Wali, R. Ali, W. Qamar, R. Khan, A. Ahmad, S.S. Aga, S. Alqahtani, N.M. Almatroudi, Multi-Therapeutic Potential of Naringenin (4′,5,7-Trihydroxyflavonone): Experimental Evidence and Mechanisms, Plants. 9 (2020) 1784. https://doi.org/10.3390/plants9121784.

[30] Sariga, A. George, R. Rajeev, D.A. Thadathil, A. Varghese, A Comprehensive Review on the Electrochemical Sensing of Flavonoids, Crit. Rev. Anal. Chem. 0 (2021) 1–41. https://doi.org/10.1080/10408347.2021.2008863.

[31] M. Hartmann, M. Berditsch, J. Hawecker, M.F. Ardakani, D. Gerthsen, A.S. Ulrich, Damage of the bacterial cell envelope by antimicrobial peptides gramicidin S and PGLa as revealed by transmission and scanning electron microscopy, Antimicrob. Agents Chemother. 54 (2010) 3132–3142. https://doi.org/10.1128/AAC.00124-10.

[32] Q. Wu, J. Zhou, The application of polyphenols in food preservation, 1st ed., Elsevier Inc., 2021. https://doi.org/10.1016/bs.afnr.2021.02.005.

[33] D. Sanver, A. Sadeghpour, M. Rappolt, F. Di Meo, P. Trouillas, Structure and Dynamics of Dioleoyl-Phosphatidylcholine Bilayers under the Influence of Quercetin and Rutin, Langmuir. 36 (2020) 11776–11786. https://doi.org/10.1021/acs.langmuir.0c01484.

[34] X. Fan, H. Ngo, C. Wu, Natural and Bio-based Antimicrobials: A Review, ACS Symp. Ser. 1287 (2018) 1–24. https://doi.org/10.1021/bk-2018-1287.ch001.

[35] A. Adamczak, M. Ożarowski, T.M. Karpiński, Antibacterial Activity of Some Flavonoids and Organic Acids Widely Distributed in Plants, J. Clin. Med. 9 (2019) 109. https://doi.org/10.3390/jcm9010109.

[36] A. Pernin, F. Dubois-Brissonnet, S. Roux, M. Masson, V. Bosc, M.N. Maillard, Phenolic compounds can delay the oxidation of polyunsaturated fatty acids and the

growth of Listeria monocytogenes: structure-activity relationships, J. Sci. Food Agric. 98 (2018) 5401–5408. https://doi.org/10.1002/jsfa.9082.

[37] T. Hattori, H. Tagawa, M. Inai, T. Kan, S. ichiro Kimura, S. Itai, S. Mitragotri, Y. Iwao, Transdermal delivery of nobiletin using ionic liquids, Sci. Rep. 9 (2019) 1–11. https://doi.org/10.1038/s41598-019-56731-1.

[38] M.F. Manzoor, N. Ahmad, Z. Ahmed, R. Siddique, X.A. Zeng, A. Rahaman, R. Muhammad Aadil, A. Wahab, Novel extraction techniques and pharmaceutical activities of luteolin and its derivatives, J. Food Biochem. 43 (2019) 1–19. https://doi.org/10.1111/jfbc.12974.

[39] F. Shakeel, N. Haq, S. Alshehri, M.A. Ibrahim, E.M. Elzayat, M.A. Altamimi, K. Mohsin, F.K. Alanazi, I.A. Alsarra, Solubility, thermodynamic properties and solute-solvent molecular interactions of luteolin in various pure solvents, J. Mol. Liq. 255 (2018) 43–50. https://doi.org/10.1016/j.molliq.2018.01.155.

[40] K. Srinivas, J.W. King, L.R. Howard, J.K. Monrad, Solubility and solution thermodynamic properties of quercetin and quercetin dihydrate in subcritical water, J. Food Eng. 100 (2010) 208–218. https://doi.org/10.1016/j.jfoodeng.2010.04.001.

[41] X. Cao, H. Li, M. Wang, X. Ren, Y. Deng, Analysis of five active ingredients of Er-Zhi-Wan, a traditional Chinese medicine water-honeyed pill, using the biopharmaceutics classification system, Biomed. Chromatogr. 34 (2020) 1–11. https://doi.org/10.1002/bmc.4757.

[42] D.D. Milinčić, D.A. Popović, S.M. Lević, A.Ž. Kostić, Ž.L. Tešić, V.A. Nedović, M.B. Pešić, Application of Polyphenol-Loaded Nanoparticles in Food Industry, Nanomaterials. 9 (2019) 1629. https://doi.org/10.3390/nano9111629.

[43] S. Alshehri, S.S. Imam, M.A. Altamimi, M. Jafar, M.Z. Hassan, A. Hussain, A. Ahad, W. Mahdi, Host-guest complex of β-cyclodextrin and pluronic F127 with Luteolin: Physicochemical characterization, anti-oxidant activity and molecular modeling studies, J. Drug Deliv. Sci. Technol. 55 (2020) 101356. https://doi.org/10.1016/j.jddst.2019.101356.

[44] M.A. Altamimi, A. Hussain, S. Alshehri, S.S. Imam, U.A. Alnemer, Development

and Evaluations of Transdermally Delivered Luteolin Loaded Cationic Nanoemulsion: In Vitro and Ex Vivo Evaluations, Pharmaceutics. 13 (2021) 1218. https://doi.org/10.3390/pharmaceutics13081218.

[45] Y.Y. Chen, K. Liu, X.Q. Zha, Q.M. Li, L.H. Pan, J.P. Luo, Encapsulation of luteolin using oxidized lotus root starch nanoparticles prepared by anti-solvent precipitation, Carbohydr. Polym. 273 (2021) 118552. https://doi.org/10.1016/j.carbpol.2021.118552.

[46] S. Alshehri, S.S. Imam, M.A. Altamimi, A. Hussain, F. Shakeel, E. Elzayat, K. Mohsin, M. Ibrahim, F. Alanazi, Enhanced Dissolution of Luteolin by Solid Dispersion Prepared by Different Methods: Physicochemical Characterization and Antioxidant Activity, ACS Omega. 5 (2020) 6461–6471. https://doi.org/10.1021/acsomega.9b04075.

[47] Z. Lei, B. Chen, Y.M. Koo, D.R. Macfarlane, Introduction: Ionic Liquids, Chem. Rev. 117 (2017) 6633–6635. https://doi.org/10.1021/acs.chemrev.7b00246.

[48] J.M. Gomes, S.S. Silva, R.L. Reis, Biocompatible ionic liquids: Fundamental behaviours and applications, Chem. Soc. Rev. 48 (2019) 4317–4335. https://doi.org/10.1039/c9cs00016j.

[49] K.S. Egorova, E.G. Gordeev, V.P. Ananikov, Biological Activity of Ionic Liquids and Their Application in Pharmaceutics and Medicine, Chem. Rev. 117 (2017) 7132–7189. https://doi.org/10.1021/acs.chemrev.6b00562.

[50] A.A.C. Toledo Hijo, G.J. Maximo, M.C. Costa, E.A.C. Batista, A.J.A. Meirelles, Applications of Ionic Liquids in the Food and Bioproducts Industries, ACS Sustain. Chem. Eng. 4 (2016) 5347–5369. https://doi.org/10.1021/acssuschemeng.6b00560.

[51] N. Nikfarjam, M. Ghomi, T. Agarwal, M. Hassanpour, E. Sharifi, D. Khorsandi, M. Ali Khan, F. Rossi, A. Rossetti, E. Nazarzadeh Zare, N. Rabiee, D. Afshar, M. Vosough, T. Kumar Maiti, V. Mattoli, E. Lichtfouse, F.R. Tay, P. Makvandi, Antimicrobial Ionic Liquid-Based Materials for Biomedical Applications, Adv. Funct. Mater. 31 (2021) 2104148. https://doi.org/10.1002/adfm.202104148.

[52] M. Niemczak, D.K. Kaczmarek, T. Klejdysz, D. Gwiazdowska, K. Marchwińska, J.

Pernak, Ionic Liquids Derived from Vitamin C as Multifunctional Active Ingredients for Sustainable Stored-Product Management, ACS Sustain. Chem. Eng. 7 (2019) 1072–1084. https://doi.org/10.1021/acssuschemeng.8b04696.

[53] L.C. Tomé, N.H.C.S. Silva, H.R. Soares, A.S. Coroadinha, P. Sadocco, I.M. Marrucho, C.S.R. Freire, Bioactive transparent films based on polysaccharides and cholinium carboxylate ionic liquids, Green Chem. 17 (2015) 4291–4299. https://doi.org/10.1039/c5gc00416k.

[54] K. Czerniak, J. Pernak, L-Carnitine-Based Bio-Ionic Liquids as Antioxidants, ChemistrySelect. 6 (2021) 1994–2001. https://doi.org/10.1002/slct.202100420.

[55] M. Demurtas, V. Onnis, P. Zucca, A. Rescigno, J.I. Lachowicz, L. De Villiers Engelbrecht, M. Nieddu, G. Ennas, A. Scano, F. Mocci, F. Cesare Marincola, Cholinium-Based Ionic Liquids from Hydroxycinnamic Acids as New Promising Bioactive Agents: A Combined Experimental and Theoretical Investigation, ACS Sustain. Chem. Eng. 9 (2021) 2975–2986. https://doi.org/10.1021/acssuschemeng.1c00090.

[56] N.A. Ahmad, K. Jumbri, A. Ramli, N.A. Ghani, H. Ahmad, M.A. Kassim, Synthesis, characterisation and antioxidant properties of ferulate-based protic ionic liquids: Experimental and modelling approaches, J. Mol. Liq. 278 (2019) 309–319. https://doi.org/10.1016/j.molliq.2019.01.048.

[57] T.E. Sintra, A. Luís, S.N. Rocha, A.I.M.C.L. Ferreira, F. Gonçalves, L.M.N.B.F. Santos, B.M. Neves, M.G. Freire, S.P.M. Ventura, J.A.P. Coutinho, Enhancing the antioxidant characteristics of phenolic acids by their conversion into cholinium salts, ACS Sustain. Chem. Eng. 3 (2015) 2558–2565. https://doi.org/10.1021/acssuschemeng.5b00751.

[58] A.M. Curreri, S. Mitragotri, E.E.L. Tanner, Recent Advances in Ionic Liquids in Biomedicine, Adv. Sci. 8 (2021) 1–18. https://doi.org/10.1002/advs.202004819.

[59] T.E. Sintra, K. Shimizu, S.P.M. Ventura, S. Shimizu, J.N. Canongia Lopes, J.A.P. Coutinho, Enhanced dissolution of ibuprofen using ionic liquids as catanionic hydrotropes, Phys. Chem. Chem. Phys. 20 (2018) 2094–2103.

https://doi.org/10.1039/c7cp07569c.

[60] M.R. Chowdhury, R.M. Moshikur, R. Wakabayashi, Y. Tahara, N. Kamiya, M. Moniruzzaman, M. Goto, Development of a novel ionic liquid-curcumin complex to enhance its solubility, stability, and activity, Chem. Commun. 55 (2019) 7737–7740. https://doi.org/10.1039/c9cc02812a.

[61] M.K. Ali, R.M. Moshikur, R. Wakabayashi, M. Moniruzzaman, N. Kamiya, M. Goto, Biocompatible Ionic Liquid Surfactant-Based Microemulsion as a Potential Carrier for Sparingly Soluble Drugs, ACS Sustain. Chem. Eng. 8 (2020) 6263–6272. https://doi.org/10.1021/acssuschemeng.9b07773.

[62] M.T. Garcia, I. Ribosa, L. Perez, A. Manresa, F. Comelles, Self-assembly and antimicrobial activity of long-chain amide-functionalized ionic liquids in aqueous solution, Colloids Surfaces B Biointerfaces. 123 (2014) 318–325. https://doi.org/10.1016/j.colsurfb.2014.09.033.

[63] M.K. Ali, R.M. Moshikur, R. Wakabayashi, M. Moniruzzaman, M. Goto, Biocompatible Ionic Liquid-Mediated Micelles for Enhanced Transdermal Delivery of Paclitaxel, ACS Appl. Mater. Interfaces. 13 (2021) 19745–19755. https://doi.org/10.1021/acsami.1c03111.

[64] R.L. Wu, X.L. Wang, F. Li, H.Z. Li, Y.Z. Wang, Green composite films prepared from cellulose, starch and lignin in room-temperature ionic liquid, Bioresour. Technol. 100 (2009) 2569–2574. https://doi.org/10.1016/j.biortech.2008.11.044.

[65] M.J. Mehta, A. Kumar, Ionic Liquid Assisted Gelatin Films: Green, UV Shielding, Antioxidant, and Antibacterial Food Packaging Materials, ACS Sustain. Chem. Eng. 7 (2019) 8631–8636. https://doi.org/10.1021/acssuschemeng.9b00423.

CHAPTER-2: AMINO ACID ESTER BASED PHENOLIC IONIC LIQUIDS AS A POTENTIAL SOLVENT FOR THE BIOACTIVE COMPOUND LUTEOLIN

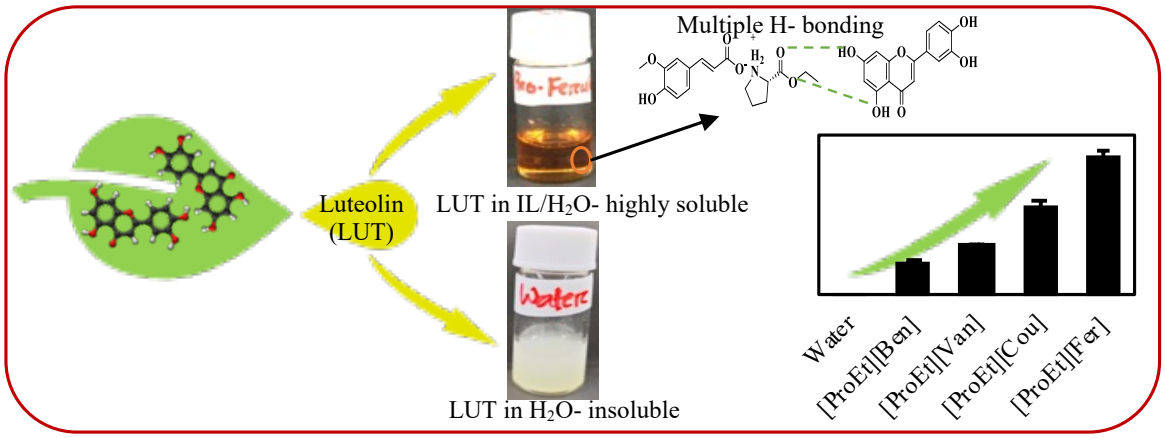

This chapter was published in Journal of Molecular Liquids 349 (2022) 118103; https://doi.org/10.1016/j.molliq.2021.118103 with permission of Elsevier.

2.1 Introduction

Ionic liquids (ILs) are molten salts synthesized by combining bulky organic cations with a wide variety of organic or inorganic anions [1]. They are considered as green alternatives to conventional toxic organic solvents owning to their tunability, low volatility, low melting point, high thermal stability, and enhanced capacity for dissolving a great variety of materials, including phenolic compounds [2–4]. Phenolic compounds – abundant in various medicinal plants, spices, fruits, and vegetables – have multifaceted biological activities, for example, as potential antiseptic, antioxidant, antimicrobial, anti-inflammatory, and anticarcinogenic compounds [2,5]. Plants synthesize various types of phenolic compound, including simple phenol, phenolic acids, stilbenes, and flavonoids as secondary metabolites for their protection from pathogens [6,7]. Among the various phenolic bioactive compounds, luteolin (LUT) is one of the most common naturally occurring and is found in celery, parsley, broccoli, carrots, apple skins, and peppers [8,9]. It has the capability to be used as a natural preservative in food processing because of its non-toxic nature and considerable antioxidant and antimicrobial properties [8,10–12]. However, LUT has poor solubility in water (0.0506 mg/mL) [13] and most conventional organic solvents at room temperature (RT), which limits its potential in the food and pharmaceutical industries [14]. To address the poor solubility issues, several modern strategies, such as nanotechnology [15], encapsulation [13], and the use of an absorption enhancer [16] have been designed. The solubility of LUT was increased 132.7 times in nanoparticles [15], 6 to 10 times in inclusion complexes with β-cyclodextrin and β-cyclodextrin: Pluronic F127 mixture [16] and 17.1 times by copolymer micelle formation [13] compared with that in pure water. However, solubility enhancement in a green solvent has not been attained yet. ILs can be used to address the low solubility of many problematic flavonoids, such as LUT, rutin, esculin, and nobiletin [12,17–19]. For example, the solubility of LUT in 1-butyl-3-methylimidazolium tetrafluoroborate and 1-hexyl-3-methylimidazolium tetrafluoroborate were significantly improved by 269.6- and 261.7-fold, respectively, compared with that in water (0.0506 mg/mL) [18]. Conventional ILs like imidazolium and phosphonium have low biodegradability and high toxicity with cell lines and aquatic organisms [20,21]. The physicochemical properties of ILs can be adjusted by alteration of cation and anion, and thus they are referred to as designer solvents [22]. However, the toxicity issue might be overcome by choosing the cations and anions of the IL from natural sources that are known as GRAS (Generally Recognized As Safe) [21,23,24]. Recently, several biocompatible cations (e.g., cholinium and amino acid esters)

and anions (e.g., amino acids, fatty acids, and carboxylic acids) are combined to form ILs that are being used to improve the solubility of flavonoids. The solubility of nobiletin was markedly improved by 450-fold in choline and geranic acid (CAGE) IL, compared with that in water [19]. To predict the thermodynamic properties, several techniques are used as a screening tool including UNIFAC [25,26], machine learning [27,28], Hansen solubility parameters [29], QSPR [30], ab initio calculation[31] and COSMO-RS [3]. Generally, most of these methods require experimental data to construct feasible training sets [32]. To select the suitable cations and anions to achieve both solubility of a certain target compound and the biocompatibility of IL itself is cumbersome and laborious. COnductor-like Screening MOdel for Real Solvents (COSMO-RS) is a convenient tool to predict the physical, thermal, and chemical properties of almost any imaginable compound mixture or system (including even experimentally unavailable entities such as reactive intermediates or transition state structures) [3]. COSMO-RS has recently gained great attraction to screen the suitable ILs for various compounds, including flavonoids. The solubility prediction of flavonoids (esculin, rutin, chrysin) in various ILs performed by COSMO-RS showed good agreement with their experimental solubilities [17,33].

The aim of this study was to screen and synthesize bio-based phenolic acids bearing amino acid ester ILs as a potent green solvent for dissolving LUT for food processing applications. Twenty cations (standard amino acid ethyl esters) and nine anions (phenolic acids) were selected and combined to form 180 ILs, which were then assessed for dissolution of LUT via COSMO-RS. Then the potential ILs were synthesized and characterized using ^{1}H NMR, Fourier-transform infrared spectroscopy (FT-IR), elemental analysis, thermal gravimetric analysis (TGA), differential scanning calorimetry (DSC), and HPLC to explore how these properties alter with the corresponding anions. The solubility of LUT in ILs was evaluated by manual shaking methods and quantified through HPLC. COSMO-RS prediction of LUT solubility was validated by determining the experimental solubility. ^{1}H NMR studies and COSMO-RS predictions were performed to gain insight into the possible solubility mechanism of LUT in ILs. Finally, a food preservation test was performed to check the efficacy of LUT with ILs.

2.2 Materials and methods

2.2.1 Materials

Luteolin (3′,4′,5,7-tetrahydroxyflavone), trans-ferulic acid, vanillic acid, trans-p-coumaric acid with purity >98.0% and 4-hydroxybenzoaic acid with purity >99.0% were purchased from Tokyo Chemical Industry Co. Ltd (Japan). Kishida Chemical Co. Ltd. (Japan) provided L (-)-proline, thionyl chloride, and ethanol with >99.0% purity. Methanol, ammonia solution, phosphoric acid, diethyl ether, and deuterated dimethylsulfoxide (DMSO-D6) were bought from Wako Pure Chemicals Industries (Japan). All other analytical grade reagents, solvents, and materials were used as received.

2.2.2 COSMO-RS

The methods used in COSMO-RS to calculate any thermodynamic property associated with chemical potential (including the activity coefficient at infinite dilution (γ^{∞})), come from both statistical thermodynamics and quantum chemistry (QC). The most alluring feature of COSMO-RS is that it just requires the molecular formula and structure of molecules as inputs for calculations. These comparatively straightforward 1D and 2D chemical representations are converted into more intricate 3D molecular geometry because of diligent optimization using *ab initio* QC calculations. A conductor-like screening model (COSMO) acts as the QC basis for COSMO-RS. One of the most well-known continuum

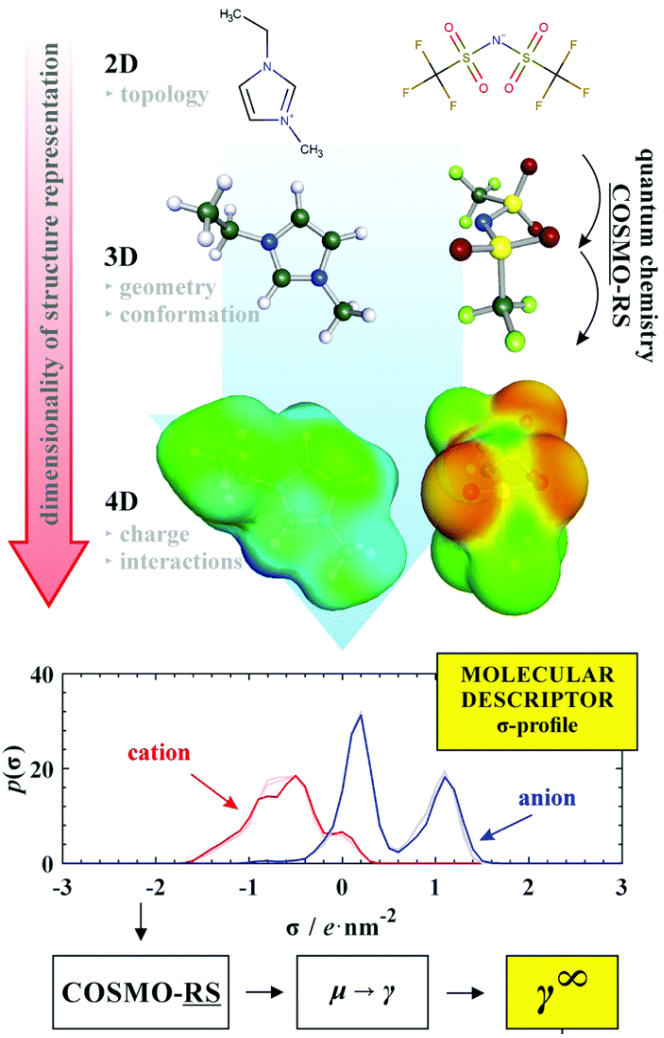

Scheme 2.1. Chemical information processing by the COSMO-RS method to obtain γ^{∞} [3]

solvation approaches, it accounts for a variety of factors connected to the influence of the solvent on the electronic state of a solute molecule in terms of electrostatics. The COSMO computation often produces a distinct surface (referred to as a cavity) built around a molecule solvated in a perfect conductor. This makes COSMO more intriguing for exploring the characteristics of molecules in liquids than traditional unimolecular QC calculations, which normally consider an isolated molecule at a temperature of T = 0 K. The distribution of charge produced at the surface of the cavity, rather than its size or shape, is the most significant COSMO-based molecular descriptor (corresponding to a different, fourth, dimension of the chemical information representation). This charge is known as the screening charge, and it is typically depicted by the surface density symbol of σ. The COSMO technique has been extended (the "RS" portion) to include actual solvents. This is accomplished by using the QC-calculated σ by means of ensemble averaging of local pairwise interactions between surface segments forming closely packed cavities. Hydrogen bonds, van der Waals dispersive forces, and electrostatic "misfit" are thought to be the causes of the interactions between segments. The probability distribution (or histogram) of the screening charge density, p(σ) is the single piece of information required in the computation of a compound's chemical potential in a mixture (μ) [3,17].

The activity coefficient is an important parameter that determines whether a given IL is effective for the separation of a given compound. In general, the value of the activity coefficient at infinite dilution (γ^{∞}) is strongly correlated with the affinity of the solutes to the ILs occurring from differences in the strength and nature between the solute– IL and IL–IL interactions [3]. Hence, it determines the potency of IL for the target compound and is useful for screening ILs. The activity coefficient at infinite dilution, γ^{∞} was calculated using the following formula [34]:

$$\gamma = \exp\left(\frac{\mu-\mu o}{RT}\right) \quad \text{.....1}$$

where μ and μ_o are the chemical potential in the solvent and of the pure compound, respectively.

COSMO-RS method determines the interaction between molecules based on a so-called sigma profile. The sigma profile (σ-profile) is the distribution of the screening charge density on the surface of that molecule. Used together with a statistical thermodynamic

expression, the resultant charge density distributions are used to compute chemical potentials of molecules in solution. σ-profile is evaluated using the equation [34].

$P(\sigma) = \sum_i^N x_i p_i(\sigma)$ ……..……..…… 2

where *i* is LUT with concentration x*i*.

2.2.3 Screening of ILs by COSMO-RS

The coordinates of the 3D molecular structures used for COSMO calculation were collected from PubChem. Furthermore, the input COSMO file was prepared using TURBOMOLE 4.5 with density functional theory (DFT) using the B3LYP (DFT-D3 BJ-damping) function with a TZVP basis set [2], [32]. The optimized geometries were verified through vibrational analysis showing that none of the structures had imaginary vibration modes. The generated output files were used for further calculations. COSMOtherm 2020 program was used for the estimation of the activity coefficient, sigma profiles, and sigma potentials.

2.2.4 Proline ethyl ester-based phenolic acids (PEEP-ILs) synthesis

L-proline ethyl ester (ProEt) was synthesized by using a procedure described in the literature [1,35]. Briefly, 5.0 gram of L(-)-proline in 50 mL dehydrated ethanol was placed in a round bottom flask. 5 mL $SOCl_2$ (thionyl chloride) was slowly added to the slurry in fume hood using a syringe and the mixture was kept under constant stirring in an ice bath for 1 hour. After 1 hour, the resultant solution was kept under vigorous agitation for 24 hours at 25^oC to produce L-proline ethyl ester hydrochloride salt (Scheme 2.2a). The reaction solution was distilled under reduced pressure to remove unreacted reactant. Then, 50 mL of diethyl ether and 10 mL of distilled water were added to the oily residue and the impurities dissolved in diethyl ether was removed by separating funnel. The L-proline ethyl ester hydrochloride salt was neutralized by adding 7.5 mL of 28% NH_3 solution (mole ratio of NH_3: salt= 2:1) and stirring in 50 mL of diethyl ether for further 2 h at 25^oC (Scheme 2.2b). The upper organic layer was collected by separating funnel and concentrated by means of reduced pressure to yield the [ProEt] cation.

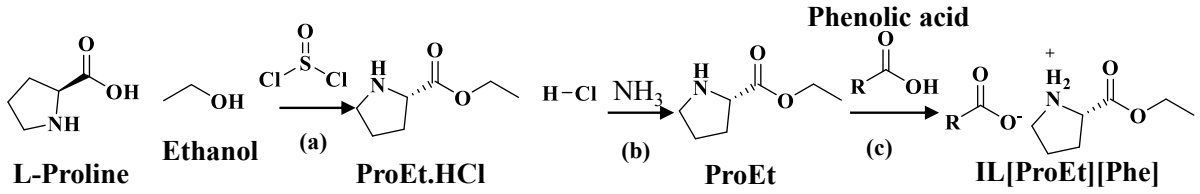

Scheme 2.2. Synthesis method for phenolic acid-based proline ethyl ester (PEEP-IL) ionic liquids. (a) $SOCl_2$ assisted esterification of l- proline by ethanol on ice for 1 hour, and then at 25°C for one day; (b) ammonium solution and diethyl ether at 25°C for 2 hours; & (c) at 40°C for 2 hours in the dark.

The synthesized ProEt and trans-ferulic acid at equal molarity were stirred in a methanolic solution for 2 hours at 40 °C to yield IL[ProEt][Fer] (Scheme 2.2c). Methanol in IL[ProEt][Fer] was then removed by evaporation under reduced pressure (<4 kPa) at >35°C. The IL[ProEt][Fer] obtained was finally freeze-dried for 12 hours. Equimolar amounts of ProEt and trans-p-coumaric acid, vanillic acid, and 4-hydroxybenzoic acid were stirred to synthesize IL[ProEt][Cou], IL[ProEt][Van], and IL[ProEt][Ben], respectively, in a similar manner to that of the IL[ProEt][Fer] synthesis. All the PEEP-ILs were characterized by ^{1}H NMR, elemental analysis, TG/DTA, DSC, and FT-IR to characterize their properties and structures.

2.2.5 NMR measurements

^{1}H NMR spectroscopy can be used for the characterization of the synthesized PEEP-ILs and it was determined on a JEOL ECZ400S 400 MHz spectrometer (Tokyo, Japan) at 25°C in deuterated dimethylsulfoxide and tetramethylsilane was used as the internal standard to confirm the proton transfer between the cation and the anion. The sensitivity of ^{1}H NMR instrument (S/N) was 500. The obtained spectra were processed in Delta NMR Processing and Control Software (version 5.3.1, JEOL). The accuracy of the NMR measurements was <0.01 ppm. The following equation was used to calculate the purities of the synthesized ILs:

$$\text{Purity (\%)} = [\Sigma I\,(\text{product})/\Sigma I\,(\text{total})] \times 100 \quad \ldots\ldots 3$$

where I represents the relative area of each signal [35].

2.2.6 Elemental analysis

Elemental analysis is a process in analytical chemistry to determine the quantity of a particular element within a molecule or material. To quantify the carbon, hydrogen, and nitrogen of the synthesized PEEP-ILs, elemental analysis on Yanaco CHNC MT-5 analyzer, Kyoto, Japan, was done.

2.2.7 Fourier transform infrared analysis

To confirm the chemical structure of the PEEP-ILs, FT-IR analysis of the PEEP-ILs was carried out with the accumulation of 20 scans in the wavenumber range 400–4000 cm^{-1} on a Perkin Elmer (Frontier FT-IR, Waltham, MA). The resolution and accuracy of FT-IR was 4 cm^{-1} and <2 cm^{-1} respectively.

2.2.8 Thermogravimetric analysis

Thermogravimetric analysis (TGA) is a thermal analysis system in which changes in physicochemical properties of materials are being observed because of increase in temperature. Thermogravimetric and derivative thermogravimetric analysis (TGA/DTG) of the PEEP-ILs sample was carried out on a Hitachi High-Technologies TG/DTA 7300 (Tokyo, Japan) to determine the thermal decomposition temperature (T_{onset}). The sensitivity of TGA was <0.2 μg. About 5–10 mg of sample was assessed in an aluminum pot using nitrogen as the purge gas. The samples were heated from 30 °C to 500 °C with 10 °C/min heating rate. Volatile solvents were removed by an isothermal hold at 70 °C for 25 min. The accuracy of the TGA measurements was <0.1%. T_{onset} was determined at the point where the initial mass was started to loss on TGA thermogram and T_{peak} was determined at the highest point on DTG graph.

2.2.9 Differential scanning calorimetry (DSC) of PEEP-ILs

DSC is a thermal analysis apparatus that determines the temperature and heat flow associated with material transitions as a function of time and temperature. The glass transition (T_g) and melting point (T_m) temperatures of the PEEP-ILs were measured by a Hitachi DSC X7000 (Tokyo, Japan). The PEEP-IL samples (8–10 mg) were placed in an aluminum pan, which was then hermetically sealed with a standard aluminum lid at the top. A blank aluminum pan with a lid was used as a reference to minimize errors in the weight

measurements. Three heating and cooling cycles were repeated for each sample from −50 to 200 °C at 5 °C/min rate to ensure reproducibility. Dry nitrogen was constantly flowing at 30 mL/min to maintain a dry and inert atmosphere inside the furnace. The accuracy of the DSC measurements was <0.5 °C. The glass transition (T_g) and melting point (T_m) temperatures were taken as the temperature at the midpoint of the concerned peaks.

2.2.10 Water solubility and partitioning coefficient determination

The water solubility and log $P_{o/w}$ of the free phenolic acids and PEEP-ILs were determined by HPLC analysis according to previously reported experiment procedures [36,37] with some modifications. The HPLC system consisted of a photo diode array (PDA) detector (MD-4010), a PU-4180 pump, an AS-4050 auto-sampler, a bottle stand (BS-4000-1), and a GL-7432 column oven controller (JASCO International Co. Ltd., HachioJi, Tokyo, Japan). The optimum separation of phenolic acids and PEEP-ILs was carried out by isocratic elution using a mobile phase consisting of water, acetonitrile, and phosphoric acid (85:13.8:1.2, v/v) [36]. The analysis was performed using an Inertsil ODS-3 column (GL Sciences Inc., Tokyo, Japan). The detection wavelengths used for the identification of phenolic acids were 254 nm for 4-hydroxybenzoic acid and vanillic acid, 280 nm for *p*-coumaric acid, 320 nm for trans-ferulic acid [37]. The temperature of the column oven was set at 25 °C. The flow rate of the mobile phase was 1.0 mL/min, and the injection volumes were 10 µL of the standards and samples. The standard stock solution was prepared at 1 mg/mL in methanol and diluted with the mobile phase at 5-80 µg/mL of phenolic acids.

An excess amount of each phenolic acid was added to milliQ water (≈1 mL) and stirred for 24 h at 25 °C. PEEP-ILs in milliQ water were allowed to equilibrate under constant agitation for 10 min. To measure the log *P* in octanol and water, 5–10 mg of the free phenolic acid and PEEP-ILs were mixed with 3 mL of water and 3 mL of 1-octanol. The mixtures were constantly agitated for 24 hours at RT. All the samples were centrifuged at 10000 rpm for 10 min, and the supernatant solution was diluted with the mobile phase. The partition coefficient, log $P_{o/w}$, was determined using the following equation:

log $P_{o/w}$ = log (concentration of solute in octanol/ concentration of solute in water) …..... 4

2.2.11 Solubility of LUT in PEEP-ILs

Excess amount of LUT was added to a glass vial containing an aqueous solution of PEEP-IL. Then, the suspension was stirred at 300 rpm by a magnetic stirring apparatus for 24 h at 25 °C. Then, the solution was centrifuged at 10,000 rpm for 15 min to separate the solid-liquid phase. The liquid phase was filtered using a 0.2 μm syringe filter (Millipore Millex-LG, PTFE) to remove the remaining solid particles. The amount of solubilized LUT in the supernatant was diluted with a mobile phase composed of methanol and 0.2% phosphoric acid aqueous solution (55:45, v/v) [38]. A fixed amount of LUT was added to methanol to prepare the stock of standard solution (1 mg/mL). The stock standard solution was diluted with the mobile phase.

The concentration of LUT in aqueous PEEP-ILs solution was determined by using the HPLC method according to a previous report with slight modifications [38]. The previously described HPLC system with Inertsil ODS-3 column was used. The mobile phase was used at a flow rate of 1.0 mL/min. The column temperature was set at 30 °C, and the injection volume was 10 μL. A linear calibration curve was established within the range 5 μg/mL to 40.0 μg/mL (correlation coefficient, $R^2 = 0.9999$) for the analysis of LUT in different PEEP-ILs. The solubility of LUT in different aqueous PEEP-IL solutions was measured at 350 nm [38].

2.2.12 Biocompatibility of PEEP-ILs

The two bacterial strains tested in this study were: *Escherichia coli* (ATCC 25922) and *Staphylococcus aureus subsp. Aureus* (ATCC 6538). The intact vial of microorganisms was activated by rehydrating the entire pellet by Mueller- Hinton (M-H) broth (Sigma-Aldrich, USA). Then the aliquot was aseptically transfer into the M-H agar and incubated the tube at 37°C for 24 hours. Single colony was transferred into M-H broth and cultured 24 hours. Microbial strains were stored at -80°C in cryovial with 30% (v/v) glycerol, and they were subcultured overnight in M-H broth before testing.

A broth microdilution method in flat-bottom polystyrene 96-well microtiter plates (Thermo Fisher Scientific, Roskilde, Denmark) was used to determine the biocompatibility of the PEEP-ILs and LUT on gram-positive *Staphylococcus aureus (S. aureus*) and gram-negative *Escherichia coli* (*E. coli*) by following the previous procedure [39]. 100% DMSO (Sigma-Aldrich) served as a diluent for LUT and the final concentration of DMSO in each well did

not exceed 5%. The bacterial inoculum was cultured overnight and diluted in M-H broth to a McFarland turbidity of 0.5 (1 x 10^8 colony forming unit (CFU)/mL). 188 µL of M-H medium, 10 µL of PEEP-ILs (312 to 40000 µg/mL diluted in water) or LUT (40 to 10000 µg/mL diluted in DMSO) with 2-fold serial dilutions and 2 µL of inoculum suspension were added in each well of microdilution tray. Bacterial suspensions with DMSO were used as control and PEEP-ILs/LUT without bacteria as blank. The trays were incubated at 37°C for 24 hours and OD_{600} was measured using a Microplate Reader (SpectraMax i3x, Molecular Devices, Inc.). MICs were determined twice and in triplicates. An incremental increase approach was also adopted to determine the exact MICs with 500 µg for PEEP-ILs [40].

2.2.13 Food Preservation Test

The food preservation ability of LUT in PEEP-ILs was confirmed on peeled red apple pieces using IL[ProEt][Fer]. Freshly cut apple was immersed in 100% milliQ water (control), 0.5% IL[ProEt][Fer] and 50 µg/mL LUT in 0.5% DMSO, 0.5% ethanol and 0.5% IL[ProEt][Fer] aqueous solution for 10 minutes. All the samples were left in the air and visually observed for up to 120 hours. The experiments were carried out two times, each consisting of three replicates [41].

2.3 Results and Discussion

2.3.1 Screening biocompatible ionic liquids for LUT solubility

One of our objectives was to synthesize biocompatible ILs as food-grade solvents, we focused on anions and cations obtained from natural sources. Furukawa et al. reported that proline and proline ethyl ester ([ProEt]) at >10 mM concentration showed higher relative cell viability in comparison to triethanolamine and choline [42]. Moshikur et al. (2018) found that ethyl ester-based ILs were safer than methyl, propyl, and butyl ester-based ILs [24]. So amino acid ethyl ester as cation may have less cytotoxicity and higher biocompatibility. To synthesize non-toxic and biocompatible ILs, one strategy is to use precursors from biocompatible sources [23]. Phenolic acids are naturally available in fruits and vegetables and, thus, may be biocompatible. In that context, 180 ILs, derived from 20 standard amino acid ethyl esters as cations and nine phenolic acids as anions, were considered for predicting the activity coefficient (gamma) at infinite dilution (γ^{∞}) of LUT in various ILs by COSMO-RS.

In all predictions of the activity coefficient, the cation and anion of an IL were considered as separate molecules with equal molar fractions. The negative $\ln\gamma^{\infty}$ values are presented in Fig. 2.1 to screen the potential LUT solvents. A lower activity coefficient specifies an enhanced affinity between LUT and IL solvent, and a higher γ^{∞} presents unfavorable interactions [43]. Among the cations, proline ethyl ester had a significantly lower activity coefficient with all the anions, thus predicting a higher solubility of LUT in proline ethyl ester-based ILs. Ferulate, p-coumarate, vanillate, and 4-hydroxybenzoate exhibited lower $\ln\gamma^{\infty}$ among the considered anions, thus suggesting higher solubility of LUT. From the COSMO-RS prediction, proline ethyl ester as the cation and 4-hydroxybenzoate, vanillate, p-coumarate, and ferulate as the anions were finally selected to synthesize PEEP-ILs.

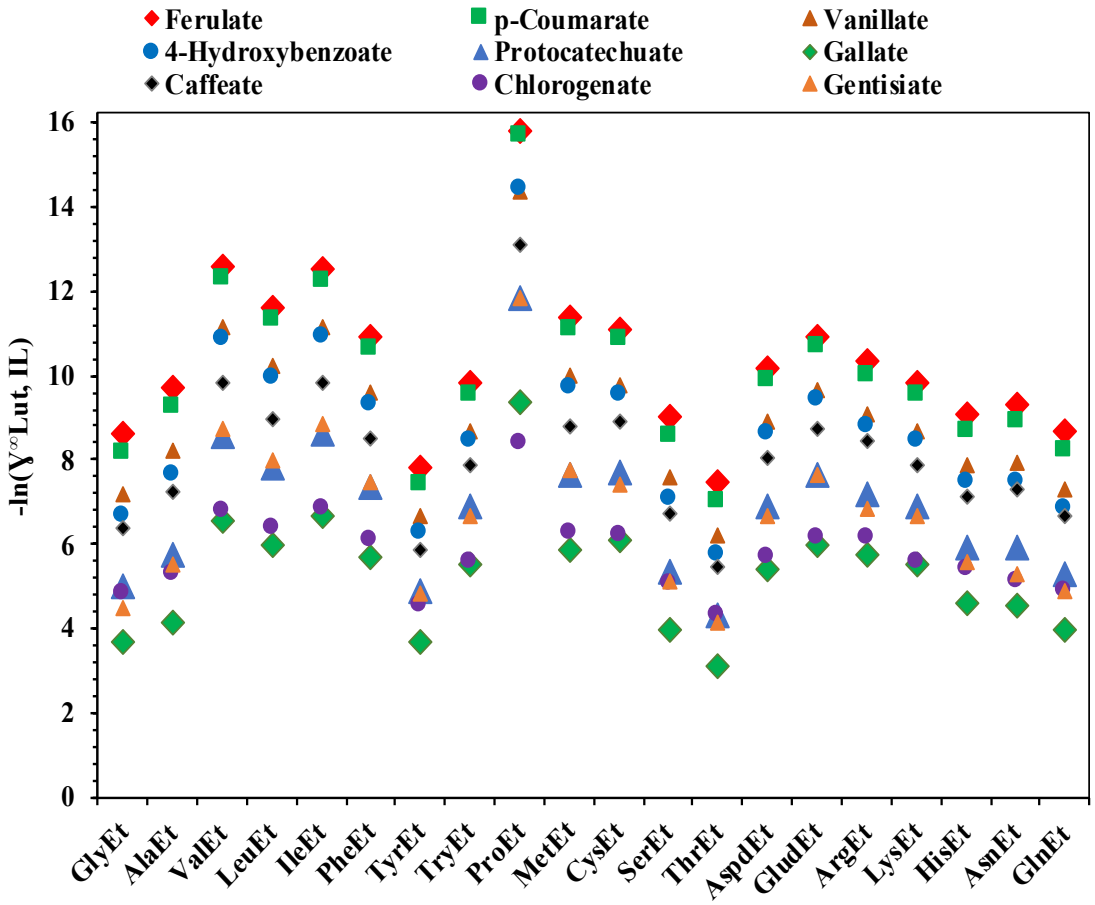

Fig. 2.1. COSMO-RS predictions of logarithmic activity coefficients of LUT at infinite dilution ($-\ln\gamma^{\infty}$) in 180 potential ILs created from 20 standard amino acid ethyl ester cations (full name of cations are given in Table 1.S1) and nine phenolic acids anions at 298 K.

2.3.2 Synthesis and characterization of PEEP-ILs

Based on the predictions of the COSMO-RS analysis, a series of new PEEP-ILs were synthesized by the neutralization of the ProEt cation with four distinct phenolic acids, namely the trans-ferulic, trans-p-coumaric acid, vanillic acid, and 4-hydroxybenzoic acid. The structures of the phenolic acids, proline ethyl ester, LUT, and the synthesized PEEP-ILs are provided in Fig. 2.2. The synthesized ProEt cation was a clear and colorless liquid at RT. All the PEEP-ILs were highly viscous, and the colors of IL[ProEt][Fer], IL[ProEt][Cou], IL[ProEt][Van], and IL[ProEt][Ben] were brown, yellow, deep yellow, and colorless, respectively.

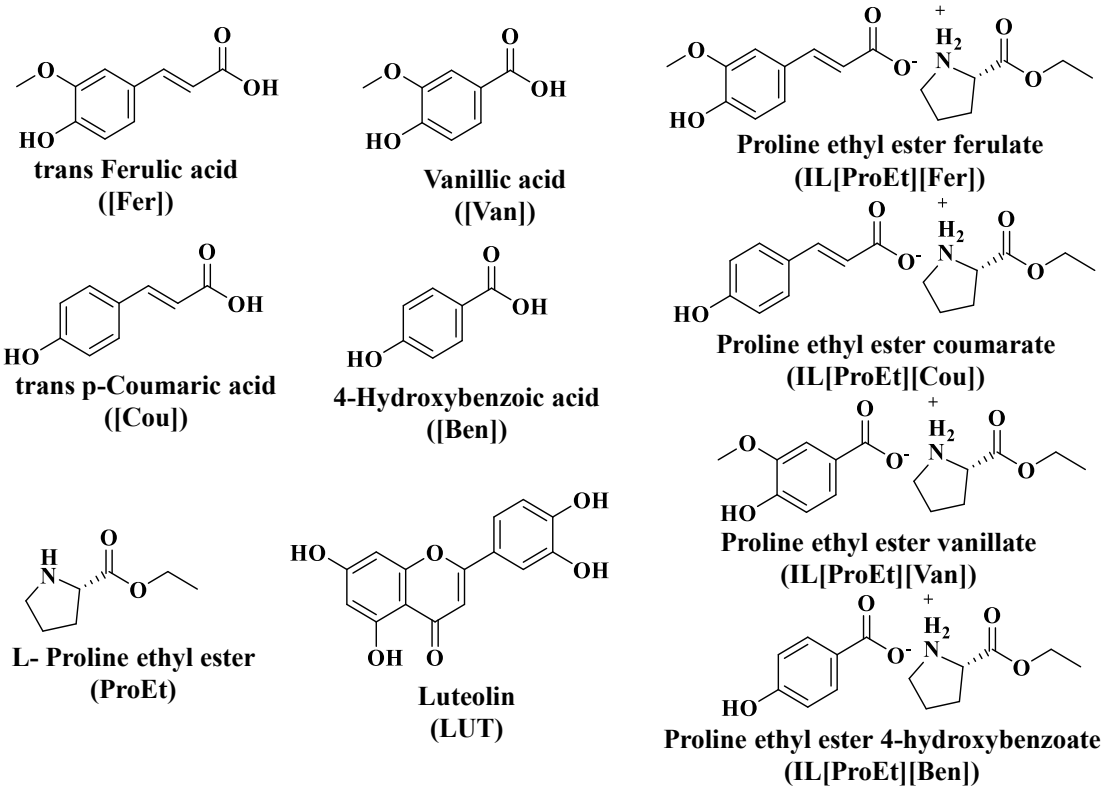

Fig. 2.2. Structures, names, and abbreviations for phenolic acids, proline ethyl ester, LUT and synthesized PEEP-ILs used in this study

All the synthesized PEEP-ILs were obtained in high yields (>98.0%) and with high purities (>93.4%) as determined by ^{1}H NMR and elemental analysis (Data not shown). The ^{1}H NMR measurements confirmed the proton transfer between [ProEt] and the phenolic acid. The protonic peak of the -COOH group in ferulic acid (at about 12.18 ppm in Fig. 2.3B) was not detected and a new peak corresponding to a protonated amine group (-NH_2) was found at 8.30 ppm (i) after the formation of IL[ProEt][Fer] (Fig. 2.3C). The proton of 2-propenoic

group (-CH=C**H**-COOH) in the IL[ProEt][Fer] showed small upfield chemical shift from 6.40 to 6.37 ppm (c). The cationic center (-NH_2) of the cation attracted the electron density of the pyrrolidine group (ring structure of ProEt) and as a result the ^{1}H NMR signals of the corresponding protons in IL[ProEt][Fer] showed upfield chemical shifts from 3.7 to 3.6 ppm (f) and 1.70 to 1.65 ppm (e); 2.1 to 2.0 ppm (e) and 3.1 to 2.9 ppm (e). These chemical shifts indicated that cation and anion was converted into IL. However, the absence of a –COOH peak in all PEEP-ILs indicated the full-ionization by proton transfer between the ProEt cation and the phenolic acids.

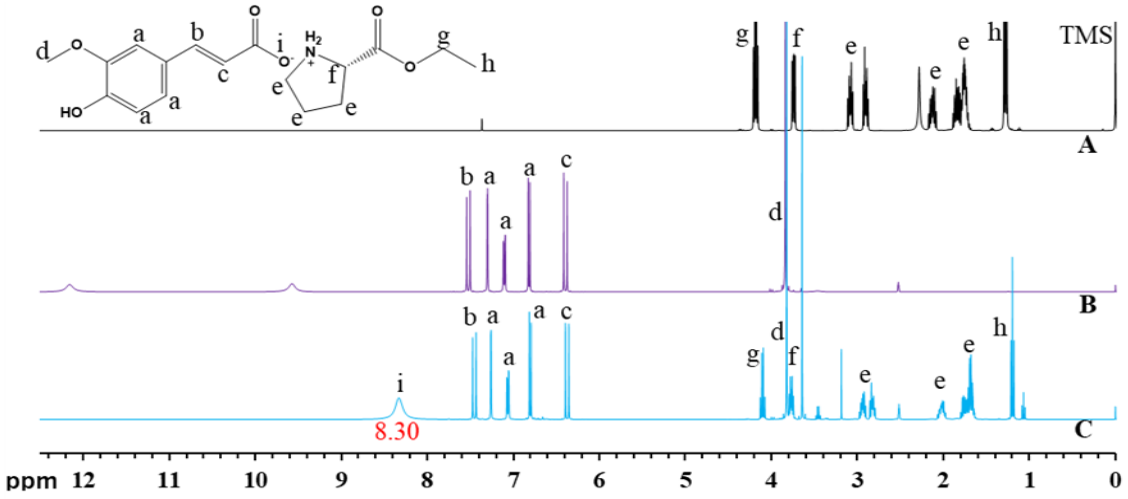

Fig. 2.3. ^{1}H NMR spectra of proline ethyl ester cation (A), free ferulic acid (B), and proline ethyl ester ferulate (IL[ProEt][Fer]) (C).

To further depict the chemical structure of the PEEP-ILs, FT-IR measurements were performed to assess the completion of the neutralization between the phenolic acid anions and the ProEt cation (Fig. 2.4). The C=O stretching peak of the carboxyl groups in ferulic acid was detected at 1661 cm^{-1}, and this peak shifted to 1689 cm^{-1}, corresponding to a C-O stretching band of the carboxylate after IL[ProEt][Fer] formation (Fig. 2.4).

Another characteristic peak was observed at 1728 cm^{-1} for the C=O stretching of the –COOR groups of ProEt, and this peak shifted to 1739 cm^{-1} in the IL[ProEt][Fer] spectrum. For all the PEEP-ILs, the characteristic peak of the -COOH group at 1660~1670 cm^{-1}, as seen in all the phenolic acids, was absent, and a new peak was observed at 1690~1695 cm^{-1}, indicating a strong electrostatic interaction between the -COOH group of the phenolic acid and the -NH_2 group of the ProEt cation. Both the ^{1}H NMR and FT-IR spectrum confirmed the formation of PEEP-ILs.

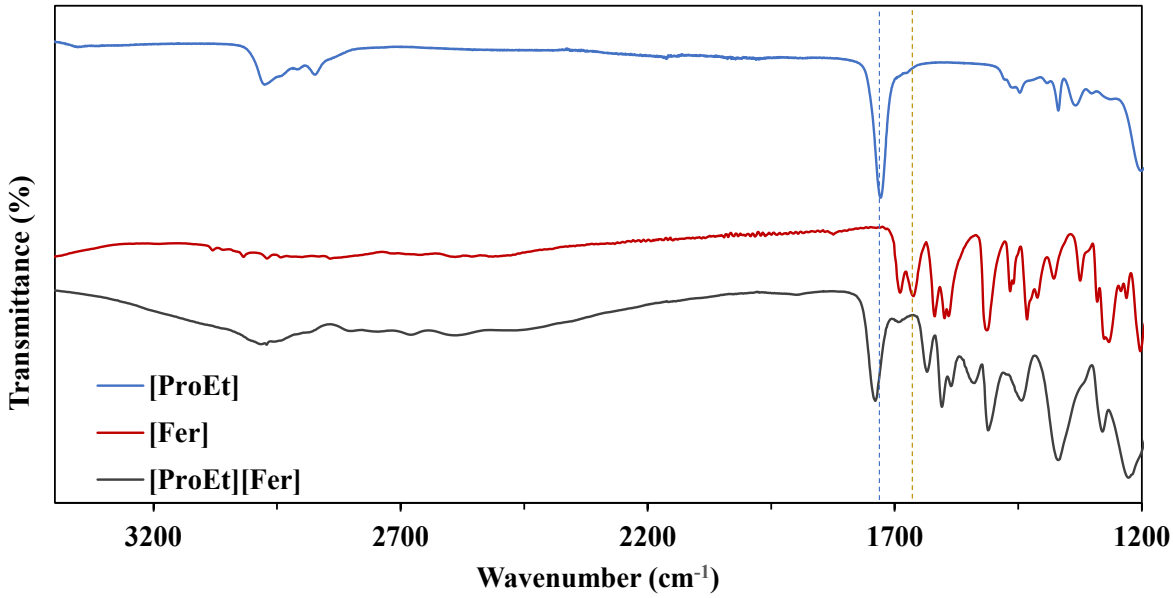

Fig. 2.4. FT-IR spectra of proline ethyl ester cation, free ferulic acid, and proline ethyl ester ferulate IL.

2.3.3 Thermophysical Properties of the PEEP-IL

The thermal stability of the PEEP-ILs was characterized by TGA and DSC to explore possible thermal interactions, such as decomposition temperatures, melting points (T_m), and phase transitions (T_g) between the ProEt cation and the phenolic acids. The TGA thermograms of the PEEP-ILs showed no loss of initial mass on heating up to ~70°C, then a slight loss of mass (for IL[ProEt][Van] 5% and for other PEEP-ILs ~2%) was observed at 70 to 75 °C (Fig. 2.5). This loss of mass may be because of the evaporation of absorbed water molecules or volatile materials. After that, a gradual loss of mass (up to 100%, except for IL[ProEt][Ben]) was observed from 75 °C to 410 °C. The hydroxycinnamic acid-based PEEP-ILs (IL[ProEt][Cou] and IL[ProEt][Fer]) started to decomposed more rapidly than the hydroxybenzoic acid-based PEEP-ILs (IL[ProEt][Ben] and IL[ProEt][Van]) because of the presence the ethylenic bond in the carboxylic group of hydroxycinnamic acid [44]. Total decomposition of IL[ProEt][Ben] did not occur at up to 500 °C, and for IL[ProEt][Cou], it was up to ~410 °C. The methoxy (-OCH_3) group containing PEEP-ILs (IL[ProEt][Fer] and IL[ProEt][Van]) completed their total decomposition at 250 °C to 260 °C, which was much lower than the other two PEEP-ILs (IL[ProEt][Cou] and IL[ProEt][Ben]). This was because the substitution of the hydrogen atom by a methoxy group in the benzene ring of phenolic acid led to rapid decomposition [45]. These findings are in good agreement with those of

previous studies on cholinium based phenolic acids [46]. However, all the PEEP-ILs showed high thermal stability, at least up to 112 °C (Table 2.1). Among all the PEEP-ILs, IL[ProEt][Ben] showed the highest thermal stability, whereas IL[ProEt][Fer] was found to be the least stable because of the presence of the methoxy group and ethylenic bond with the phenolic acid, which leads to a decrease of the thermal stability, in agreement with previous studies [45,47].

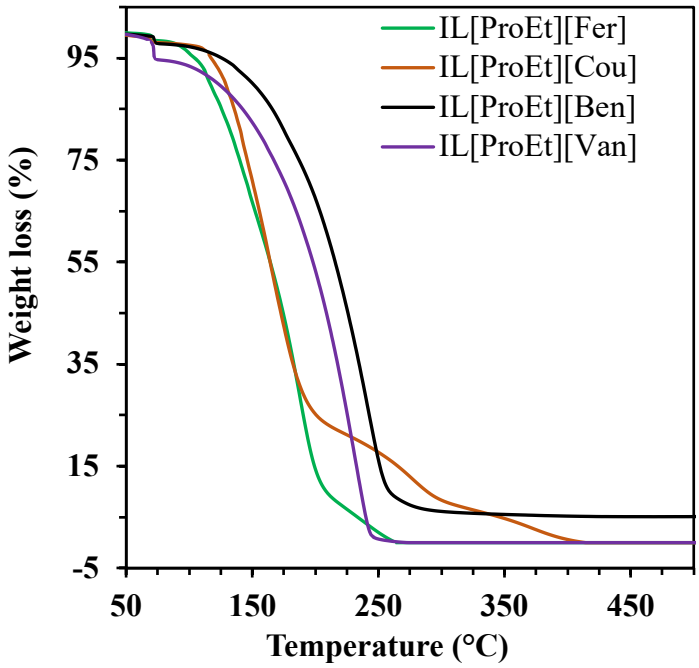

Fig. 2.5. TGA thermograms of the PEEP-ILs were measured under a nitrogen atmosphere from 30 °C to 500 °C with 10 °C/min heating rate.

To explore the phase transition temperatures, including the glass transition (T_g) and the melting point (T_m) temperatures, DSC analysis of the PEEP- ILs was recorded from −50 to 200 °C with a rate of 2 °C/min. Three DSC cycles of each of the PEEP-ILs were recorded because of the variation of temperatures and enthalpies between the freshly melted and reheated samples. The phase transition features (i.e., T_g and T_m) of the synthesized PEEP-ILs mainly depend on the structure of the phenolic acid anions. The T_g values of IL[ProEt][Fer], IL[ProEt][Cou], IL[ProEt][Van], and IL[ProEt][Ben] were found to be 6.6, 1.5, 3.6 and 4.2 °C, respectively, whereas the T_m values were 52.7, 86.4, 110.0, and 127 °C, respectively (Table 2.1). IL[ProEt][Fer] and IL[ProEt][Van] showed comparatively lower melting points than those of IL[ProEt][Cou] and IL[ProEt][Ben] because of the presence of the methoxy group in the benzene ring that leads to a decrease in the melting points of the PEEP-ILs. Similarly, IL[ProEt][Fer] and IL[ProEt][Cou] showed comparatively lower

melting points than those of IL[ProEt][Van] and IL[ProEt][Ben] because of the addition of an ethylenic bond in the alkyl chain of the carboxylic acid group. These results are in good agreement with those of previous studies on cholinium- and other cation-based phenolic acids [44,45,48].

Table 2.1. Thermal behavior of the PEEP-ILs.

PEEP-ILs	**TGA (°C)**		**DSC (°C)**	
	T_{onset}	$T_{peak(50\%)}$	T_g [a]	T_m
IL[ProEt][Fer]	113.6	190.5	6.6	52.7[b]
IL[ProEt][Cou]	116.4	163.9	1.5	86.4 [a]
IL[ProEt][Van]	138.4	234.7	3.6	110.0[b]
IL[ProEt][Ben]	141.5	245.1	4.2	127[b]

T_g and T_m were determined from [a]= first cycle and [b]= second cycle.

2.3.4 Water solubility and partitioning coefficient of the PEEP-ILs

The aqueous solubility of the PEEP-ILs was measured by HPLC to evaluate their solvation properties at RT. As expected, the aqueous solubility of all PEEP-ILs was significantly enhanced compared with the corresponding phenolic acids because of the formation of the IL moieties with the ProEt cation (Table 2.2). A similar trend was observed when the phenolic acids were converted in an ionic form with a cholinium cation [46,47]. However, IL[ProEt][Cou] showed the highest aqueous solubility (821.3 mg/mL, 1039 times higher than that of free p-coumaric acid, 0.79 mg/mL) among the PEEP-ILs, the others followed in this order: IL[ProEt][Cou] > IL[ProEt][Ben] > IL[ProEt][Van] > IL[ProEt][Fer]. The reason for the higher aqueous solubility of IL[ProEt][Cou] might be the absence of a methoxy group (-OCH_3) in the benzene ring, which may reduce the steric hindrance between the formation of a hydrogen bond between the IL and water molecules [1]. The methoxy group containing PEEP-ILs (IL[ProEt][Van] and IL[ProEt][Fer]) showed lower aqueous solubility compared with those of the methoxy group free PEEP-ILs (IL[ProEt][Ben] and IL[ProEt][Cou]), which is in good agreement with data from previous studies [46]. In addition, the hydroxycinnamic acid-based IL[ProEt][Fer] showed lower aqueous solubility than those of the hydroxybenzoic acid-based PEEP-ILs (IL[ProEt][Ben] and IL[ProEt][Van]), because the presence of an ethylenic bond in the carboxylic group of

hydroxycinnamic acid sterically hinders the formation of the hydrogen bonds between the IL and water molecules [1,44]. However, the ProEt containing phenolic acid-based ILs showed considerably higher aqueous solubility than those of cholinium bearing phenolic acid-based ILs. The aqueous solubility of IL[ProEt][Fer] was 3.8-fold higher than that of IL[Cho][Fer] [46]. These findings suggest that the basic counterpart of the phenolic acid-based ILs may have an influence on the overall solubility in water. Moreover, all the PEEP-ILs were freely soluble (>100 mg/mL) in polar organic solvents (i.e., ethanol, methanol, 1-propanol, 2-propanol, and dimethylsulfoxide) and insoluble (<0.1 mg/mL) in nonpolar solvents (i.e., toluene and cyclohexane), which indicates that all the synthesized ILs were hydrophilic in nature.

Table 2.2. Water solubility and partitioning coefficients of the PEEP-ILs measured by HPLC at RT

PEEP-ILs	**Solubility (mg/mL)**	**log $P_{o/w}$**
IL[ProEt][Fer]	681.62 ± 1.43	-0.341 ± 0.015
Ferulic acid	0.81 ± 0.005	1.46 ± 0.029
IL[ProEt][Cou]	821.29 ± 5.72***	-0.307 ± 0.005^{ns}
p-Coumaric acid	0.79 ± 0.007	1.64 ± 0.042
IL[ProEt][Van]	712.91 ± 3.99^{ns}	-0.364 ± 0.005^{ns}
Vanillic acid	1.59 ± 0.019	1.13 ± 0.022
IL[ProEt][Ben]	781.00 ± 4.73**	-0.309 ± 0.047^{ns}
4-Hydroxyenzoic acid	4.95 ± 0.040	1.15 ± 0.008

Data are shown as the mean ± standard deviation, n =3; ns=non-significant, $^{**}p<0.01$, $^{***}p<0.001$.

The log *P* values of the PEEP-ILs –a key parameter for envisaging the hydrophilicity/ lipophilicity– are also shown in Table 2.2. All the synthesized ILs were hydrophilic in nature, with log *P* ranges from -0.307 to -0.364. Conversion of the corresponding phenolic acids into their ILs form changed their hydrophobic nature into hydrophilic, although no relation was found between the partition coefficients and the structural features on the ILs.

2.3.5 Solubility of LUT in the PEEP-ILs

The drug-solubilizing ability of the PEEP-ILs was evaluated using LUT as a poorly water-soluble bioactive compound. The concentration of LUT in water and in different aqueous

solutions of PEEP-ILs was measured by HPLC with a predetermined standard curve. A set of aqueous PEEP-ILs solutions composed of 10% to 60 % of IL[ProEt][Fer] were prepared. Since all the PEEP-ILs are highly viscous at RT, aqueous solutions of more than 60% IL were too viscous to stir, so this was our maximum loading of the IL. As expected, the solubility of LUT was increased significantly with the concentration of the ILs in the solution (Fig. 2.6A). The solubility of LUT in 10% IL[ProEt][Fer] aqueous solution was found 0.64 mg/mL and was improved 67-fold in 60% IL[ProEt][Fer] solution, thereby showing the importance of the IL for the solubility enhancement of a drug in water. In the 60% PEEP-IL solutions, the solubility of LUT was highest in IL[ProEt][Fer] and lowest in IL[ProEt][Ben] (Fig. 2.6B).

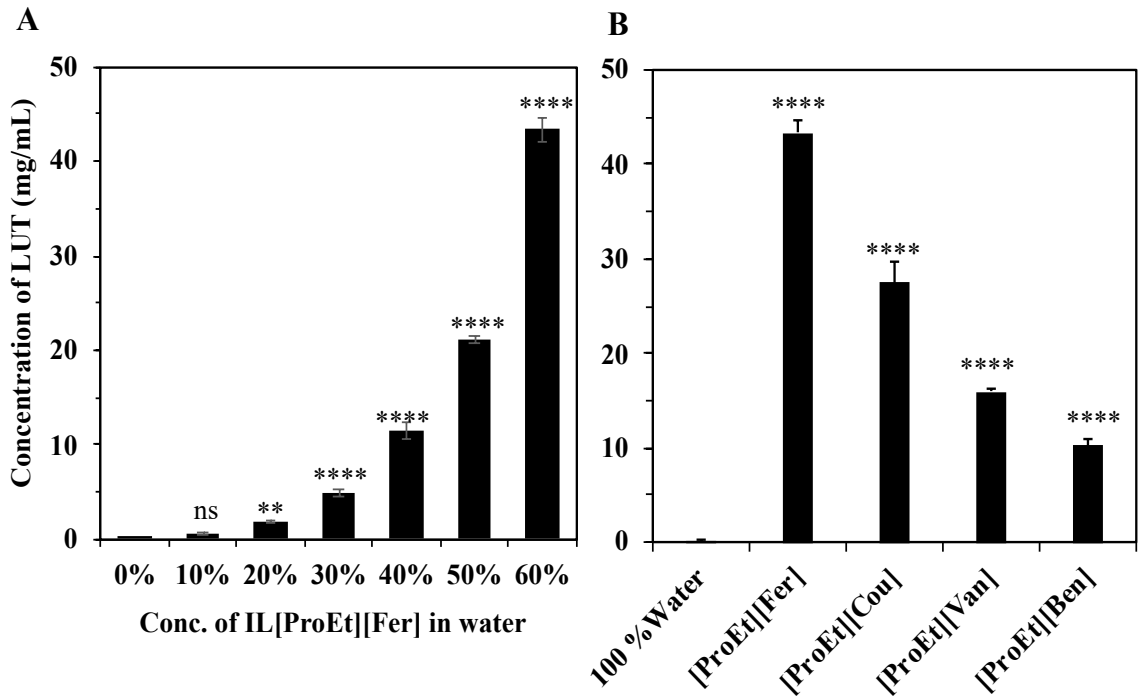

Fig. 2.6. Experimental solubility of LUT determined by HPLC analysis in A) different concentrations of IL[ProEt][Fer] and B) different 60% PEEP-ILs aqueous solvents at RT. Data are shown as the mean ± standard deviation, n =3; ns=non-significant, $^{**}p<0.01$, $^{****}p<0.0001$.

Interestingly, the solubility of LUT in solutions of IL[ProEt][Fer], IL[ProEt][Cou], IL[ProEt][Van], and IL[ProEt][Ben] was significantly enhanced by 879.9-, 557.7-, 323.2- and 207.4-fold, compared with that in water (0.049 mg/mL), respectively. Among the 60% IL-containing solutions, the IL[ProEt][Fer]-containing solution showed the highest LUT solubility, which was 4.2-, 2.7- and 1.5-fold higher than the IL[ProEt][Ben], IL[ProEt][Van] and IL[ProEt][Cou]-containing solutions, respectively. The reason for the higher solubility

of LUT in 60% IL[ProEt][Fer]-containing solution might be the presence of the methoxy group (-OCH_3) in the benzene ring and an addition of an ethylenic bond in the alkyl chain of the carboxylic group that leads to a strong intermolecular interaction between the LUT and IL, resulting in improved LUT dissolution [44,45]. Similarly, the hydroxycinnamic acid-based IL-containing solutions showed higher solubility of LUT than the hydroxybenzoic acid-based IL solutions, regardless of a methoxy group on the benzene ring. Although the solubility of LUT in 60% IL[ProEt][Van] and IL[ProEt][Ben] was lower than the other two ILs, it was still significantly higher than nobiletin (another flavonoid) solubility in choline and geranic acid (CAGE) IL (7.2 mg/mL), and comparable to 1-hexyl-3-methylimidazolium tetrafluoroborate (13.24 mg/mL) and 1-butyl-3-methylimidazolium tetrafluoroborate (13.64 mg/mL) [18,19].

2.3.6 Dissolution Mechanism

The solubilization mechanism of LUT in PEEP-ILs was investigated using experimental data and COSMO-RS predictions. Generally, ILs with high polarity can act as either an H-bond donor or acceptor, and so they have high dissolving power to break inter- and intramolecular H-bonds [32]. The sigma (σ) potential of LUT and the sigma (σ) profiles of anions and LUT can explain their intermolecular interaction between LUT and the ILs (Fig. 2.7). The σ potentials and the σ profiles are divided into three different regions: hydrogen bond donor region ($\sigma < -1$ e/Å^2), nonpolar region ($-1 < \sigma < 1$ e/Å^2), and hydrogen bond acceptor region ($\sigma > 1$ e/Å^2). A negative chemical potential on the σ potential represents more attractive interactions between molecules while the positive chemical potential denotes a repulsive interaction [43].

The σ potential of LUT indicates favorable interactions with hydrogen bond acceptor and donor regions and slight interactions with nonpolar regions (Fig. 2.7A). The σ profiles of anions were characterized by peaks in three regions (Fig. 2.7B). Among the studied IL anions, ferulate, p-coumarate, vanillate, and 4-hydroxybenzoate showed similar peaks in both the hydrogen bond donor and acceptor regions, while differences were observed in the nonpolar region. It showed that ferulate had the highest peak in the nonpolar region among the anions, which may favor the nonpolar-nonpolar interaction between LUT and thus displayed the highest solubility. The solubility trends of the anion series agree with the experimental solubility.

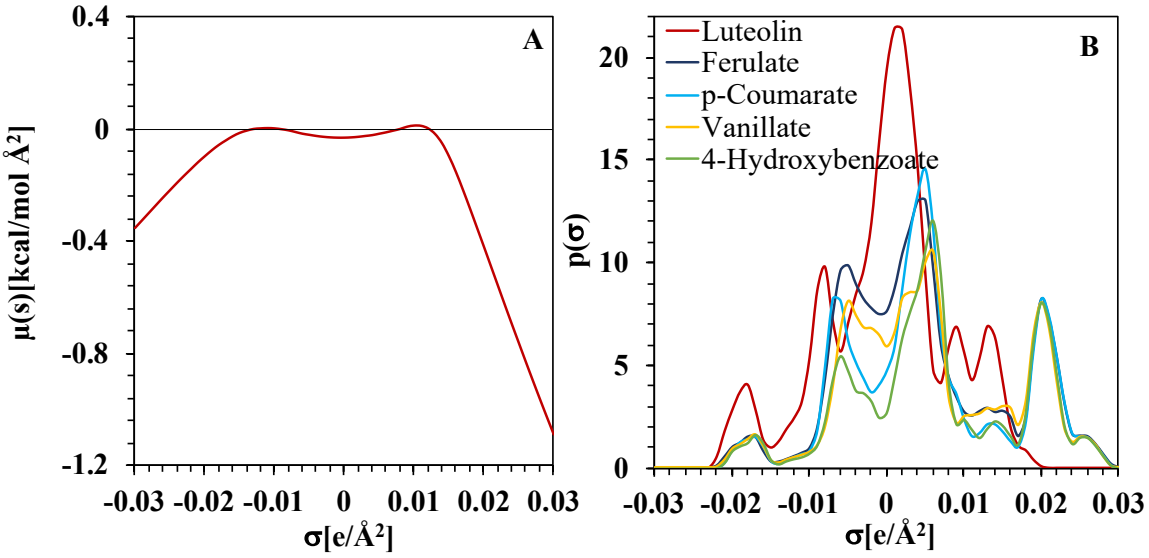

Fig. 2.7. COSMO-RS predicted sigma (σ) potential of LUT (A) and sigma (σ) profiles of LUT and anions (B)

An ^{1}H NMR study was conducted by analyzing the spectrum of free LUT, IL-water solution, and LUT-containing IL-water solution, as shown in Fig. 2.8. The characteristic peaks of the hydroxyl groups in the free LUT were observed in the region of 9.30 to 11.0 ppm, which were absent in the spectrum of the LUT-containing IL-water solution, indicating that there was a hydrogen bonding interaction between the LUT molecules and the ILs. The hydroxyl groups of the free LUT may interact with the carbonyl groups of the ILs, in which the hydrogen atoms of hydroxyl groups in LUT act as a hydrogen bond donor, and the oxygen atoms of the carbonyl groups of the ILs act as a hydrogen bond acceptor. These multiple hydrogen-bonding interactions between the LUT molecule and ILs may be a driving force for the solubilization of LUT in IL solutions. In addition, the characteristic H peaks of the ethylene and benzene ring of the phenolic acid and NH_2 of the ProEt in the IL-water solution were shifted at 6.80-6.81, 7.07-7.08, 7.25, and 7.43-7.47 ppm from 6.81-6.82, 7.06-7.07, 7.24, and 7.42-7.46 ppm, respectively, when LUT was added into the IL-water solution. The LUT molecule may participate in multiple intermolecular interactions with the IL-water mixture, including hydrogen bonding and π–π interactions between the benzene ring of the ILs and LUT, cation–π interactions between $+NH_2$ group of the cations and the π-electron of the benzene rings in LUT, resulting in the dissolution of LUT in IL-containing aqueous solutions. These results agree well with other studies on the use of fatty acid-based amino acid ester IL to dissolve the hydrophobic drugs ibuprofen, glibenclamide in choline-tryptophan IL, and the use of CAGE to dissolve nobiletin molecules [1,19,21,49].

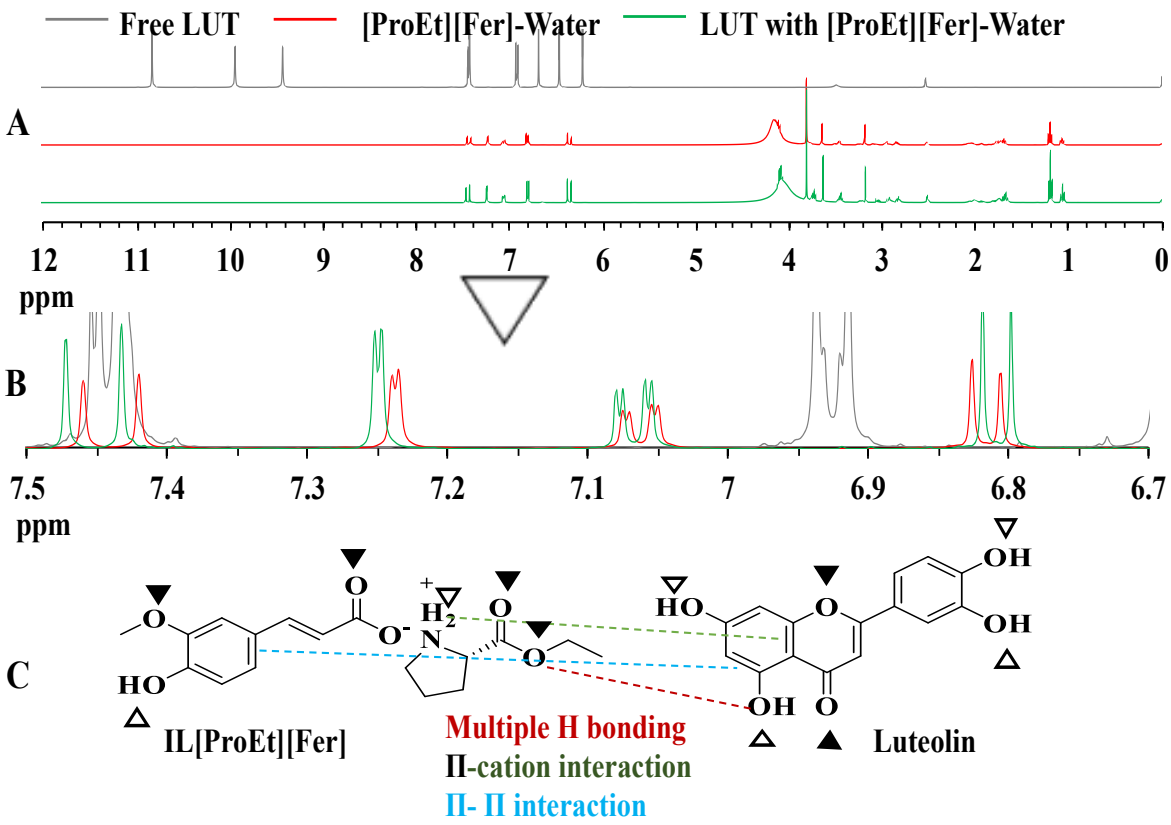

Fig. 2.8. ^{1}H NMR spectra of LUT-IL[ProEt][Fer] complexes as a representative LUT- PEEP ILs mixture. (A) ^{1}H NMR spectra of free LUT, IL[ProEt][Fer]-Water, and LUT with IL[ProEt][Fer]-Water in DMSO-d6, (B) zoomed-in view of the overlapped ^{1}H NMR spectra between 6.7 to 7.5 ppm, (C) possible multiple hydrogen bonding sites between LUT and IL[ProEt][Fer]. The open triangles (Δ) are the possible hydrogen bond donors, and filled triangles (▲) are the possible hydrogen bond acceptors.

2.3.7 Validation of the COSMO-RS prediction with experiment data

The COSMO-RS prediction of LUT solubility was validated by experimentally determining the solubility. The activity coefficient of LUT in 60% PEEP-ILs aqueous solution was compared with the experimental solubility. The correlation coefficient (R^2) was found to be 0.94 from the regression curve. The theoretical solubility was calculated using the equation of regression curves. The percentage average absolute deviation between the theoretical and experimental solubility was also calculated and found to be 10.58%. The obtained deviation is acceptable since 7- 10% average absolute deviation between predicted and experimental values have been reported in previous studies [32,34,50].

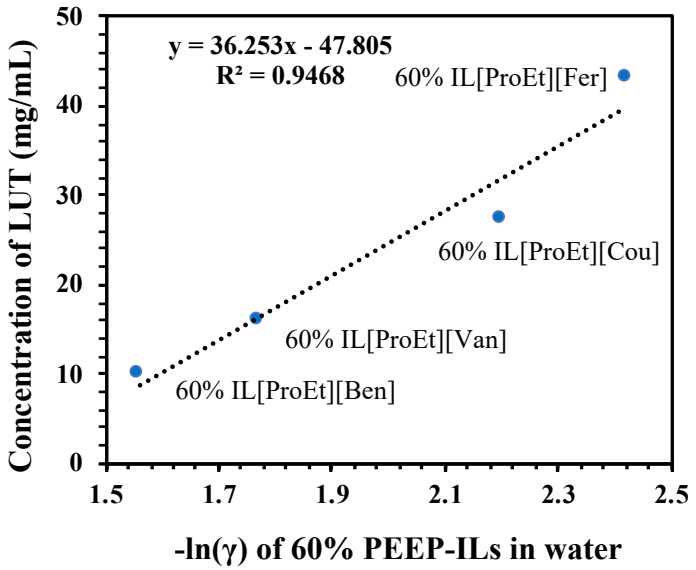

Fig. 2.9. The linear regression curve between COSMO-RS predicted -ln(γ) and the experimental solubility of LUT in PEEP-ILs at 298K.

2.3.8 Biocompatibility of PEEP-ILs

To evaluate the biocompatibility of synthesized PEEP-ILs using ecotoxicity test, the minimum inhibitory concentration (MIC) was determined against gram-positive *S. aureus* and gram-negative *E. coli*. *S. aureus* and *E. coli* are common bacterial strains as indicators in ecotoxicity studies for their short generation time [51]. The potential ecotoxicity of PEEP-ILs against E. coli and S. aureus is summarized in Table 2.3. Generally, the higher the MIC value, the lower the toxicity [52]. IL[ProEt][Fer] and IL[ProEt][Cou] showed the lowest toxicity against both *E. coli* and *S. aureus*, whereas the highest toxicity was found for IL[ProEt][Van]. The MIC values of IL[ProEt][Fer], IL[ProEt][Cou], IL[ProEt][Ban] and IL[ProEt][Van] were 7000, 6000, 6000 and 5000 µg/mL, respectively, against *E. coli*. The MIC values of IL[ProEt][Fer], IL[ProEt][Cou], IL[ProEt][Ban] and IL[ProEt][Van] against *S. aureus* were 7000, 7000, 6500 and 5500 µg/mL, respectively. Interestingly, the toxicity of corresponding phenolic acids was significantly reduced after the formation of PEEP-ILs. It has been reported the MIC value of free vanillic acid and free p-coumaric acid against *E. coli* ATCC 25922 was 750 µg/mL and against *S. aureus* ATCC 6538 was 1000 and 1500 µg/mL, respectively, which are higher toxic, compared with the corresponding ProEt-based ILs [39]. The fully dissociations of phenolate anions in ILs probably reduced the toxicity of ILs, compared with free acids [53]. The MIC of PEEP-ILs were significantly higher than some of conventional imidazolium, pyridinium, pyrrolidinium, piperidinium and

morpholinium based ILs (Table 2.3) which indicated low toxicity of PEEP-ILs. The result showed that all the synthesized PEEP-ILs were relatively harmless (>1000 μg/mL) [54].

Table 2.3. Minimum inhibitory concentration (MIC) of PEEP-ILs against *S. aureus* and *E. coli,* μg/mL.

Name of PEEP-ILs	MIC (μg/mL)	
	E. coli	***S. aureus***
IL[ProEt][Fer]	7000	7000
IL[ProEt][Cou]	6000	7000
IL[ProEt][Van]	5000	5500
IL[ProEt][Ben]	6000	6500
3-dodecyl-1-methylimidazolium bromide [55]	20	2.5
N-dodecyl-N-methylpyrrolidinium bromide [55]	80	10
N-methyl-N-dodecylpiperidinium bromide [55]	40	5
N-dodecyl-N-methylmorpholinium bromide [55]	156.2	20
2-methyl-1-(2-phenoxyethyl)pyridinium bromide [54]	32	16
1-(2-phenoxyethyl)pyridazin-1-ium bromide [54]	32	64

2.3.9 Food Preservation Test

The food preservation ability of the LUT on peeled red apple pieces [56] using IL[ProEt][Fer] was observed for up to 120 hours. It was apparent that the sample (apple piece) in 50 μg/mL LUT in 0.5% IL[ProEt][Fer] aqueous solution looked fresher than the control (milliQ water) and the samples in 50 μg/mL LUT in 0.5% DMSO, 50 μg/mL LUT in 0.5% ethanol, and 0.5% IL[ProEt][Fer] aqueous solution probably because of the decreased enzymatic activity, air-oxidation, and microbial activity (Fig. 2.10). The unwanted browning reaction that occurs in fruits and vegetables by tyrosinase blight their organoleptic properties. LUT as a tyrosinase inhibitor can inhibit undesirable enzymatic browning by reversible noncompetitive inhibition and also have whitening effects on the skin [57]. Here LUT with IL[ProEt][Fer] aqueous solution maintained better organoleptic properties of the red apple slices, possibly by preventing or slowing down the microbial growth and the enzymatic reaction. A recent study of LUT application in sweet cherry showed that 100- 200 μg/mL LUT improved the organoleptic quality by reducing the

incidence of postharvest decay, namely weight loss, soluble solid content, and titratable acids. LUT also improved the antioxidative capacity by activating the phenylpropanoid metabolic pathway and demonstrated inhibitory effects on fungal growth [41]. Thus, this result indicated the applicability of the LUT in food preservation.

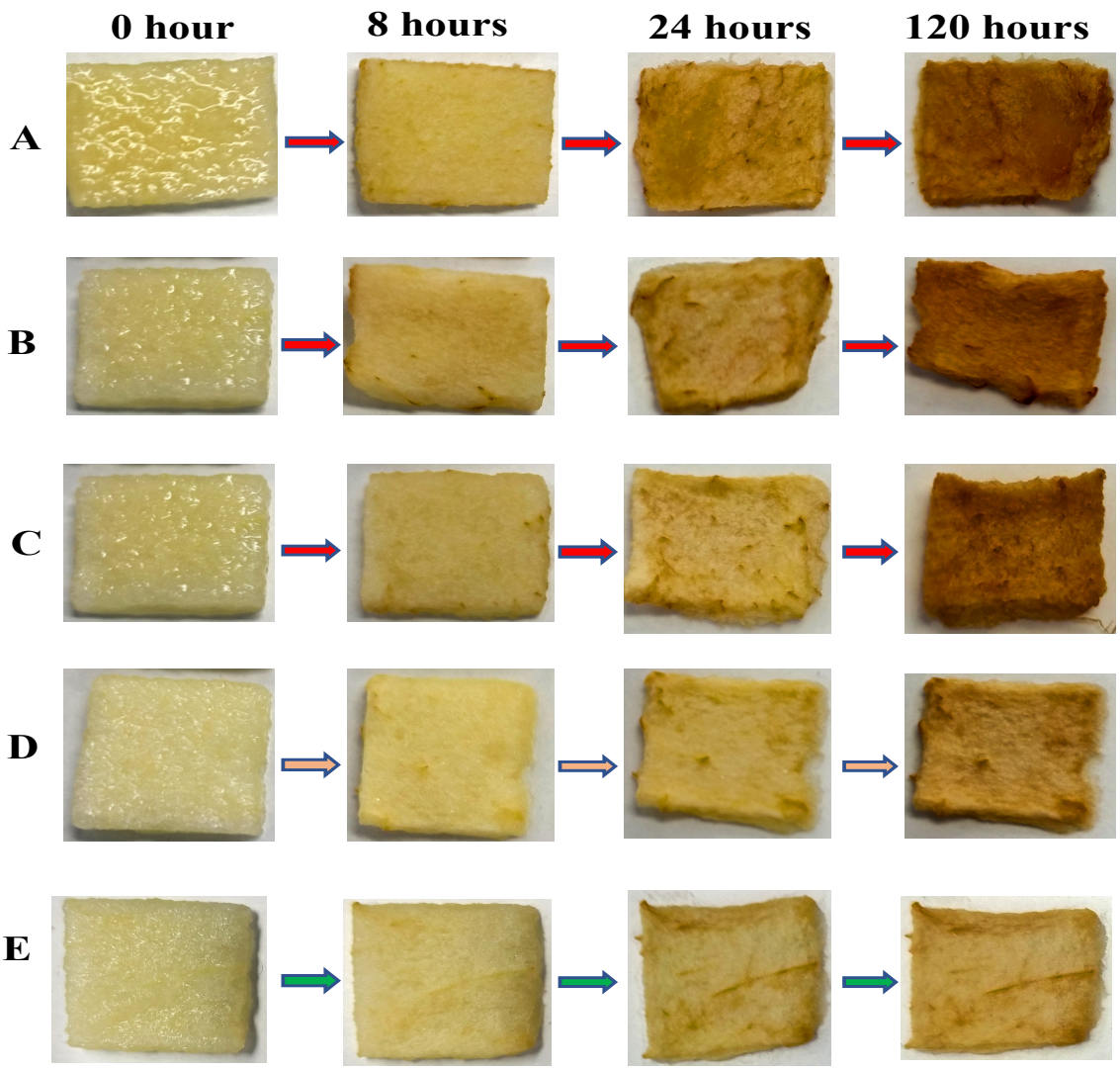

Fig. 2.10. Food preservation test of LUT on peeled red apple piece immersed for 10 minutes in A) Control (MilliQ water), B) 50 µg/mL LUT in 0.5% DMSO, C) 50 µg/mL LUT in 0.5% ethanol, D) 0.5% IL[ProEt][Fer], and E) 50 µg/mL LUT in 0.5% IL[ProEt][Fer].

2.4 Conclusion

COSMO-RS was used to screen the potential ILs for predicting LUT solubility. Four PEEP-ILs were synthesized by simple neutralization of proline ethyl ester with bioactive phenolic acids (trans-ferulic, vanillic, trans-p-coumaric, and 4-hydroxybenzoic acid), and their

physico-thermal properties were investigated. All the PEEP-ILs were viscous at RT with high yields (>98.0%) and purities (>93.4%). Characterization studies (including NMR, FT-IR, elemental analysis, DSC, and TGA) demonstrated the successful synthesis of PEEP-ILs with excellent thermal stabilities. The solubility of LUT in aqueous ILs was evaluated, and proline ethyl ester ferulate was found to be the best solubilizer of LUT. Multiple hydrogen bonding, π–π interactions, and cation–π interactions between LUT and ILs were the characteristic mechanism of solubility. An ecotoxicity test indicated PEEP-ILs as green solvents were relatively harmless. LUT in PEEP-ILs demonstrated superior organoleptic properties on red apple slices. These results indicated that the synthesized PEEP-ILs could be used as a potential solvent to apply poorly soluble phytochemicals to food. However, further work is required to apply phytochemicals through ILs in the food industry.

2.5 References

[1] R. Md Moshikur, M.R. Chowdhury, H. Fujisawa, R. Wakabayashi, M. Moniruzzaman, M. Goto, Design and Characterization of Fatty Acid-Based Amino Acid Ester as a New “green” Hydrophobic Ionic Liquid for Drug Delivery, ACS Sustain. Chem. Eng. 8 (2020) 13660–13671. https://doi.org/10.1021/acssuschemeng.0c03419.

[2] N.A. Ahmad, K. Jumbri, A. Ramli, N.A. Ghani, H. Ahmad, M.A. Kassim, Synthesis, characterisation and antioxidant properties of ferulate-based protic ionic liquids: Experimental and modelling approaches, J. Mol. Liq. 278 (2019) 309–319. https://doi.org/10.1016/j.molliq.2019.01.048.

[3] K. Paduszyński, An overview of the performance of the COSMO-RS approach in predicting the activity coefficients of molecular solutes in ionic liquids and derived properties at infinite dilution, Phys. Chem. Chem. Phys. 19 (2017) 11835–11850. https://doi.org/10.1039/c7cp00226b.

[4] M.R. Chowdhury, R.M. Moshikur, R. Wakabayashi, Y. Tahara, N. Kamiya, M. Moniruzzaman, M. Goto, Development of a novel ionic liquid-curcumin complex to enhance its solubility, stability, and activity, Chem. Commun. 55 (2019) 7737–7740. https://doi.org/10.1039/c9cc02812a.

[5] N. Alsaud, K. Shahbaz, M. Farid, Application of deep eutectic solvents in the

extraction of polyphenolic antioxidants from New Zealand Manuka leaves (Leptospermum Scoparium): Optimization and antioxidant activity, J. Mol. Liq. 337 (2021) 116385. https://doi.org/10.1016/j.molliq.2021.116385.

[6] S.M. Vilas-Boas, P. Brandão, M.A.R. Martins, L.P. Silva, T.B. Schreiner, L. Fernandes, O. Ferreira, S.P. Pinho, Solubility and solid phase studies of isomeric phenolic acids in pure solvents, J. Mol. Liq. 272 (2018) 1048–1057. https://doi.org/10.1016/j.molliq.2018.10.108.

[7] X. Fan, H. Ngo, C. Wu, Natural and Bio-based Antimicrobials: A Review, ACS Symp. Ser. 1287 (2018) 1–24. https://doi.org/10.1021/bk-2018-1287.ch001.

[8] C. Marrassini, A. Idrissi, I. De Waele, K. Smail, N. Tchouar, M. Moreau, A. Mezzetti, Organic solvent-luteolin interactions studied by FT-Raman, Vis-Raman, UV-Raman spectroscopy and DFT calculations, J. Mol. Liq. 205 (2015) 2–8. https://doi.org/10.1016/j.molliq.2014.08.014.

[9] K.W. Choy, D. Murugan, X.F. Leong, R. Abas, A. Alias, M.R. Mustafa, Flavonoids as natural anti-inflammatory agents targeting nuclear factor-kappa B (NFκB) signaling in cardiovascular diseases: A mini review, Front. Pharmacol. 10 (2019) 1–8. https://doi.org/10.3389/fphar.2019.01295.

[10] W. Qian, M. Liu, Y. Fu, J. Zhang, W. Liu, J. Li, X. Li, Y. Li, T. Wang, Antimicrobial mechanism of luteolin against Staphylococcus aureus and Listeria monocytogenes and its antibiofilm properties, Microb. Pathog. 142 (2020) 104056. https://doi.org/10.1016/j.micpath.2020.104056.

[11] K. Rashed, A. Ćirić, J. Glamočlija, M. Soković, Antibacterial and antifungal activities of methanol extract and phenolic compounds from Diospyros virginiana L., Ind. Crops Prod. 59 (2014) 210–215. https://doi.org/10.1016/j.indcrop.2014.05.021.

[12] J.N. Pedersen, S. Liu, Y. Zhou, T. Balle, X. Xu, Z. Guo, Synergistic effects of binary ionic liquid-solvent systems on enzymatic esterification of esculin, Food Chem. 310 (2020) 125858. https://doi.org/10.1016/j.foodchem.2019.125858.

[13] W. Qing, Y. Wang, H. Li, F. Ma, J. Zhu, X. Liu, Preparation and Characterization of Copolymer Micelles for the Solubilization and In Vitro Release of Luteolin and

Luteoloside, AAPS PharmSciTech. 18 (2017) 2095–2101. https://doi.org/10.1208/s12249-016-0692-y.

[14] F. Shakeel, N. Haq, S. Alshehri, M.A. Ibrahim, E.M. Elzayat, M.A. Altamimi, K. Mohsin, F.K. Alanazi, I.A. Alsarra, Solubility, thermodynamic properties and solute-solvent molecular interactions of luteolin in various pure solvents, J. Mol. Liq. 255 (2018) 43–50. https://doi.org/10.1016/j.molliq.2018.01.155.

[15] L. Wang, C. Zhong, Y. Zu, X. Zhao, Y. Deng, W. Wu, X. Sun, L. Wang, M. Wu, Preparation and characterization of luteolin nanoparticles for enhance bioavailability and inhibit liver microsomal peroxidation in rats, J. Funct. Foods. 55 (2019) 57–64. https://doi.org/10.1016/j.jff.2019.01.054.

[16] S. Alshehri, S.S. Imam, M.A. Altamimi, M. Jafar, M.Z. Hassan, A. Hussain, A. Ahad, W. Mahdi, Host-guest complex of β-cyclodextrin and pluronic F127 with Luteolin: Physicochemical characterization, anti-oxidant activity and molecular modeling studies, J. Drug Deliv. Sci. Technol. 55 (2020) 101356. https://doi.org/10.1016/j.jddst.2019.101356.

[17] Z. Guo, B.M. Lue, K. Thomasen, A.S. Meyer, X. Xu, Predictions of flavonoid solubility in ionic liquids by COSMO-RS: Experimental verification, structural elucidation, and solvation characterization, Green Chem. 9 (2007) 1362–1373. https://doi.org/10.1039/b709786g.

[18] K. Yang, Y. Song, L. Ge, J. Su, Y. Wen, Y. Long, Measurement and correlation of the solubilities of luteolin and rutin in five imidazole-based ionic liquids, Fluid Phase Equilib. 344 (2013) 27–31. https://doi.org/10.1016/j.fluid.2013.01.026.

[19] T. Hattori, H. Tagawa, M. Inai, T. Kan, S.-I. Kimura, S. Itai, S. Mitragotri, Y. Iwao, transdermal delivery of nobiletin using ionic liquids, Sci. RepoRtS |. 9 (2019) 20191. https://doi.org/10.1038/s41598-019-56731-1.

[20] A. Tarannum, N.P. Lobo, J.R. Rao, N.N. Fathima, Are aqueous solutions of choline-based ionic liquid biocompatible cross-linkers for collagen?, J. Mol. Liq. 303 (2020). https://doi.org/10.1016/j.molliq.2020.112654.

[21] M.A. Alawi, I.I. Hamdan, Als.A. Sallam, N.A. Heshmeh, Solubility enhancement of

glibenclamide in choline-tryptophan ionic liquid: Preparation, characterization and mechanism of solubilization, J. Mol. Liq. 212 (2015) 629–634. https://doi.org/10.1016/j.molliq.2015.10.006.

[22] M. Guncheva, P. Ossowicz, E. Janus, S. Todinova, D. Yancheva, Elucidation of the effect of some cholinium amino acid ionic liquids on the thermal and the conformational stability of insulin, J. Mol. Liq. 283 (2019) 257–262. https://doi.org/10.1016/j.molliq.2019.03.074.

[23] R. Md Moshikur, M.R. Chowdhury, M. Moniruzzaman, M. Goto, Biocompatible ionic liquids and their applications in pharmaceutics, Green Chem. 22 (2020) 8116–8139. https://doi.org/10.1039/d0gc02387f.

[24] R.M. Moshikur, M.R. Chowdhury, R. Wakabayashi, Y. Tahara, M. Moniruzzaman, M. Goto, Characterization and cytotoxicity evaluation of biocompatible amino acid esters used to convert salicylic acid into ionic liquids, Int. J. Pharm. 546 (2018) 31–38. https://doi.org/10.1016/j.ijpharm.2018.05.021.

[25] Z. Lei, J. Zhang, Q. Li, B. Chen, UNIFAC model for ionic liquids, Ind. Eng. Chem. Res. 48 (2009) 2697–2704. https://doi.org/10.1021/ie801496e.

[26] S. Gracin, T. Brinck, Å.C. Rasmuson, Prediction of solubility of solid organic compounds in solvents by UNIFAC, Ind. Eng. Chem. Res. 41 (2002) 5114–5124. https://doi.org/10.1021/ie011014w.

[27] Z. Song, H. Shi, X. Zhang, T. Zhou, Prediction of CO2 solubility in ionic liquids using machine learning methods, Chem. Eng. Sci. 223 (2020) 115752. https://doi.org/10.1016/j.ces.2020.115752.

[28] F. Yusuf, T. Olayiwola, C. Afagwu, Application of Artificial Intelligence-based predictive methods in Ionic liquid studies: A review, Fluid Phase Equilib. 531 (2021) 112898. https://doi.org/10.1016/j.fluid.2020.112898.

[29] A. Benazzouz, L. Moity, C. Pierlot, V. Molinier, J.M. Aubry, Hansen approach versus COSMO-RS for predicting the solubility of an organic UV filter in cosmetic solvents, Colloids Surfaces A Physicochem. Eng. Asp. 458 (2014) 101–109. https://doi.org/10.1016/j.colsurfa.2014.03.065.

[30] K. Paduszyński, F. Yusuf, T. Olayiwola, C. Afagwu, A. Benazzouz, L. Moity, C. Pierlot, V. Molinier, J.M. Aubry, Z. Song, H. Shi, X. Zhang, T. Zhou, S. Gracin, T. Brinck, Å.C. Rasmuson, P.R. Duchowicz, E.A. Castro, A.A. Lapkin, M. Peters, L. Greiner, S. Chemat, K. Leonhard, M.A. Liauw, W. Leitner, Z. Lei, J. Zhang, Q. Li, B. Chen, QSPR studies on aqueous solubilities of drug-like compounds, Ind. Eng. Chem. Res. 223 (2009) 115752. https://doi.org/10.1021/ie801496e.

[31] A.A. Lapkin, M. Peters, L. Greiner, S. Chemat, K. Leonhard, M.A. Liauw, W. Leitner, Screening of new solvents for artemisinin extraction process using ab initio methodology, Green Chem. 12 (2010) 241–25. https://doi.org/10.1039/b922001a.

[32] M. Lotfi, M. Moniruzzaman, M. Sivapragasam, S. Kandasamy, M.I. Abdul Mutalib, N.B. Alitheen, M. Goto, Solubility of acyclovir in nontoxic and biodegradable ionic liquids: COSMO-RS prediction and experimental verification, J. Mol. Liq. 243 (2017) 124–131. https://doi.org/10.1016/j.molliq.2017.08.020.

[33] X. Dong, Y. Cao, N. Wang, P. Wang, M. Li, Systematic study on solubility of chrysin in different organic solvents: The synergistic effect of multiple intermolecular interactions on the dissolution process, J. Mol. Liq. 325 (2021) 115180. https://doi.org/10.1016/j.molliq.2020.115180.

[34] H.W. Khan, A.V.B. Reddy, M.M.E. Nasef, M.A. Bustam, M. Goto, M. Moniruzzaman, Screening of ionic liquids for the extraction of biologically active compounds using emulsion liquid membrane: COSMO-RS prediction and experiments, J. Mol. Liq. 309 (2020) 113122. https://doi.org/10.1016/j.molliq.2020.113122.

[35] R.M. Moshikur, M.R. Chowdhury, R. Wakabayashi, Y. Tahara, M. Moniruzzaman, M. Goto, Ionic liquids with methotrexate moieties as a potential anticancer prodrug: Synthesis, characterization and solubility evaluation, J. Mol. Liq. 278 (2019) 226–233. https://doi.org/10.1016/j.molliq.2019.01.063.

[36] M. Luczkiewicz, W. Cisowski, P. Kaiser, R. Ochocka, A. Piotrowski, Comparative analysis of phenolic acids in mistletoe plants from various hosts, Acta Pol. Pharm. - Drug Res. 58 (2001) 373–379.

[37] P. Mattila, J. Kumpulainen, Determination of free and total phenolic acids in plant-derived foods by HPLC with diode-array detection, J. Agric. Food Chem. 50 (2002) 3660–3667. https://doi.org/10.1021/jf020028p.

[38] L.P. Li, H. Di Jiang, Determination and assay validation of luteolin and apigenin in human urine after oral administration of tablet of Chrysanthemum morifolium extract by HPLC, J. Pharm. Biomed. Anal. 41 (2006) 261–265. https://doi.org/10.1016/j.jpba.2005.10.019.

[39] L. Sanhueza, R. Melo, R. Montero, K. Maisey, L. Mendoza, M. Wilkens, Synergistic interactions between phenolic compounds identified in grape pomace extract with antibiotics of different classes against Staphylococcus aureus and Escherichia coli, PLoS One. 12 (2017) 1–15. https://doi.org/10.1371/journal.pone.0172273.

[40] M.U. Amin, M. Khurram, B. Khattak, J. Khan, Antibiotic additive and synergistic action of rutin, morin and quercetin against methicillin resistant Staphylococcus aureus, BMC Complement. Altern. Med. 15 (2015) 1–12. https://doi.org/10.1186/s12906-015-0580-0.

[41] X. Liu, X. Cui, D. Ji, Z. Zhang, B. Li, Y. Xu, T. Chen, S. Tian, Luteolin-induced activation of the phenylpropanoid metabolic pathway contributes to quality maintenance and disease resistance of sweet cherry, Food Chem. 342 (2021) 128309. https://doi.org/10.1016/j.foodchem.2020.128309.

[42] S.Y. Furukawa, G. Hattori, S. Sakai, N. Kamiya, Highly efficient and low toxic skin penetrants composed of amino acid ionic liquids, RSC Adv. 6 (2016) 87753–87755. https://doi.org/10.1039/c6ra16926k.

[43] L.F. Lepre, S. Sabelle, F. Beaumard, A. Detroyer, M.-C. Frantz, A. Padua, M.C. Gomes, Screening Ionic Solvents for Enhancing the Solubility of Water-Insoluble Natural Dyes, Ind. Eng. Chem. Res. 60 (2021) 8555–8564. https://doi.org/10.1021/acs.iecr.1c00785.

[44] A. Xu, L. Chen, X. Xu, Z. Xiao, R. Liu, R. Gao, M. Yuan, L. Zhang, Recyclable choline nicotinate and ferulate aqueous solutions as efficient lignin solvents, Polymers (Basel). 10 (2018) 1–10. https://doi.org/10.3390/polym10080840.

[45] N.A. Ahmad, K. Jumbri, A. Ramli, H. Ahmad, M.B.A. Rahman, R.A. Wahab, Design and molecular modelling of phenolic-based protic ionic liquids, J. Mol. Liq. 308 (2020). https://doi.org/10.1016/j.molliq.2020.113062.

[46] M. Demurtas, V. Onnis, P. Zucca, A. Rescigno, J.I. Lachowicz, L. De Villiers Engelbrecht, M. Nieddu, G. Ennas, A. Scano, F. Mocci, F. Cesare Marincola, Cholinium-Based Ionic Liquids from Hydroxycinnamic Acids as New Promising Bioactive Agents: A Combined Experimental and Theoretical Investigation, ACS Sustain. Chem. Eng. 9 (2021) 2975–2986. https://doi.org/10.1021/acssuschemeng.1c00090.

[47] T.E. Sintra, A. Luís, S.N. Rocha, A.I.M.C.L. Ferreira, F. Gonçalves, L.M.N.B.F. Santos, B.M. Neves, M.G. Freire, S.P.M. Ventura, J.A.P. Coutinho, Enhancing the antioxidant characteristics of phenolic acids by their conversion into cholinium salts, ACS Sustain. Chem. Eng. 3 (2015) 2558–2565. https://doi.org/10.1021/acssuschemeng.5b00751.

[48] S. Hayouni, A. Robert, N. Ferlin, H. Amri, S. Bouquillon, New biobased tetrabutylphosphonium ionic liquids: Synthesis, characterization and use as a solvent or co-solvent for mild and greener Pd-catalyzed hydrogenation processes, RSC Adv. 6 (2016) 113583–113595. https://doi.org/10.1039/c6ra23056c.

[49] M.K. Ali, R.M. Moshikur, R. Wakabayashi, M. Moniruzzaman, M. Goto, Biocompatible Ionic Liquid-Mediated Micelles for Enhanced Transdermal Delivery of Paclitaxel, ACS Appl. Mater. Interfaces. 13 (2021) 19745–19755. https://doi.org/10.1021/acsami.1c03111.

[50] R. Anantharaj, T. Banerjee, COSMO-RS based predictions for the desulphurization of diesel oil using ionic liquids: Effect of cation and anion combination, Fuel Process. Technol. 92 (2011) 39–52. https://doi.org/10.1016/j.fuproc.2010.08.018.

[51] M. Sivapragasam, J.R. Jaganathan, J.M. Levêque, M. Moniruzzaman, M.I. Abdul Mutalib, Microbial biocompatibility of phosphonium- and ammonium-based ionic liquids, J. Mol. Liq. 273 (2019) 107–115. https://doi.org/10.1016/j.molliq.2018.10.022.

[52] A. Yazdani, M. Sivapragasam, J.M. Leveque, M. Moniruzzaman, Microbial Biocompatibility and Biodegradability of Choline-Amino Acid Based Ionic Liquids, J. Microb. Biochem. Technol. 08 (2016) 415–421. https://doi.org/10.4172/1948-5948.1000318.

[53] A. Pernin, L. Guillier, F. Dubois-Brissonnet, Inhibitory activity of phenolic acids against Listeria monocytogenes: Deciphering the mechanisms of action using three different models, Food Microbiol. 80 (2019) 18–24. https://doi.org/10.1016/j.fm.2018.12.010.

[54] K.S. Egorova, V.P. Ananikov, Fundamental importance of ionic interactions in the liquid phase: A review of recent studies of ionic liquids in biomedical and pharmaceutical applications, J. Mol. Liq. 272 (2018) 271–300. https://doi.org/10.1016/j.molliq.2018.09.025.

[55] W. Florio, S. Becherini, F. D'Andrea, A. Lupetti, C. Chiappe, L. Guazzelli, Comparative evaluation of antimicrobial activity of different types of ionic liquids, Mater. Sci. Eng. C. 104 (2019) 109907. https://doi.org/10.1016/j.msec.2019.109907.

[56] M.J. Mehta, A. Kumar, Ionic Liquid Assisted Gelatin Films: Green, UV Shielding, Antioxidant, and Antibacterial Food Packaging Materials, ACS Sustain. Chem. Eng. 7 (2019) 8631–8636. https://doi.org/10.1021/acssuschemeng.9b00423.

[57] L. Zhang, X. Zhao, G.J. Tao, J. Chen, Z.P. Zheng, Investigating the inhibitory activity and mechanism differences between norartocarpetin and luteolin for tyrosinase: A combinatory kinetic study and computational simulation analysis, Food Chem. 223 (2017) 40–48. https://doi.org/10.1016/j.foodchem.2016.12.017.

CHAPTER-3: CHOLINE OLEATE BASED MICELLAR SYSTEM AS A NEW APPROACH FOR LUTEOLIN FORMULATION

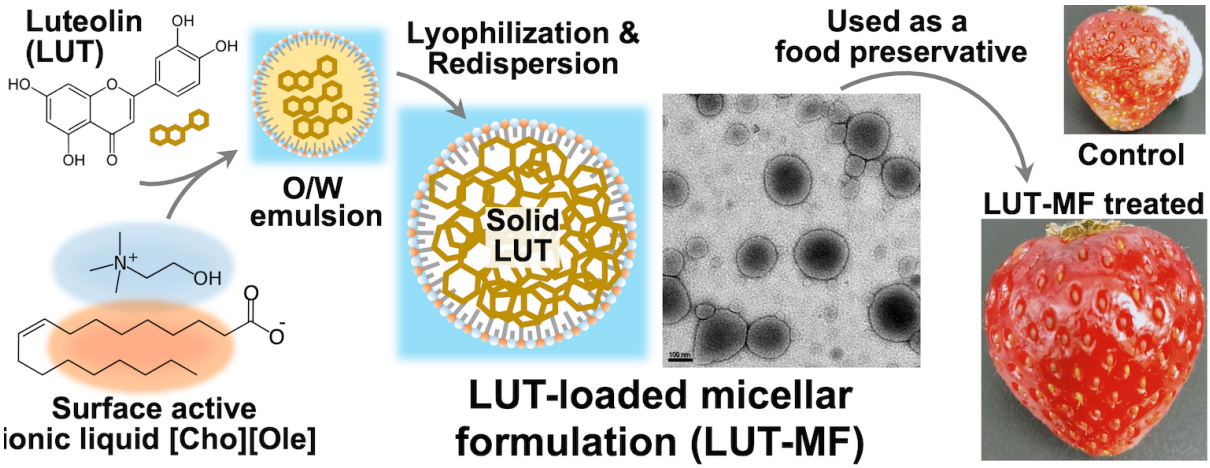

This chapter was published in Journal of Molecular Liquids 365 (2022) 120151; https://doi.org/10.1016/j.molliq.2022.120151 with permission of Elsevier.

3.1 Introduction

Food antimicrobials are usually added to foods to enhance their shelf life by maintaining organoleptic properties including taste, texture, appearance, and freshness [1,2]. Various synthetic and semi-synthetic chemicals (e.g., sodium/potassium benzoate, sorbate, nitrite, and nitrate) are widely used as preservatives in food processing owing to their potential antibacterial and antifungal properties [2]. However, the use of these chemical preservatives in food has been considered a health risk to humans—even when used at levels below the limits recommended by regulatory agencies—because of their undesirable side effects such as skin problems, sneezing and breathing trouble, gastrointestinal discomfort, and cancer [2,3]. Recently, natural preservatives derived from plants have been used as potential green alternatives to chemical preservatives. They have been reported to effectively preserve food without compromising its shelf life, durability, or resistance to microbial attacks [1]. Various natural food preservatives, such as eugenol, thymol, carvacrol, vanillin, terpene, cinnamic acid, curcumin, quercetin, and luteolin are available [1,4]. Luteolin (LUT, 3′,4′,5,7-tetrahydroxyflavone) is a yellow weakly acidic tetrahydroxy flavonoid with poor aqueous solubility (1.09 ± 0.16 μg/mL) [5], which is naturally found in vegetables (e.g., radicchio, celery, peppermint, broccoli, carrots, and pepper), medicinal herbs (e.g., oregano and thyme), and fruits (e.g., belimbi, lemons, and mango) [6,7]. Due to its non-toxic side effects (LD_{50} 219.8−793.7 mg/kg in humans), LUT has already been commercially developed as a health food and can be found in cosmetic products [6]. LUT has potential for use in food processing also owing to its considerable antioxidant and antimicrobial properties that delay food spoilage [8,9]. LUT also shows various other therapeutic activities such as hepatoprotective [5,10], neuroprotective [11], and anticancer activities [12]. However, limited aqueous solubility, poor bioavailability, and low stability to oxidation impede the potential of LUT in both the food and pharmaceutical industries [13,14]. Different approaches are therefore being explored to overcome the drawbacks of LUT.

Surface active agent (surfactant)-based self-assembled structures (e.g., micelles, emulsions, and liposomes) have been used as carriers to encapsulate bioactive compounds to protect them from the adverse effects of pH, oxygen, and light as well as from contacting and reacting with other food components. Generally, the solubility and absorbability, and stability to gravitational separation and aggregation of LUT carriers, decrease with increasing formulation particle size [13,15]. Smaller particles have greater surface area per

unit volume and penetrate easily into water rich areas of food where spoilage bacteria generally grow [3]. The particle sizes of LUT-loaded nanoemulsion vehicles, nanovesicles, nanosized vesicles, and oxidized lotus root starch (OLRS) nanoparticles were 290 nm [16], 373–459 nm [17], 189.92 nm [18], and 305 nm [9], respectively. However, many formulations require a high concentration of surfactant to stabilize the micelles in aqueous media. For example, the LUT nanoemulsion formed by cremophor EL and labrasol (2:1) required 28% (w/w) surfactant [19], while the LUT SNEDDS formulated from Tween-80 and Transcutol-HP (1:1) required 40 wt% surfactant [10]. Such a high amounts of conventional surfactant in food products present health risks, and their use is limited by different regulatory agencies [20]. Moreover, several common cationic and anionic surfactants are toxic and non-biodegradable [21,22]. Therefore, low toxicity surfactants that can form small nanocarriers at low concentration are required for the formulation of LUT delivery systems for food products. The carrier materials chosen for encapsulation play a crucial role in presenting the biological activities of the encapsulated compounds [23].

Recently, surface active ionic liquids (SAILs)—molten salts composed of organic cations with organic or inorganic anions—have been established as potential alternatives to conventional surfactants for various purposes including food and pharmaceutical applications [24,25]. There have been reports of ILs being used to deliver hydrophobic phytochemical drugs such as quercetin [26], curcumin [21], rutin [27] and nobiletin [28]. Bio-based SAILs can provide better surface-active properties, biocompatibility, and high temperature stability, as well as lower toxicity than conventional surfactants [29–31]. The IC_{50} of choline oleate against mammalian cell line NIH 3T3 was found to be 0.59 mM which is lower than the traditional ionic surfactant SDS (IC_{50}= 0.16 mM) and similar cytotoxicity of the conventional surfactant Tween 80 (IC_{50}= 0.68 mM) [32]. Choline, an essential nutrient related to vitamin B-complex, and fatty acids are generally recognized as safe (GRAS) substance and food additive [33]. The combination of choline and oleic acid, a long chain fatty acid (C18:1), to produce choline oleate IL ([Cho][Ole]), is considered low toxicity for food industry applications [32,33].

The aim of this study was to formulate and investigate nano-sized micellar formulation of LUT using a low carrier material concentration to enhance LUT dissolution and bioactivity. The LUT-loaded micellar formulation (LUT-MF) was prepared using the solid-in-water nanodispersion technique [34]. LUT-MFs were optimized in terms of the organic phase

component, concentration of [Cho][Ole], and mixing method, and the particle size and size distribution, morphology, encapsulation efficiency, and maximum aqueous solubility were evaluated. The dissolution rate, antioxidant activity, and *in vitro* antibacterial properties of the LUT-MF were also assessed to support their application in the food industry. Finally, LUT-MFs were used on strawberry fruits as a model food to evaluate their food preservation effects.

3.2 Materials and methods

3.2.1 Materials

Tokyo Chemical Industry Co. Ltd (Kita-Ku, Tokyo, Japan) provided luteolin with purity >98.0%. HPLC grade methanol, acetone, phosphoric acid, cyclohexane, silver oxide, deuterated dimethylsulfoxide (DMSO-d_6), and sodium dodecylsulfate (SDS) were purchased from Wako Pure Chemicals Industries (Osaka, Japan). Tween 80 was obtained from Sigma Aldrich (Missouri, USA). Wako Pure Chemicals Industries (Osaka, Japan) supplied choline chloride and oleic acid. All other reagents, solvents, and materials were analytical grade and used as received.

3.2.2 Synthesis of choline oleate ([Cho][Ole])

The [Cho][Ole] was synthesized by following reported procedure (Scheme 3.1) [29]. Briefly, choline chloride (5 mg) and an excess amount of silver oxide in presence of water were stirred vigorously in dark place at room temperature for 2 h. The mixture was filtered and evaporated to get choline hydroxide ([Cho][OH]). The resultant [Cho][OH] was neutralized with an equimolar oleic acid in methanol solution by stirring at room temperature for 24 h. The solvent was evaporated at 40°C under 20 hPa, and the [Cho][Ole] was freeze-dried for 24 h to eliminate residual water. ^{1}H NMR and FT-IR were used to confirm the proton transfer between [Cho][OH] and oleic acid.

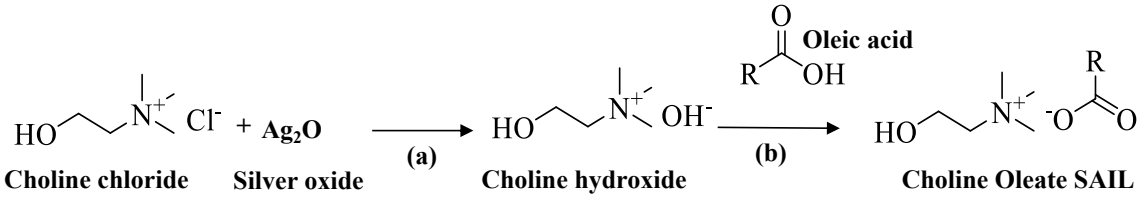

Scheme 3.1. Synthetic process of the SAIL[Cho][Ole]. (a) Precipitation of silver chloride in water at room temperature for 2 h in the dark to obtain choline hydroxide. (b) Stirring

choline hydroxide and the oleic acid in methanol at room temperature for 24 h yields the [Cho][Ole].

3.2.3 Preparation and characterization of LUT-MF

LUT-MF was prepared using a solid-in-water nanodispersion technique adapted from a previously reported method with some modifications [34]. Briefly, 1 mL of organic phase (acetone: methanol: cyclohexane = 5:10:85, v/v) containing 1 mg of LUT and 3 mL of an aqueous phase of SAIL [Cho][Ole] (5 mg/mL) were emulsified and the prepared O/W emulsion was lyophilized to obtain solid LUT-[Cho][Ole] complex. The solid complex was redispersed in water to obtain LUT-MF. The mean particle size (z-average) and size distribution as polydispersity index (PDI) were measured by dynamic light scattering (DLS). The morphologies of the LUT-MF and blank formulation (LUT-free MF carrier) were observed using transmission electron microscopy. To confirm the encapsulation of LUT in the micellar formulation, XRD patterns of free LUT, lyophilized LUT-MF, LUT-free MF carrier, and a physical mixture (free LUT and LUT-free MF carrier) were obtained using an X-ray diffractometer.

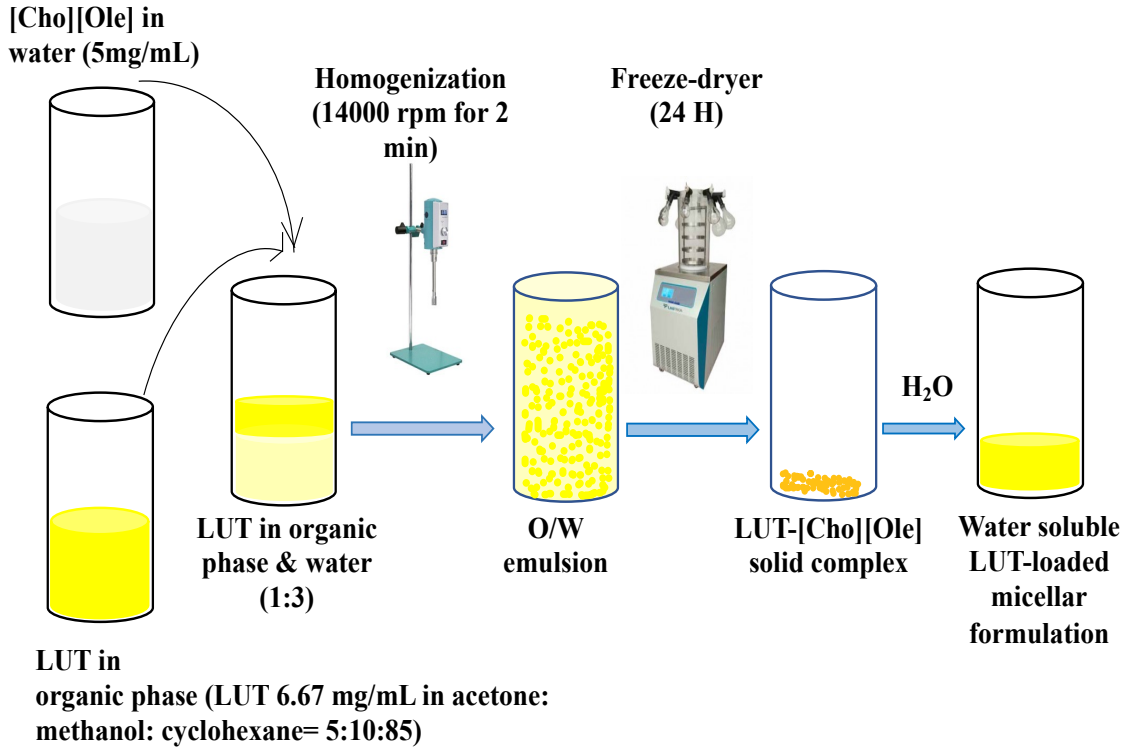

Scheme 3.2. Preparation steps of LUT loaded micellar formulation preparation.

3.2.4 HPLC measurement of LUT

The LUT content of different samples (encapsulation efficiency, maximum aqueous solubility, and dissolution rate) was measured using a HPLC system (JASCO International Co. Ltd., Tokyo, Japan). The mobile phase was composed of methanol and 0.2% phosphoric acid aqueous solution at a ratio of 55:45 (v/v) [35], and the flow rate of the mobile phase was 1.0 mL/min. Chromatographic separation was carried out on an Inertsil ODS-3 column (4.6 × 250 mm, 5 µm, GL Sciences Inc., Japan) at 350 nm. The temperature of the column oven was set at 30°C and the injection volume for the standards and samples was 10 µL. The standard LUT stock solution was prepared at 1 mg/mL in methanol and diluted with mobile phase at 2–32 µg/mL.

3.2.4.1 Encapsulation efficiency (EE)

The EE of LUT-MF was evaluated using a filtration method [29] and compared with formulations prepared with the same composition and preparation method as used for the optimized LUT-MF, but using Tween 80 and SDS as surfactants. LUT-MF and formulations prepared with Tween 80 and SDS were filtered through a 0.2 µm membrane (Millipore Millex-LG, PTFE) to separate the non-encapsulated LUT. The filtered (encapsulated LUT) and unfiltered samples (total LUT) were injected into the HPLC system for analysis. The EE (%) was determined using the following equation.

EE (%) = Concentration of LUT in filtered sample/ Concentration of LUT in unfiltered sample × 100

3.2.4.2 Solubility of the LUT formulation

The maximum solubility of LUT-MF in water was assessed using HPLC to measure the concentration of LUT as described in the literature [21] and the results were compared with formulations prepared with Tween 80 and SDS instead of [Cho][Ole]. The LUT-surfactant solid formulation (after lyophilization) was dissolved in 1 mL of Milli-Q water in a glass vial by gentle shaking and rotating. The LUT-surfactant aqueous solution was then transferred to another glass vial containing the solid formulation and this process was repeated until the solution became turbid. The undissolved LUT solid was removed by centrifugation (10,000 rpm for 10 min) and the supernatant was filtered to separate the non-encapsulated LUT using a 0.2 µm syringe filter. The non-encapsulated formulation showed

a mean particle size of 1339.0 nm. The filtered aqueous solutions were diluted with mobile phase and analyzed by HPLC to quantify the solubility of the formulations.

3.2.5 Dissolution rate

Free LUT in an aqueous solution containing 20% DMSO (denoted LUT suspension) and LUT-MF were evaluated to determine the release patterns into 25 mL of phosphate-buffered saline (PBS, pH 7.4) containing 30% ethanol at 37°C, through a dialysis membrane (regenerated cellulose membrane) [14]. One milliliter of LUT-MF or LUT suspension was loaded into a previously activated membrane (Spectrum Laboratories, Inc., Rancho Dominguez, California, USA, molecular weight cut-off of 12–14 kDa). The dialysis bag was hermetically tied on both sides using plastic clips and immersed in the release media. The release media was stirred constantly at 100 rpm. Sampling of the release media (1 mL aliquots) was performed at different time points (0.08–24 h) and the same volume of preheated fresh media was added to maintain the total volume. Each sample (1 mL withdrawn) was first filtered using a membrane filter, and then diluted with the HPLC mobile phase. Triplicate samples were analyzed using HPLC and the LUT concentration was determined by measuring the absorbance at 350 nm.

3.2.6 Stability assay

The stability of LUT-MF was evaluated using DLS measurement and visual observation following long term storage at different temperatures, and exposure to freeze-thaw cycles. The formulations were stored at 4, 25, and 37°C for 30 days and the particle size and PDI were measured using DLS every five days. In addition, formulations in a clear glass vial were stored in a freezer (−25°C) for 12 h and then thawed at room temperature (~25°C) for 12 h. The particle size and PDI of the formulations were measured by DLS and visually observed before and after conducting the freeze-thaw cycles (up to 5 times)[19]. The experiment was repeated three times.

3.2.7 Antioxidant activity

The antioxidant activities of optimized LUT-MF and free LUT were assessed using 1,1-diphenyl-2-picrylhydrazyl (DPPH) method following previously reported procedure with some modifications [17]. Different concentrations (5, 10, 25, and 50 μg/mL) of LUT-MF,

free LUT, and ascorbic acid were prepared in methanol solution. DPPH in methanol (175 µL, 0.1 mM) was added to 25 µL samples of LUT-MF, ascorbic acid, and free LUT in a 96-well plate. Milli-Q water was added to the DPPH solution as a control. The reaction mixtures were incubated at 25°C for 30 min in the dark. The absorbance of the mixtures was measured at 517 nm using a microplate reader (SpectraMax i3x, Molecular Devices, Inc.). The percentage of DPPH scavenging activity was calculated as follows:

$$\text{Antioxidant activity (\%)} = \left(\frac{A_C - A_S}{A_C}\right) \times 100$$

where A_C is the absorbance of DPPH in Milli-Q water (control) and A_S is the absorbance of the test sample.

3.2.8 Antibacterial assays

Bacterial culture

In vitro antibacterial activities of LUT-MF were tested against two gram-positive bacteria *Staphylococcus aureus* (*S. aureus*) ATCC 6538 and *Bacillus subtilis* (*B. subtilis*) ATCC 6051 and two gram-negative bacteria *Escherichia coli* (*E. coli*) ATCC 25922 and *Salmonella enterica* (*S. enterica*) ATCC 8400. Stock cultures of bacteria were stored at -80°C in cryovial and they were grown into the Mueller-Hinton (M-H) agar (Sigma-Aldrich) for 24 h at 37°C. Single colony from M-H agar plate was cultured on M-H broth for 24 h and diluted in M-H broth to a McFarland turbidity of 0.5 (1 x 10^8 colony forming unit (CFU)/mL) before testing.

3.2.8.1 MIC and MBC determination

The minimum inhibitory concentration (MIC) and minimum bactericidal concentration (MBC) of optimized LUT-MF was determined in flat-bottom polystyrene 96-well microplates (Thermo Fisher Scientific, Roskilde, Denmark) by serial microdilution method as described in literatures with some modifications [36,37]. Solid LUT-MF (after lyophilization) were dissolved in M-H broth medium to a 6 mg/mL concentration of LUT, filtered by 0.2 µm membrane filter and serially diluted in 96-well plate. To evaluate the antimicrobial properties of [Cho][Ole], different concentrations of [Cho][Ole] (60, 50, 40, 30, 25, 20, 15 and 10 mg/mL) were prepared in MHB. Ten microliters of bacteria inoculum

(1 x 10^6 CFU/mL) were added in each well containing 90 µL of M-H broth with LUT-MF or [Cho][Ole]. Bacterial suspensions with M-H broth (without LUT-MF or [Cho][Ole]) were used as control and M-H broth with LUT-MF and [Cho][Ole] (without bacteria) as blank. The microplates were incubated at 37°C for 24 h and absorbance was measured at 600 nm using a microplate reader (SpectraMax i3x, Molecular Devices, Inc.). An incremental increase approach of 200 µg/mL was also adopted to determine the exact MICs with for LUT. The MIC was determined twice and in triplicates. To determine MBC the overnight treated suspension was diluted and spotted on M-H agar plates and incubated for further 18 h at 37°C for CFU counting. The MBC was measured as the lowest concentration resulting all bacterial death.

3.2.8.2 Bacterial time-kill assay

To compare the antimicrobial activity of LUT-MF with a commercial preservative (sodium benzoate), the growth kinetics of gram-positive *S. aureus* and *B. subtilis*, and gram-negative *E. coli* and *S. enterica* were investigated following literature with modification [38]. The treatment formulations, i.e., LUT-MF (1.5 mg/mL) and sodium benzoate (15.0 mg/mL, and 1.5 mg/mL) were prepared in M-H broth and compared with control (M-H media only). Bacteria were cultured with M-H broth at 37°C for 24 h and 15 µL diluted bacterial suspension (10^6 CFU/mL) was added with 150 µL of the formulations (M-H broth containing LUT-MF or sodium benzoate) in a 96 well plate. The growth of bacteria was monitored by measuring optical density (OD_{600}) at 2, 4, 6, 8, 18 and 30 h and the growth kinetics of bacteria were plotted as OD versus time.

3.2.9 Food preservation test

Strawberries were used as the food model because of their limited post-harvest shelf life. Fresh strawberry fruits from a local supermarket in Fukuoka, Japan were sorted and selected based on uniform size (average weight 14.0 ± 2.0 g) as well as being free of visible mechanical damage and fungal infection. The strawberries were sanitized by immersion in sterilized deionized water for 3 min and were split into 3 groups (30 strawberries per group)—a Milli-Q water treated group, sodium benzoate (15 mg/mL) treated group, and LUT-MF (1.5 mg LUT per mL water) treated group—for physicochemical analysis and visual observation. The strawberries were submerged in Milli-Q water, sodium benzoate, or LUT-MF for 3 min at 25°C. Ten strawberries were then packed in 500 mL clamshell boxes

(dimensions: 17.8 cm × 11.1 cm × 5.1 cm) with a lid and 4 holes in each of the 4 sides, three boxes were prepared per treatment. The clamshell boxes of strawberries were stored at 10°C and natural incubator humidity (30–35%). The physicochemical properties of the strawberries were determined on day 0, 4, and 8. Sensory evaluation of the strawberry samples was conducted at 0 and 8 days. The preservation test was repeated in duplicate.

3.2.9.1 Physicochemical properties of strawberries

Weight loss

To estimate the weight loss, ten strawberries in each group were weighed at day 0, 4, and 8 using a digital balance (± 0.01 mg) (SECURA225D-1SJP Sartorius, Germany). Weight loss was calculated as the percentage loss compared with the initial weight and the mean with standard deviation was reported from the average values of duplicate measurements.

Decay

Strawberries were visually observed for grey mold infection, brown spots, and softening of wounded areas, and the presence of these features was counted as decay. The results are presented as a decay percentage by dividing the number of samples exhibiting decay by the total number of samples multiplied by 100.

pH and total soluble solids

Five strawberries in each group were wrapped in cheesecloth at 0, 4, and 8 days then squeezed with a hand press to collect the juice. The pH of the obtained juice was determined using a digital pH meter (HM-30R, DKK-TOA corporation). The total soluble solids (TSS) content was determined using a Brix refractometer and the results are expressed as a percentage (%) at 20°C.

3.2.9.2 Sensory quality evaluation

The color, shriveling, decay, aroma, and firmness of strawberries treated with Milli-Q water, sodium benzoate and LUT-loaded MF were evaluated by a panel comprising 15 people according to a published method [39]. The panel included faculty members and undergraduate, graduate, and postgraduate students (9 males and 6 females; aged between 20 and 62 years). Sensory quality evaluation of the color, shriveling, decay, aroma, and firmness of coded samples was executed subjectively using a 1–5 rating scale where 5 =

excellent, 4 = good, 3 = acceptable, 2 = poor, and 1 = very poor. This technique was carried out to support the effectiveness of LUT-loaded MF as a natural antimicrobial to preserve the organoleptic properties of food products.

Scores and description

	1 Very poor	2 Poor	3 Acceptable	4 Good	5 Excellent
Color	Very dark purplish-red; extremely overripe or senescent	Overripe; very dark red	Fully red	Fully light red	Three-quarter to fully light red
Shriveling	Extremely wilted and dry	Severe shriveling, fruit is shriveled and calyx is wilted and dry	Shriveling evident, fruit and calyx show evident signs of moisture loss	Minor signs of shriveling, calyx slightly wilted	Field-fresh fruit, and calyx appear very fresh and turgid
Decay	100 %, characteristic sporulation, the fruit is either partial or completely rotten	75 %, moderate to heavy mycelium growth	50 %, spots with decay and some mycelium growth	25 %, slight brown discoloration of the tissues, probable decay	0%, no visible changes in the tissues
Aroma	Very poor, unpleasant aroma	Poor	Acceptable	Good	Excellent, characteristic strawberry odor
Firmness	Extremely soft and deteriorated	Soft and leaky	Minor signs of softness	Firm but less turgid	Very firm and turgid

3.3 Results and discussion

3.3.1 Preparation and optimization of LUT-MF

The formulations were produced by adding aqueous [Cho][Ole] to organic solvent containing LUT (1 mg/mL), followed by lyophilization to remove the organic phase and encapsulate LUT solid in [Cho][Ole]. The absence of organic phase in LUT-MF was

confirmed by ^{1}H NMR. The roles of the organic solvents, mixing method, and [Cho][Ole] concentration in each micellar formulation (MF) were thoroughly investigated by considering the particle size and stability of the formulations. A mixture of organic solvents (methanol: acetone = 2:1) was used to solubilize LUT and then this solution was mixed with cyclohexane to form the LUT solubilized organic phase. The necessity of each organic component in the preparation was investigated by evaluating the particle size and PDI. Organic solvent (methanol, acetone, and cyclohexane)-mediated formulation resulted in a monomodal distribution of LUT-MF particles with average particle size of 75.43 nm and PDI of 0.137. In contrast, the formulations without methanol-acetone or cyclohexane exhibited polymodal distribution with PDI >0.4; therefore, organic solvents were considered essential for the preparation of homogenous formulations.

Aqueous [Cho][Ole] surfactant was used to reduce the interfacial tension and played a vital role in reducing the particle size and increasing the stability of LUT in the MF. When no [Cho][Ole] was added to the formulation a broad peak with a PDI of 0.370 was observed at 1339.0 nm. Initially with an increase in [Cho][Ole] concentration, the particle size of the MF decreased to minimum value of 72.1 nm at 20 mg/mL and then begun to increase. This trend shows good agreement with a previous study [5]. It is thought that the optimal amount of [Cho][Ole] adsorbs on the surface of the LUT particles preventing aggregation of the formulation and stabilizing the particles dispersed in the water phase. Excess [Cho][Ole] may then condense on the micelles and increase their particle size [5]. A monomodal distribution (single peak; PDI < 0.2) was observed for formulations containing 15 and 20 mg/mL [Cho][Ole]; however, the formulation with 20 mg/mL [Cho][Ole] became turbid with multiple peaks after 10 days, while the 15 mg/mL [Cho][Ole] formulation remained stable. Thus, we concluded that 15 mg/mL [Cho][Ole] was an optimal concentration for preparing stable LUT-MF.

The effects of different mixing methods including stirring, vortexing, and high energy methods such as high-pressure homogenization and sonication, on LUT-MF were evaluated using 1 mg/mL organic solvent-mediated LUT with 15 mg/mL [Cho][Ole]. LUT-MFs were not clear on visual inspection when prepared by sonication for 30 min and vortexing for 5 min. Although, a clear solution was formed with constant stirring for 24 h at 500 rpm, the formulation became turbid with a polymodal distribution after 10 days of storage at 25°C. Only the formulation prepared by homogenization at 14,000 rpm for 2 min was clear with

a monomodal distribution after 10 days. Homogenization is thought to have stabilized the formulation by reducing the particle size of the oil-in-water emulsion more effectively than the stirring, vortexing, and sonication processes [40]. Therefore, the optimized LUT-MF was achieved using 15 mg/mL [Cho][Ole] in presence of an organic phase (acetone, methanol, and cyclohexane) with homogenization (14,000 rpm for 2 min) and LUT-MF demonstrated uniform distribution of particle size (75.43 nm) and PDI (0.137) without any sedimentation.

3.3.2 Particle size and morphology assessment of LUT-MFs

DLS measurements were carried out to investigate the particle size and size distribution of the LUT-MF in aqueous solution. The particle size of the LUT-MF was 73.12 nm, while that of the blank formulation was 56.40 nm. The size of the LUT-MF increased with increasing LUT content, which indicated encapsulation of LUT in the micellar core of [Cho][Ole]. In addition, the PDI of LUT-MF was found to be 0.136 when 1 mg/mL LUT was loaded, indicating monomodal size distribution of the formulation. The morphology of the MFs with/without LUT was determined by TEM (Fig. 3.1A–3.1B). The TEM images of the LUT-MF and the blank MF clearly show spherical structures in the nanometer range. The successful encapsulation of LUT in [Cho][Ole] was indicated by an increase in the particle diameter. In a previous study, encapsulation of LUT in oxidized lotus root starch nanoparticles and methoxy polyethylene glycol-polylactide-co-glycolide copolymer micelles showed greater particle size than the blank formulations, which is consistent with the findings of this study [9,41]. As the concentration of LUT in the LUT-MF increased from 0.0 mg/mL to 3.0 mg/mL, the particle size increased from 56.40 nm to 94.57 nm (Fig. 3.1C), which also supported the conclusion that LUT was incorporated into the micelles and the amount of LUT loaded into the micelles could be controlled.

The XRD patterns of free LUT, lyophilized LUT-MF, LUT-free MF carrier (Blank), and a physical mixture (free LUT and blank) were determined and are presented in Fig. 3.1D. Free LUT showed several sharp peaks at 13.8°, 15.3°, 16.9°, 22.5°, 26.6°, 27.4°, 28.6°, and 29.6°, which suggested that free LUT was present as a crystalline phase [42]. The physical mixture of free LUT with blank-MF showed similar sharp peaks with lower intensities. The sharp peaks of free LUT were not detected for LUT-MF, indicating that the LUT in the MF was amorphous or encapsulated by [Cho][Ole]. This finding is in good agreement with previous reports [9,42].

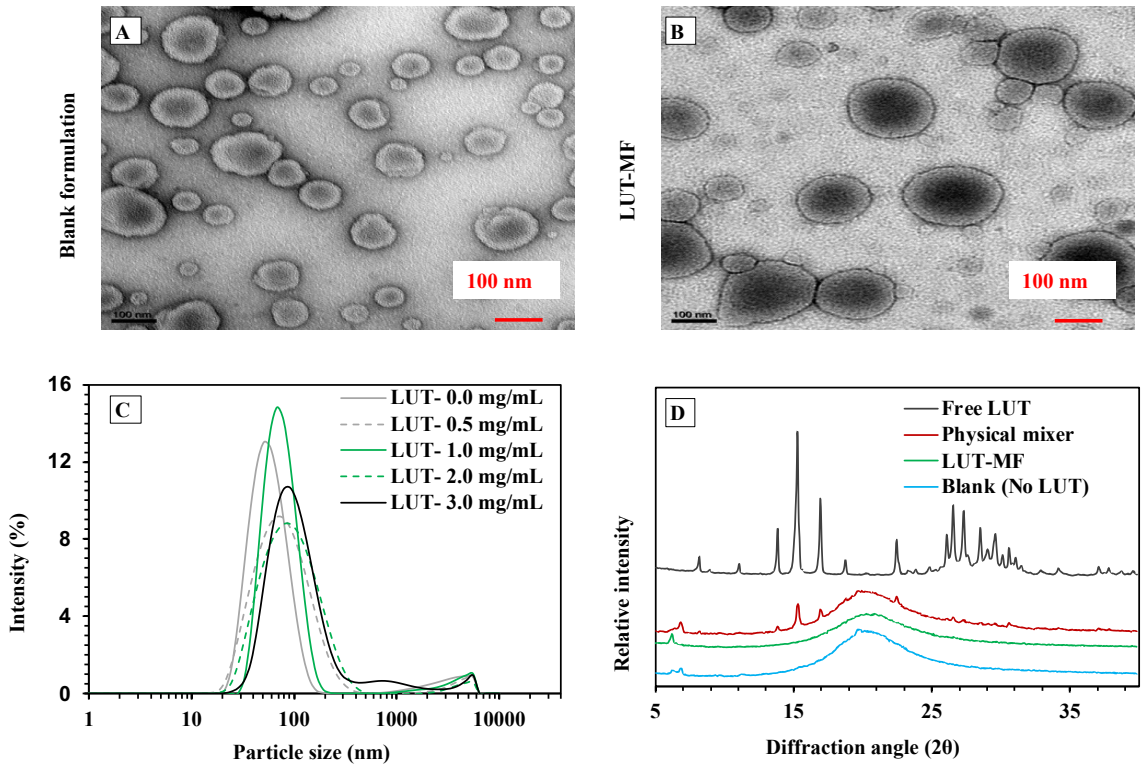

Fig. 3.1. TEM images of blank formulation (A) and LUT-MF (B) (20 k resolution, scale bar 100 nm). (C) Particle size of LUT-MFs containing different concentrations of LUT. (D) XRD patterns of free LUT, LUT-MF, LUT-free MF carrier (Blank), and a physical mixture (free LUT and blank).

3.3.3 Encapsulation efficiency and aqueous solubility of LUT-MFs

The encapsulation efficiency (EE) of LUT in the [Cho][Ole]-based MF was investigated using a filtration method and compared with LUT formulations assembled using non-ionic surfactant (Tween 80) or anionic surfactant (SDS). The EE of the [Cho][Ole]-based formulation was 94.3 %, while those of the Tween 80-based and SDS-based formulations were 33.0% and 23.5%, respectively (Table 3.1). The EE of LUT in carriers assembled using quinoa protein or oxidized lotus root starch was reported to be 42.7% and 87.2%, respectively, indicating that the EE of LUT in our formulation was higher than those in previous reports [9,42]. The long alkyl chain of oleate in [Cho][Ole] interacted strongly with nanosized LUT solids to stably coat their surface. The solubility of LUT in the [Cho][Ole]-based MF was significantly higher than the solubility of LUT in water. The maximum solubility of LUT in [Cho][Ole]-based MF was 8.97 ± 0.60 mg/mL, which is 177−8229 times higher than that in water depending on the reported value (1.09−50.6 μg/mL) [5,41]. The micellar formulations based on [Cho][Ole] developed in this study showed significantly

higher (60 times) aqueous LUT solubility than a previously reported LUT nanoparticle formulation based on polyvinylpyrrolidone-k30, for which the solubility of LUT was 150 μg/mL [5]. The possible reasons behind the higher encapsulation and maximum solubility for choline oleate-based formulations are intermolecular interactions between LUT molecule and [Cho][Ole] such as hydrogen-bonding interaction, cation- π interactions and π- π interactions [29,43].

Table 3.1 Encapsulation efficiency, EE (%), and maximum solubility (mg/mL) of LUT-MF using different surfactants.

Surfactant	EE, %	Maximum solubility, mg/mL
[Cho][Ole]	94.30 ± 7.56	8.97 ± 0.60
Tween- 80	33.03 ± 0.46^{ns}	1.31 ± 0.01^{ns}
SDS	23.47 ± 2.30^{ns}	1.28 ± 0.09^{ns}

Data are shown as the mean ± standard deviation, n= 3; ns= non-significant.

3.3.4 Dissolution rate

The release behavior of LUT-MF and free LUT in an aqueous solution of 20% DMSO (LUT suspension), into PBS (pH 7.4) containing 30% ethanol through a dialysis membrane, was investigated using HPLC. The addition of ethanol was needed to prevent the precipitation of LUT in the release media. LUT-MF showed rapid LUT release up to 2 h and then a steady release up to 12 h, while much lower release of LUT was observed from the LUT suspension (Fig. 3.2). The cumulative release rates of LUT from LUT suspension and LUT-MF after 24 h were 20.7% and 81.6%, respectively. LUT-MF showed 3.94 times higher release than LUT suspension after 24 h, which is attributed to improved dissolution of LUT by [Cho][Ole] that may be due to the poor solubility of LUT in PBS in the absence of carrier materials.

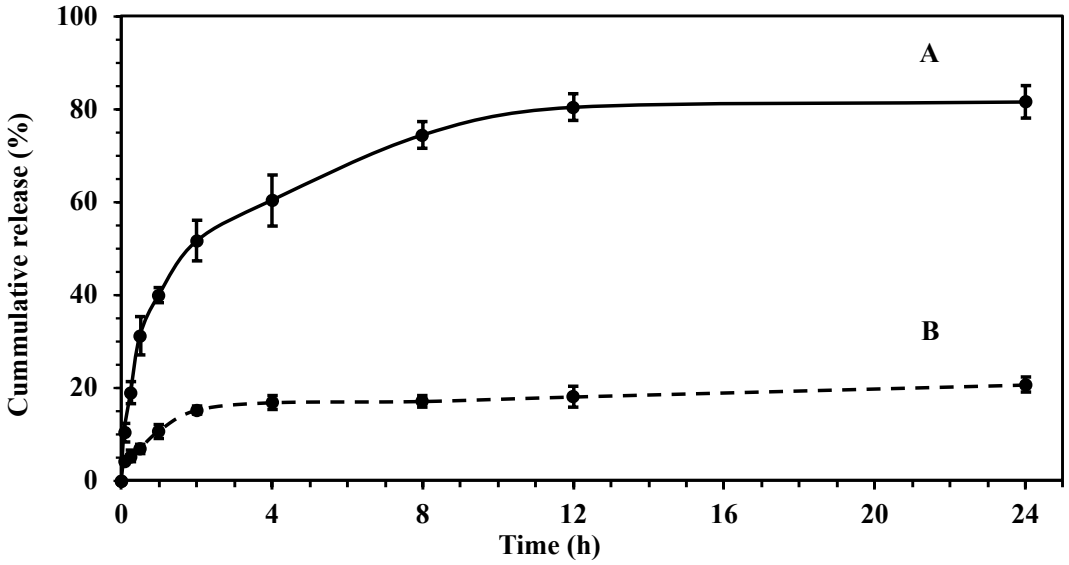

Fig. 3.2. Cumulative release of LUT from (A) LUT-loaded micellar formulation (LUT-MF) and (B) a free LUT aqueous solution containing 20% DMSO (LUT suspension), into PBS media containing 30% ethanol (v/v).

3.3.5 Stability of LUT-MF

Particle stability is crucial to the bioactivity of micelles and particle size changes are a useful benchmark for estimating stability [11]. Long term storage at different temperatures and freeze- thaw cycles were used to evaluate the stability of the optimized LUT-MF through changes in the particle size and PDI. The particle size of LUT-MF was measured at 0, 10, 15, 20, 25, and 30 days of storage at 4, 25, and 37°C (Fig. 3.3A, 3.3B, & 3.3.C). The particle size of the formulations increased from 72.5 nm (0 day) to 93.4 nm after 30 days storage at 4°C and 122.6 nm after 30 days storage at 25°C, but the formulations were clear, and no phase separation, aggregation, or sedimentation was observed. The particle size of the samples stored at 37°C increased from 72.5 nm (0 day) to176.3 nm after 30 days and the sample exhibited some turbidity. This result indicated that the stability of the optimized formulation depended on the storage temperature. Similar trends in droplet size increment for β-carotene-loaded Pickering emulsions stabilized by complex nanoparticles, was observed when the temperature was raised above 40°C. The droplet size increased due to the greater chance of collisions between droplets and self-aggregation at comparatively high temperature [44]. The optimized LUT-MF withstood five freeze-thaw cycles with no LUT phase separation, aggregation, or precipitation (Fig. 3.3D). These findings clearly indicate

that the optimized LUT-MF remained stable at 4°C and 25°C, freeze-thaw cycles had very little effect on the MF, and centrifugation cycles had no effect.

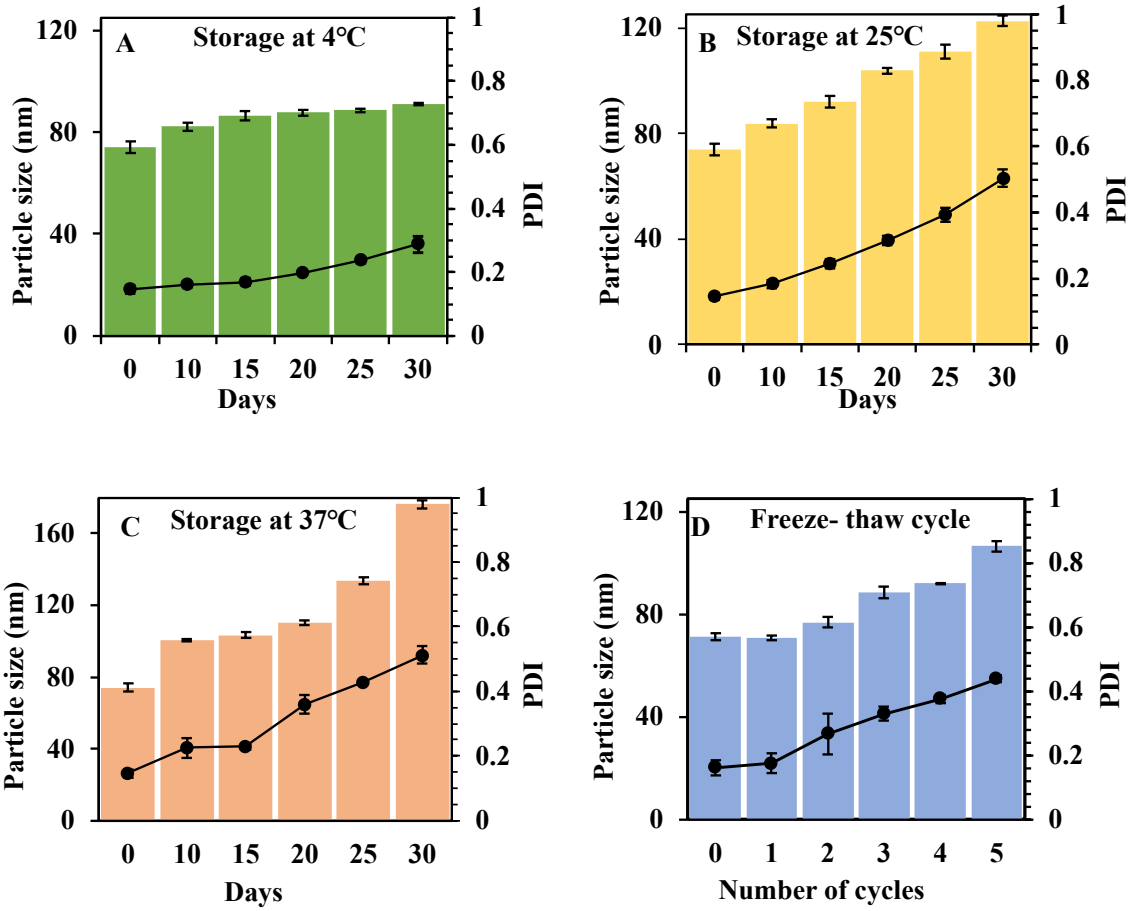

Fig. 3.3. Stability of LUT-MFs. Particle size and PDI of LUT-MF stored at 4°C (A), 25°C (B), and 37°C (C) over time. Effects of freeze-thaw cycles (D) on the particle size and PDI of LUT-MF. Column graphs show the particle size in nm and line graphs show the PDI.

3.3.6 Antioxidant activity

The antioxidant activity of LUT-MF was estimated by assessing the scavenging of the stable free-radical DPPH and compared with the performance of free LUT and ascorbic acid. Slightly lower antioxidant activity was observed in ascorbic acid at each tested concentration than in LUT-MF and free LUT (Fig. 3.4). A similar antioxidant activity in LUT and ascorbic acid has been reported in literature where the antioxidant activity evaluation of LUT and ascorbic acid was conducted in 2,2′-azobis(2-methylpropionamidine) dihydrochloride–luminol and hemoglobin–hydrogen peroxide–luminol systems [45]. The free LUT and LUT-MF showed similar antioxidant potential at lower concentrations (5 and 10 µg/mL LUT). As the concentration of LUT increased from

10 to 25 µg/mL, the antioxidant activity of LUT-MF also gradually increased. The presence of IL surfactant in LUT-MF facilitated a higher antioxidant activity than that was observed in free LUT owing to the solubility of LUT being increased. It can be inferred that efficient encapsulation in micelles or nanoparticles improves antioxidant activity, which agrees with previous reports [9,46].

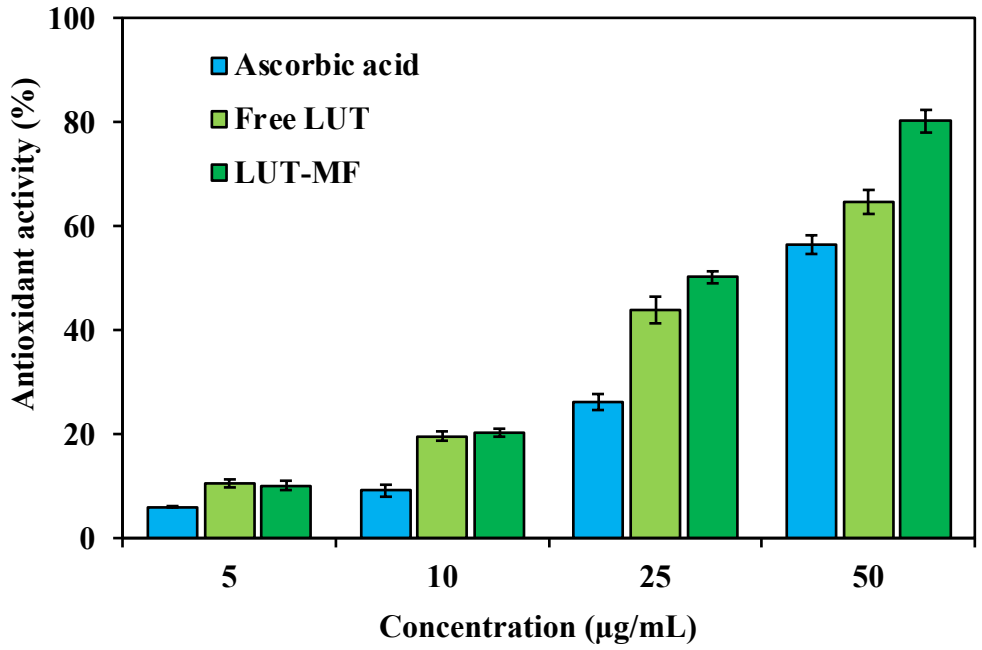

Fig. 3.4. Antioxidant activity of methanolic solutions of ascorbic acid, free LUT, and LUT-MF.

3.3.7 Antibacterial assay

The *in vitro* antimicrobial activity of LUT-MF was evaluated in terms of the MIC and MBC against gram-positive *S. aureus* and *B. subtilis* and gram-negative *E. coli* and *S. enterica* and the results are presented in Table 3.2. LUT-MF demonstrated comparatively higher antimicrobial activities against *B. subtilis* and *E. coli.* It has been reported that LUT in DMSO solution resulted in very low MICs (16 µg/mL against *S. aureus* ATCC- 25923 and 32 µg/mL against *Listeria monocytogenes* ATCC- 19115) [8], whereas the MIC of LUT in 20% DMSO solution was 500 µg/mL against clinical isolates of *E. coli* and *S. aureus* [47], indicating the possible significant role of DMSO in the antimicrobial studies. The controlled release of LUT observed in this study may contribute to the antimicrobial activities. Approximately 50% of the loaded LUT was released from LUT-MF after 2 h, leading to slow action (Fig.3.2). In contrast, LUT dissolved in DMSO worked immediately, which may be the reason for the higher antimicrobial activity of LUT dissolved in DMSO. Here,

LUT-MF dissolved in water demonstrated similar antibacterial activity (MIC 500 to >1000 μg/mL against *S. aureus* and *E. coli*) to other flavonoids (kaempferol, quercetin, and rutin) dissolved in 20% DMSO in water solution [47]. [Cho][Ole] demonstrated mild antibacterial activities against the tested bacteria (MIC 25000- 30000 μg/mL and MBC >60000 μg/mL) which is consistent with the previous study (Table 3.2) [48]. The MBC values of LUT-MF were significantly higher than the MIC values. The MIC and MBC results are not fully coherent with the general pattern, which is summarized as gram-positive bacteria having higher sensitivity than gram-negative bacteria. Cell membrane damage and changes in the cell morphology of *S. aureus* and *Listeria monocytogenes* have been described as potent antibacterial mechanisms of LUT in the literature [8]. Owing to its lower MIC and MBC values, LUT-MF has the potential to be used as an antimicrobial agent in food preservation.

Table 3.2 Antibacterial activity of LUT-MF and [Cho][Ole] against selected bacteria in terms of MIC and MBC.

Samples	***S. aureus***		***B. subtilis***		***E. coli***		***S. enterica***	
	MIC	**MBC**	**MIC**	**MBC**	**MIC**	**MBC**	**MIC**	**MBC**
Lut-MF	800	1200	600	1000	600	1000	1000	1500
[Cho][Ole]	25000	>60000	30000	>60000	25000	>60000	30000	>60000

3.3.8 Bacterial time-kill assay

The *in vitro* growth kinetics of *S. aureus*, *B. subtilis*, *E. coli,* and *S. enterica* were evaluated to compare the antibacterial effects of LUT-MF and sodium benzoate and the results are shown in Fig.3.5. As the MICs of sodium benzoate against *E. coli* and *S. enterica* are 10.73 mg/mL and 10.375 mg/mL, respectively [49], we used 15 mg/mL sodium benzoate. To compare the effect of similar concentrations, 1.5 mg/mL sodium benzoate was also studied to reflect the concentration of LUT in LUT-MF. It was found that treatment with 1.5 mg/mL sodium benzoate resulted in similar growth kinetics to those of the control (bacterial growth in M-H broth only). The growth of all the bacteria tested in the control and sodium benzoate (1.5 mg/mL) reached a peak after 18 h, then declined, possibly owing to the lack of nutrients and increased metabolic products. LUT-MF (1.5 mg/mL) and sodium benzoate (15.0 mg/mL) inhibited the growth of both gram-positive and gram-negative bacteria and showed similar bacteriostatic or bactericidal effects. In a previous study, carvacrol in an ovalbumin

inclusion complex demonstrated similar inhibition of *Bacillus cereus* and *Salmonella* growth up to 24 h, with the ovalbumin reported to enhance the access of carvacrol to the membrane and inside the cytoplasm of bacteria [38]. LUT-MF (1.5 mg/mL) and sodium benzoate (15.0 mg/mL) were used for the food preservation test owing to their higher antibacterial activities.

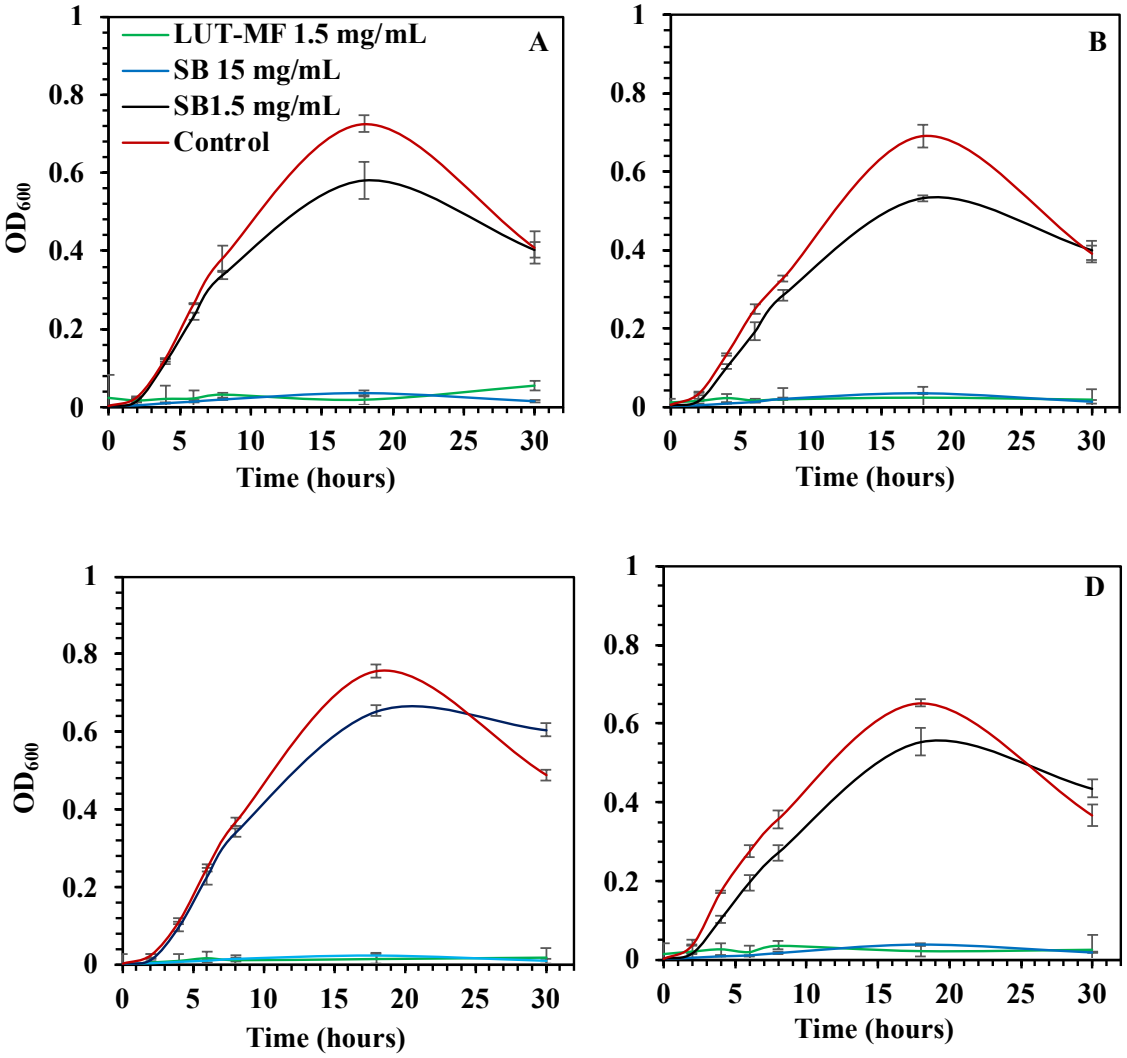

Fig. 3.5. *In vitro* bacterial time-kill assays for LUT-MF, sodium benzoate (SB) 1.5 mg/mL, and sodium benzoate (SB) 15.0 mg/mL against *Staphylococcus aureus* (A), *Bacillus subtilis* (B), *Escherichia coli* (C), and *Salmonella enterica* (D).

3.3.9 Food preservation test

To evaluate the preservative effect of LUT-MF treatment, the physicochemical properties and sensory qualities of strawberry fruits were assessed and compared with those of

strawberries treated with the commercial preservative sodium benzoate (15 mg/mL), and untreated (Milli-Q treated) samples.

3.3.9.1 Physicochemical properties

Strawberries are one of the most perishable fruits and are prone to severe water loss due to their thin skin. Low weight loss indicates fruit freshness and water loss by transpiration is the main weight loss route [50]. The percentage weight losses of strawberries treated with LUT-MF and sodium benzoate were compared with that of Milli-Q treated strawberries throughout storage at 10°C (Fig. 3.6A). The percentage of weight loss of strawberries in all three groups increased with storage time. The weight losses of the LUT-MF and sodium benzoate treated samples on day 4 were 3.54% and 3.88%, respectively, which were significantly lower than that of the Milli-Q treated strawberries (4.62%). On day 8, both LUT-MF and sodium benzoate significantly prevented weight loss (7.78% and 8.70%, respectively) compared with Milli-Q (10.01%). These results are in good agreement with previous findings that LUT solution prevented the weight loss of sweet cherry in a dose-dependent manner [51]. The LUT-MF treated samples showed marked weight conservation, likely owing to the antioxidant properties of LUT-MF resulting in the protection of cells from natural free radical damage. In a previous study, the weight loss of non-contaminated strawberries was compared with that of strawberries artificially contaminated with *Botrytis cinerea* and less weight loss was observed for non-contaminated strawberries than for contaminated strawberries, indicating that microbial activity could be a factor in the weight loss [50]. As LUT-MF demonstrated significant antimicrobial activity, lower microbial activity in LUT-MF treated strawberries may be another reason for the lower weight loss.

The decay percentages of strawberries subjected to different treatments during the storage period at 10°C are shown in Fig. 3.6B. Decay increased with time in all three groups, but the increment of decay percentage was significantly different among the groups. The decay percentages of the control (Milli-Q treated) strawberries were 40% and 75% after 4 and 8 days of storage, respectively. Sodium benzoate (15 mg/mL) treated strawberries showed a lower decay percentage than the control strawberries on day 4 and 8 (15% and 40%, respectively). As the concentration of sodium benzoate applied to the strawberries was above the MIC value, it significantly prevented the growth of microorganisms and maintained low microbial decay of the strawberry samples. LUT-MF treated samples showed no decay at day 4 and only 15% decay on day 8, which is significantly less decay

than was observed for the sodium benzoate treated samples, demonstrating the potential of LUT-MF as a preservative. The high performance of LUT-MF in comparison to sodium benzoate may be a result of their different mechanism of action on microorganisms. Sodium benzoate inhibits the growth of microorganisms largely by obstructing the enzymatic functions vital for oxidative phosphorylation, whereas LUT inhibits microorganisms by damaging cell membranes and altering cellular morphology in the planktonic state [8,49].

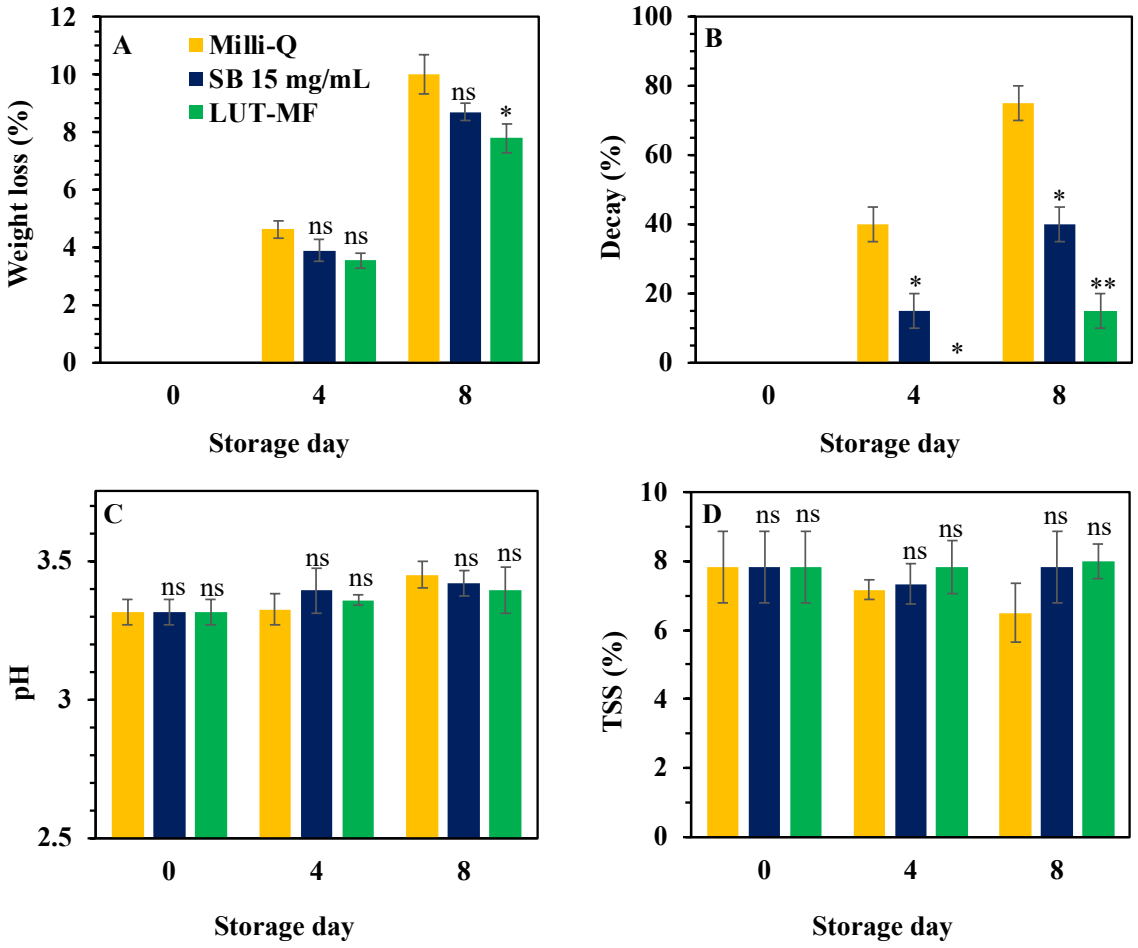

Fig. 3.6. Effects of LUT-loaded micellar formulation (LUT-MF) and sodium benzoate (15 mg/mL) on weight loss (A), decay (B), pH (C), and total soluble solid contents (D) of strawberries over 8 days of storage at 10°C in natural incubator humidity. Data are shown as the mean ± standard deviation, n= 3; ns= non-significant, *p<0.1, **p<0.01.

The pH changes of strawberries treated with different formulations are presented in Fig. 3.6C. On day 0, the pH of strawberry juice was 3.32. On day 4 and 8, the pH increased slightly compared with day 0, but no significant variation in pH was observed among the three groups. As shown in Fig. 3.6D, the total soluble solids (TSS) content of the

strawberries was 7.8% at the initial stage of storage and did not change considerably throughout the storage period in any of the three treatment groups. Similarly, Shankar, Khodaei and Lacroix (2021) observed no significant changes in the TSS content of strawberries packed in chitosan-essential oil-silver nanoparticles after 6 days of storage at 25°C [52].

3.3.9.2 Sensory quality evaluation

Overall appearance, lack of decay, flavor, and texture are the initial driving factors behind consumer food purchases [39]. In this study, the sensory parameters of color, shriveling, decay, aroma, and firmness were subjectively evaluated, and the results are presented in Fig. 3.7. The strawberry samples treated with LUT-MF showed notably higher color ratings than the Milli-Q treated strawberries (3.40 ± 0.27 compared with 2.60 ± 0.17, respectively) after 8 days of storage, while the color score of fresh strawberries was 4.86 ± 0.24 at day 0. The LUT-MF treated strawberries exhibited a significantly lower shriveling score than Milli-Q treated strawberries after 8 days of storage. LUT-MF inhibited decay and maintained the firmness of the strawberry samples compared with Milli-Q treatment. The sensory scores for color, shriveling, decay, aroma, and firmness for the LUT-MF treated strawberries were 3.40 ± 0.27, 4.14 ± 0.28, 4.37 ± 0.12, 4.32 ± 0.47, and 4.21 ± 0.57, respectively, and 2.60 ± 0.17, 2.96 ± 0.17, 2.16 ± 0.27, 2.89 ± 0.20, and 2.25 ± 0.25, respectively, for strawberries treated with Milli-Q water. The higher scores for LUT-MF treated strawberries indicate the good quality of the strawberries compared with the Milli-Q water treated fruits. The LUT-MF treated strawberries also showed better sensory ratings for decay, shriveling, and color than sodium benzoate treated strawberries after 8 days of storage, but no substantial variation in ratings for aroma and firmness was identified. Similar sensory evaluation ratings for strawberries were also observed for cannabidiol treatment at 10°C storage in a previous report [53]. Enzymatic browning by polyphenol oxidase and peroxidase enzymes affects the flavor, appearance, and decay of fruits and vegetables and LUT effectively prevents the peroxidase activities in a non-competitive manner [54]. In contrast, LUT augments phenylpropanoid metabolic activities, leading to increased flavonoid and anthocyanin contents, which may contribute to the defense mechanisms of fruits against adverse environmental conditions and microbial attacks [51]. LUT-MF is thought to have suppressed the browning and decay of strawberries and maintained good organoleptic properties by inhibiting oxidase and peroxidase and microbial activity. The LUT-MF

treatment successfully preserved the overall quality of the strawberries for 8 days, which indicates the effectiveness of LUT-MF as a food preservative.

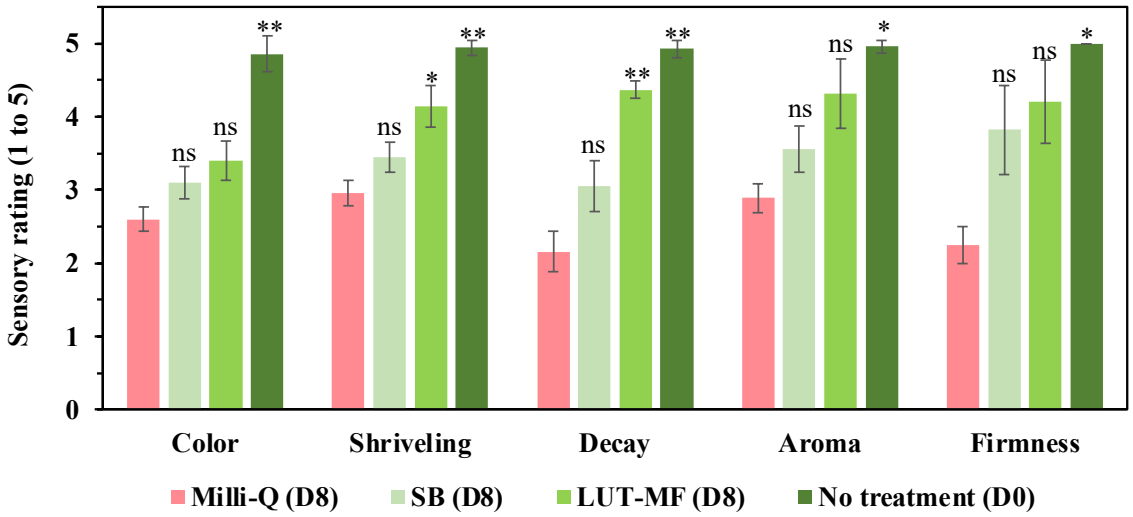

Fig. 3.7. Sensory quality ratings (1–5 scale) for fresh strawberries at 0 day (No treatment, D0), and strawberries treated with LUT-MF, sodium benzoate (SB, D8), and Milli-Q water, and stored at 10°C for 8 days. The sensory panel comprised 15 people including faculty members, and undergraduate, graduate, and postgraduate students (9 males and 6 females; aged between 20 and 62 years). Data are shown as the mean ± standard deviation, n= 3; ns= non-significant, *p<0.1, **p<0.01.

3.4 Conclusions

We prepared and optimized a water-based formulation of poorly water-soluble LUT in surface active [Cho][Ole] IL using a solid-in-water nanodispersion technique. The spherical LUT-MF particles developed with 15 mg/mL [Cho][Ole] and an organic phase showed nanoscale particle size (<100 nm) and enhanced encapsulation efficiency, aqueous solubility, and stability. The LUT-MF demonstrated efficient antioxidant and *in vitro* antibacterial activities, indicating their potential for food preservation. LUT-MF treated strawberries showed marked weight maintenance and less decay than sodium benzoate treated samples and controls after 8 days at 10°C. The LUT-MF treated strawberry samples also exhibited better sensory ratings for shriveling, decay, and color than sodium benzoate treated samples after 8 days of storage. This technique could be used for other water-insoluble flavonoids and would offer a new approach as a promising antioxidant and antimicrobial formulation platform for the application of other natural preservative agents in the food industry. Future

research should focus on the performance of this approach under a variety of environmental conditions with other food items during processing, transport, and storage.

3.5 References

[1] X. Fan, H. Ngo, C. Wu, Natural and Bio-based Antimicrobials: A Review, ACS Symp. Ser. 1287 (2018) 1–24. https://doi.org/10.1021/bk-2018-1287.ch001.

[2] K.R. Ng, X. Lyu, R. Mark, W.N. Chen, Antimicrobial and antioxidant activities of phenolic metabolites from flavonoid-producing yeast: Potential as natural food preservatives, Food Chem. 270 (2019) 123–129. https://doi.org/10.1016/j.foodchem.2018.07.077.

[3] G. Granata, S. Stracquadanio, M. Leonardi, E. Napoli, G.M.L. Consoli, V. Cafiso, S. Stefani, C. Geraci, Essential oils encapsulated in polymer-based nanocapsules as potential candidates for application in food preservation, Food Chem. 269 (2018) 286–292. https://doi.org/10.1016/j.foodchem.2018.06.140.

[4] I. Gutiérrez-del-Río, J. Fernández, F. Lombó, Plant nutraceuticals as antimicrobial agents in food preservation: terpenoids, polyphenols and thiols, Int. J. Antimicrob. Agents. 52 (2018) 309–315. https://doi.org/10.1016/j.ijantimicag.2018.04.024.

[5] L. Wang, C. Zhong, Y. Zu, X. Zhao, Y. Deng, W. Wu, X. Sun, L. Wang, M. Wu, Preparation and characterization of luteolin nanoparticles for enhance bioavailability and inhibit liver microsomal peroxidation in rats, J. Funct. Foods. 55 (2019) 57–64. https://doi.org/10.1016/j.jff.2019.01.054.

[6] Z. Wang, M. Zeng, Z. Wang, F. Qin, J. Chen, Z. He, Dietary Luteolin: A Narrative Review Focusing on Its Pharmacokinetic Properties and Effects on Glycolipid Metabolism, J. Agric. Food Chem. 69 (2021) 1441–1454. https://doi.org/10.1021/acs.jafc.0c08085.

[7] S. Sarmah, S. Pahari, V.K. Belwal, M. Jana, A. Singha Roy, Elucidation of molecular interaction of bioactive flavonoid luteolin with human serum albumin and its glycated analogue using multi-spectroscopic and computational studies, J. Mol. Liq. 318 (2020) 114147. https://doi.org/10.1016/j.molliq.2020.114147.

[8] W. Qian, M. Liu, Y. Fu, J. Zhang, W. Liu, J. Li, X. Li, Y. Li, T. Wang, Antimicrobial mechanism of luteolin against Staphylococcus aureus and Listeria monocytogenes and its antibiofilm properties, Microb. Pathog. 142 (2020) 104056. https://doi.org/10.1016/j.micpath.2020.104056.

[9] Y.Y. Chen, K. Liu, X.Q. Zha, Q.M. Li, L.H. Pan, J.P. Luo, Encapsulation of luteolin using oxidized lotus root starch nanoparticles prepared by anti-solvent precipitation, Carbohydr. Polym. 273 (2021) 118552. https://doi.org/10.1016/j.carbpol.2021.118552.

[10] F. Shakeel, M.M. Alamer, P. Alam, A. Alshetaili, N. Haq, F.K. Alanazi, S. Alshehri, M.M. Ghoneim, I.A. Alsarra, Hepatoprotective effects of bioflavonoid luteolin using self-nanoemulsifying drug delivery system, Molecules. 26 (2021) 1–15. https://doi.org/10.3390/molecules26247497.

[11] L. Tan, C. Liang, Y. Wang, Y. Jiang, S. Zeng, R. Tan, Pharmacodynamic effect of luteolin micelles on alleviating cerebral ischemia reperfusion injury, Pharmaceutics. 10 (2018) 1–17. https://doi.org/10.3390/pharmaceutics10040248.

[12] P. Zhu, L. Chen, Y. Zhao, C. Gao, J. Yang, X. Liao, D. Liu, B. Yang, A novel host-guest complex based on biotin functionalized polyamine-β-cyclodextrin for tumor targeted delivery of luteolin, J. Mol. Struct. 1237 (2021) 130339. https://doi.org/10.1016/j.molstruc.2021.130339.

[13] F. Garavand, M. Jalai-Jivan, E. Assadpour, S.M. Jafari, Encapsulation of phenolic compounds within nano/microemulsion systems: A review, Food Chem. 364 (2021) 130376. https://doi.org/10.1016/j.foodchem.2021.130376.

[14] Y.M. Jeong, J.H. Ha, S.N. Park, Cytoprotective effects against UVA and physical properties of luteolin-loaded cationic solid lipid nanoparticle, J. Ind. Eng. Chem. 35 (2016) 54–62. https://doi.org/10.1016/j.jiec.2015.12.014.

[15] W. Li, H. Chen, Z. He, C. Han, S. Liu, Y. Li, Influence of surfactant and oil composition on the stability and antibacterial activity of eugenol nanoemulsions, Lwt. 62 (2015) 39–47. https://doi.org/10.1016/j.lwt.2015.01.012.

[16] K. Shin, H. Choi, S.K. Song, J.W. Yu, J.Y. Lee, E.J. Choi, D.H. Lee, S.H. Do, J.W.

Kim, Nanoemulsion Vehicles as Carriers for Follicular Delivery of Luteolin, ACS Biomater. Sci. Eng. 4 (2018) 1723–1729. https://doi.org/10.1021/acsbiomaterials.8b00220.

[17] S.S. Imam, S. Alshehri, M.A. Altamimi, A. Hussain, K.H. Alyahya, W.A. Mahdi, W. Qamar, Formulation and Evaluation of Luteolin-Loaded Nanovesicles: In Vitro Physicochemical Characterization and Viability Assessment, ACS Omega. 7 (2022) 1048–1056. https://doi.org/10.1021/acsomega.1c05628.

[18] I. Kazmi, F.A. Al-Abbasi, M.S. Nadeem, H.N. Altayb, S. Alshehri, S.S. Imam, Formulation, optimization and evaluation of luteolin-loaded topical nanoparticulate delivery system for the skin cancer, Pharmaceutics. 13 (2021) 1–17. https://doi.org/10.3390/pharmaceutics13111749.

[19] M.A. Altamimi, A. Hussain, S. Alshehri, S.S. Imam, U.A. Alnemer, Development and Evaluations of Transdermally Delivered Luteolin Loaded Cationic Nanoemulsion: In Vitro and Ex Vivo Evaluations, Pharmaceutics. 13 (2021) 1218. https://doi.org/10.3390/pharmaceutics13081218.

[20] H. Li, Y. Yuan, J. Zhu, T. Wang, D. Wang, Y. Xu, Zein/soluble soybean polysaccharide composite nanoparticles for encapsulation and oral delivery of lutein, Food Hydrocoll. 103 (2020) 105715. https://doi.org/10.1016/j.foodhyd.2020.105715.

[21] M.R. Chowdhury, R.M. Moshikur, R. Wakabayashi, Y. Tahara, N. Kamiya, M. Moniruzzaman, M. Goto, Development of a novel ionic liquid-curcumin complex to enhance its solubility, stability, and activity, Chem. Commun. 55 (2019) 7737–7740. https://doi.org/10.1039/c9cc02812a.

[22] R.M. Moshikur, M.K. Ali, R. Wakabayashi, M. Moniruzzaman, M. Goto, Formation and potential application of micelles composed of biocompatible N-lauroyl-amino acid ionic liquids surfactant, J. Mol. Liq. 320 (2020) 114424. https://doi.org/10.1016/j.molliq.2020.114424.

[23] P. Wang, Y. Wu, A review on colloidal delivery vehicles using carvacrol as a model bioactive compound, Food Hydrocoll. 120 (2021) 106922. https://doi.org/10.1016/j.foodhyd.2021.106922.

[24] R.M. Moshikur, M.K. Ali, M. Moniruzzaman, M. Goto, Recent advances in surface-active ionic liquid-assisted self-assembly systems for drug delivery, Curr. Opin. Colloid Interface Sci. 56 (2021) 101515. https://doi.org/10.1016/j.cocis.2021.101515.

[25] S. Uddin, M.R. Islam, M.R. Chowdhury, R. Wakabayashi, N. Kamiya, M. Moniruzzaman, M. Goto, Lipid-Based Ionic-Liquid-Mediated Nanodispersions as Biocompatible Carriers for the Enhanced Transdermal Delivery of a Peptide Drug, ACS Appl. Bio Mater. 4 (2021) 6256–6267. https://doi.org/10.1021/acsabm.1c00563.

[26] P. Singla, O. Singh, S. Chabba, R.K. Mahajan, Pluronic-SAILs (surface active ionic liquids) mixed micelles as efficient hydrophobic quercetin drug carriers, J. Mol. Liq. 249 (2018) 294–303. https://doi.org/10.1016/j.molliq.2017.11.044.

[27] R. Caparica, A. Júlio, M.E.M. Araújo, A.R. Baby, P. Fonte, J.G. Costa, T. Santos de Almeida, Anticancer Activity of Rutin and Its Combination with Ionic Liquids on Renal Cells, Biomolecules. 10 (2020) 233. https://doi.org/10.3390/biom10020233.

[28] T. Hattori, H. Tagawa, M. Inai, T. Kan, S. ichiro Kimura, S. Itai, S. Mitragotri, Y. Iwao, Transdermal delivery of nobiletin using ionic liquids, Sci. Rep. 9 (2019) 1–11. https://doi.org/10.1038/s41598-019-56731-1.

[29] M.K. Ali, R.M. Moshikur, R. Wakabayashi, M. Moniruzzaman, M. Goto, Biocompatible Ionic Liquid-Mediated Micelles for Enhanced Transdermal Delivery of Paclitaxel, ACS Appl. Mater. Interfaces. 13 (2021) 19745–19755. https://doi.org/10.1021/acsami.1c03111.

[30] A.K. Das, R.A. Sequeira, T.K. Maity, K. Prasad, Bio-ionic liquid promoted selective coagulation of κ-carrageenan from Kappaphycus alvarezii extract, Food Hydrocoll. 111 (2021) 106382. https://doi.org/10.1016/j.foodhyd.2020.106382.

[31] X. Liu, C. Ji, Q. Yang, Z. Bao, X. Fan, Y. Yang, H. Xing, Carboxylate ionic liquids combining low cytotoxicity toward HepG2 cell and high separation efficiency for bioactive molecules, ACS Sustain. Chem. Eng. 5 (2017) 1974–1981. https://doi.org/10.1021/acssuschemeng.6b02778.

[32] M.K. Ali, R.M. Moshikur, R. Wakabayashi, Y. Tahara, M. Moniruzzaman, N. Kamiya, M. Goto, Synthesis and characterization of choline–fatty-acid-based ionic

liquids: A new biocompatible surfactant, J. Colloid Interface Sci. 551 (2019) 72–80. https://doi.org/10.1016/j.jcis.2019.04.095.

[33] A.A.C. Toledo Hijo, H.D.F.Q. Barros, G.J. Maximo, C.B.B. Cazarin, L.B.E. da Costa, J.F.B. Pereira, M.R. Maróstica Junior, A.J.A. Meirelles, Subacute toxicity assessment of biobased ionic liquids in rats, Food Res. Int. 134 (2020) 109125. https://doi.org/10.1016/j.foodres.2020.109125.

[34] R. Wakabayashi, R. Ishiyama, N. Kamiya, M. Goto, A novel surface-coated nanocarrier for efficient encapsulation and delivery of camptothecin to cells, Medchemcomm. 5 (2014) 1515–1519. https://doi.org/10.1039/c4md00179f.

[35] I.M. Shimul, R.M. Moshikur, K. Minamihata, M. Moniruzzaman, N. Kamiya, M. Goto, Amino Acid Ester based Phenolic Ionic Liquids as a Potential Solvent for the Bioactive Compound Luteolin: Synthesis, Characterization, and Food Preservation Activity, J. Mol. Liq. 349 (2022) 118103. https://doi.org/10.1016/j.molliq.2021.118103.

[36] G. Granata, S. Stracquadanio, M. Leonardi, E. Napoli, G.M.L. Consoli, V. Cafiso, S. Stefani, C. Geraci, Essential oils encapsulated in polymer-based nanocapsules as potential candidates for application in food preservation, Food Chem. 269 (2018) 286–292. https://doi.org/10.1016/j.foodchem.2018.06.140.

[37] P. Shao, H. Zhang, B. Niu, L. Jiang, Antibacterial activities of R-(+)-Limonene emulsion stabilized by Ulva fasciata polysaccharide for fruit preservation, Int. J. Biol. Macromol. 111 (2018) 1273–1280. https://doi.org/10.1016/j.ijbiomac.2018.01.126.

[38] S. Rao, G. Xu, X. Lu, R. Zhang, L. Gao, Q. Wang, Z. Yang, X. Jiao, Characterization of ovalbumin-carvacrol inclusion complexes as delivery systems with antibacterial application, Food Hydrocoll. 105 (2020) 105753. https://doi.org/10.1016/j.foodhyd.2020.105753.

[39] K. Kelly, V.M. Whitaker, M.C. do N. Nunes, Physicochemical characterization and postharvest performance of the new Sensation® 'Florida127' strawberry compared to commercial standards, Sci. Hortic. (Amsterdam). 211 (2016) 283–294. https://doi.org/10.1016/j.scienta.2016.09.012.

[40] X. Wang, Y. Jiang, Y.W. Wang, M.T. Huang, C.T. Ho, Q. Huang, Enhancing anti-inflammation activity of curcumin through O/W nanoemulsions, Food Chem. 108 (2008) 419–424. https://doi.org/10.1016/j.foodchem.2007.10.086.

[41] W. Qing, Y. Wang, H. Li, F. Ma, J. Zhu, X. Liu, Preparation and Characterization of Copolymer Micelles for the Solubilization and In Vitro Release of Luteolin and Luteoloside, AAPS PharmSciTech. 18 (2017) 2095–2101. https://doi.org/10.1208/s12249-016-0692-y.

[42] K. Liu, X.Q. Zha, Q.M. Li, L.H. Pan, J.P. Luo, Hydrophobic interaction and hydrogen bonding driving the self-assembling of quinoa protein and flavonoids, Food Hydrocoll. 118 (2021) 106807. https://doi.org/10.1016/j.foodhyd.2021.106807.

[43] M.K. Ali, R.M. Moshikur, R. Wakabayashi, M. Moniruzzaman, N. Kamiya, M. Goto, Biocompatible Ionic Liquid Surfactant-Based Microemulsion as a Potential Carrier for Sparingly Soluble Drugs, ACS Sustain. Chem. Eng. 8 (2020) 6263–6272. https://doi.org/10.1021/acssuschemeng.9b07773.

[44] Y. Wei, C. Wang, X. Liu, A. Mackie, M. Zhang, L. Dai, J. Liu, L. Mao, F. Yuan, Y. Gao, Co-encapsulation of curcumin and β-carotene in Pickering emulsions stabilized by complex nanoparticles: Effects of microfluidization and thermal treatment, Food Hydrocoll. 122 (2022) 107064. https://doi.org/10.1016/j.foodhyd.2021.107064.

[45] A.M. Popov, A.N. Osipov, E.A. Korepanova, O.N. Krivoshapko, A.A. Artyukov, A.A. Klimovich, A study of the antioxidant and membranotropic activities of luteolin using different model systems, Biophys. (Russian Fed. 61 (2016) 843–850. https://doi.org/10.1134/S0006350916060221.

[46] S. Chen, Q. Li, D.J. McClements, Y. Han, L. Dai, L. Mao, Y. Gao, Co-delivery of curcumin and piperine in zein-carrageenan core-shell nanoparticles: Formation, structure, stability and in vitro gastrointestinal digestion, Food Hydrocoll. 99 (2020) 105334. https://doi.org/10.1016/j.foodhyd.2019.105334.

[47] A. Adamczak, M. Ożarowski, T.M. Karpiński, Antibacterial Activity of Some Flavonoids and Organic Acids Widely Distributed in Plants, J. Clin. Med. 9 (2019) 109. https://doi.org/10.3390/jcm9010109.

[48] L.R. Jorge, L.K. Harada, E.C. Silva, W.F. Campos, F.C. Moreli, G. Shimamoto, J.F.B. Pereira, J.M. Oliveira, M. Tubino, M.M.D.C. Vila, V.M. Balcão, Non-invasive Transdermal Delivery of Human Insulin Using Ionic Liquids: In vitro Studies, Front. Pharmacol. 11 (2020) 1–17. https://doi.org/10.3389/fphar.2020.00243.

[49] M. Harich, B. Maherani, S. Salmieri, M. Lacroix, Evaluation of antibacterial activity of two natural bio-preservatives formulations on freshness and sensory quality of ready to eat (RTE) foods, Food Control. 85 (2018) 29–41. https://doi.org/10.1016/j.foodcont.2017.09.018.

[50] S. Hajji, I. Younes, S. Affes, S. Boufi, M. Nasri, Optimization of the formulation of chitosan edible coatings supplemented with carotenoproteins and their use for extending strawberries postharvest life, Food Hydrocoll. 83 (2018) 375–392. https://doi.org/10.1016/j.foodhyd.2018.05.013.

[51] X. Liu, X. Cui, D. Ji, Z. Zhang, B. Li, Y. Xu, T. Chen, S. Tian, Luteolin-induced activation of the phenylpropanoid metabolic pathway contributes to quality maintenance and disease resistance of sweet cherry, Food Chem. 342 (2021) 128309. https://doi.org/10.1016/j.foodchem.2020.128309.

[52] S. Shankar, D. Khodaei, M. Lacroix, Effect of chitosan/essential oils/silver nanoparticles composite films packaging and gamma irradiation on shelf life of strawberries, Food Hydrocoll. 117 (2021) 106750. https://doi.org/10.1016/j.foodhyd.2021.106750.

[53] H. Inselberg, M.C. do Nascimento Nunes, Using Cannabidiol as a potential postharvest treatment to maintain quality and extend the shelf life of strawberries, Postharvest Biol. Technol. 173 (2021) 111416. https://doi.org/10.1016/j.postharvbio.2020.111416.

[54] F. Li, Y. Fu, H. Yang, Y. Tang, The inhibition mechanism of luteolin on peroxidase based on multispectroscopic techniques, Int. J. Biol. Macromol. 166 (2021) 1072–1081. https://doi.org/10.1016/j.ijbiomac.2020.10.262.

CHAPTER-4: FORMULATION AND CHARACTERIZATION OF CHOLINE OLEATE BASED MICELLES FOR CO-DELIVERY OF LUTEOLIN, NARINGENIN, AND QUERCETIN

4.1 Introduction

Flavonoids, the most prevalent class of plant polyphenols, can be divided into several subfamilies such as flavones (such as luteolin), flavanols (such as catechins), flavanones (such as naringenin), flavonols (such as quercetin), and isoflavones [1] [2]. Flavonoids are connected to a variety of advantages for human health as well as plant defense mechanisms. Flavonoids and other phenylpropanoids act as effective antimicrobials or immune boosters for plants, defend them from a variety of abiotic and biotic stresses and boost their immunity to a wide range of diseases. Flavonoids, which are components of the human diet and provide health advantages, have anti-inflammatory, anti-allergic, anti-inflammatory, hepatoprotective, and anti-proliferative properties [1,3–6]. Large number of these compounds perform as antimicrobial and antioxidant agents, destroying microbial cells and obstructing the pathways used by microbes to produce bioactive molecules. The researchers' interest in studying flavonoids' numerous positive functions in the industry of food and drugs has been fueled by customers' growing demand for natural products. Luteolin (Lut), quercetin (Quer), naringenin (Nar) and other flavonoids are mainly found in various fruits, vegetables, beverages as well as in flowers, leaves, seeds, etc. [3,4,7]. Luteolin has cardioprotective, anticarcinogenic, antioxidant, and antimicrobial properties and is prevalent in radicchio, celery, peppermint, broccoli, carrots, pepper, oregano, thyme, belimbi, lemons, and other foods [8,9]. Quercetin, a naturally occurring pentahydroxyflavone, is commonly present in foods like onions (Allium cepa), apples, red wine, tomatoes, red grapes, tea, and kale and it has just been granted GRAS (Generally Recognized As Safe) classification by the USFDA. Numerous therapeutic properties of quercetin include anti-inflammatory, anti-cancer, antioxidant, antiviral, and antibacterial effects [3,10,11]. Fruits including grapefruit, orange juice, tomatoes, and bergamot are rich sources of naringenin (4′,5,7-trihydroxyflavanone). Anti-inflammatory, antioxidant, anticancer, anti-diabetic, hepatoprotective, and neuroprotective activity are some of its possible health-promoting properties [1,12,13].

Thousands of flavonoids and other phenylpropanoids captured in the epidermis of therapeutic plants, spices, and herbs to fight a variety of microbes [5]. Perhaps their synergistic potentialities give plants a stronger defense against different diseases and serve as potent antimicrobials or immunological boosters. Numerous investigations also demonstrated the reduction of minimal effective doses for their combinations [14,15]. A

wide variety of microorganisms may thrive well in most foodstuffs. Food deterioration is caused by food spoilage and pathogenic microorganisms, including bacteria, yeasts, molds, parasites, protozoa, pathogenic algae, and their toxins [16]. Different types of antibacterial drugs are required due to the variations in their structural composition and sensitivity to certain adverse environments [17]. Different flavonoids exhibit antimicrobial activity through various mechanisms. For instance, luteolin's antibacterial effects on *Trueperella pyogenes* include affecting the integrity of the cell wall and membranes, modifying protein expressions, inhibiting nucleic acid synthesis, and interrupting energy metabolism [18]. The antibacterial properties of quercetin have been demonstrated through cell membrane damage, altered permeability, inhibition of nucleic acid and protein synthesis, and mitochondrial dysfunction and antifungal effects through decreased cell adhesion and effects on the genes involved in biofilm formation [3,19]. While naringenin disrupts the fatty acid composition and protein conformation in membranes and preferentially form groove binding to genomic DNA [20]. Higher concentrations of phytochemical substances, such as flavonoids and essential oils, are needed to inhibit bacteria in foods as opposed to laboratory media for their rapid dissemination in foods and denaturation with food components [21]. Since the use of natural preservatives can change the flavor of foods and go beyond the flavor threshold of consumer acceptability, higher concentrations may have an organoleptic impact [22]. Combinations of flavonoids could reduce any negative organoleptical effects and generate synergistic benefits against spoilage and pathogenic microbes [22–25]. However, the hydrophobic ring structure of flavonoids restricts their bio-functionality. The bioactivities of luteolin are hindered by its low water solubility (1.09 ± 0.16 μg/mL) [8] and poor bioavailability (26 ± 6%) [26]. Quercetin has poor aqueous solubility (2.15 μg/mL) [27], poor bioavailability (4%) [28], and a serious photosensitivity-related problem. The low aqueous solubility (46 ± 6 μg/mL) of naringenin results in poor bioavailability (4- 5.81%), poor permeability, instability and the substantial first pass metabolism before reaching the systemic circulation [4,29]. Due to the poor solubility of flavonoids in hydrophilic matrices, their application in hydrophilic food systems is limited. Appropriate delivery systems could overcome the limitations of flavonoids such as low solubility, poor bioactivity, and alteration of food organoleptic properties. Encapsulation of flavonoids in microemulsions, nanoemulsion, solid lipid nanoparticles, liposomes, or micelles-based system can be a promising delivery system in food. A high surfactant concentration and a large particle size in formulation are limitations of emulsion and solid lipid nanoparticle-based delivery systems [8,23]. Biocompatible surface-active ionic liquids,

such as choline oleate, have been revealed as suitable substitutes for traditional surfactants in the delivery of hydrophobic phytochemical drugs for their superior surface-active characteristics, high thermal stability, and lower toxicity [30,31]. Recently, the micelle-based delivery has become a cutting-edge method because of their capacity for self-assembly, the controlled release profile, and the high drug encapsulation efficiency. Thus, luteolin, quercetin, and naringenin can all be co-delivered together as a micelle to increase their solubility and performance in the food system at lower concentrations.

The aim of this work was to develop choline oleate assisted micellar formulations of luteolin, quercetin and naringenin in combinations to increase their solubility and bioactivity. Three different formulations were selected by visual observation from the six prepared formulations. The selected formulations, naringenin loaded micellar formulation (Nar-MF), luteolin and naringenin loaded micellar formulation (LN-MF), and luteolin, naringenin and quercetin loaded micellar formulation (LNQ-MF), were characterized by DLS, XRD and TEM. The encapsulation efficiency, loading capacity and maximum aqueous dispersibility were measured. Finally, their in vitro release profile, the antioxidant capacity, and the antibacterial capability were also evaluated.

4.2 Materials and methods

4.2.1 Materials

Tokyo Chemical Industry Co. Ltd, Japan supplied Luteolin (purity >98.0%) and Sigma Aldrich (USA) provided naringenin, and quercetin (purity ≥95%). Choline chloride, oleic acid, silver oxide, methanol, phosphoric acid, and cyclohexane were purchased from Wako Pure Chemicals Industries, Japan. All other required reagents were analytical grade. The choline oleate ([Cho][Ole]) was synthesized by a previously described procedure [8].

4.2.2 Preparation of micellar formulations

The previously published method was slightly modified to adapt the nanodispersion process for the preparation of micellar formulations [8,32] Briefly, Lut, Nar and Quer were dissolved in the acetone-methanol (1:2) mixed solution at 6.67 mg/mL concentration. Fifty μL of each Lut, Nar or Quer solution (total 150 μL) was mixed with 850 μL of cyclohexane to produce the organic phase. Surface active choline oleate was solubilized at 5 mg/mL

concentration to yield the aqueous phase. Oil-in-water emulsion of LNQ was prepared by mixing the oil phase and the aqueous phase at 1:3 ratio using a high pressure homogenizer (Polytron, Kinematica, Bohemia, NY, USA) at 16000 rpm for 2.5 min. Liquid nitrogen was used for 30 minutes to freeze the emulsion immediately. A solid LNQ–[Cho][Ole] formulation was obtained after freeze-drying the oil-in-water emulsion. The obtained LNQ–[Cho][Ole] solids were dispersed in water to give a precipitate free dispersion of luteolin, naringenin and quercetin (LNQ) loaded micellar formulation (LNQ-MF). To prepare Nar-MF and Quer-MF, 1 mL of the organic phase containing 1.0 mg of naringenin, and quercetin were used respectively. One mL of the organic phase containing 0.5 mg of corresponding flavonoid was used for LN-MF, LQ-MF, NQ-MF.

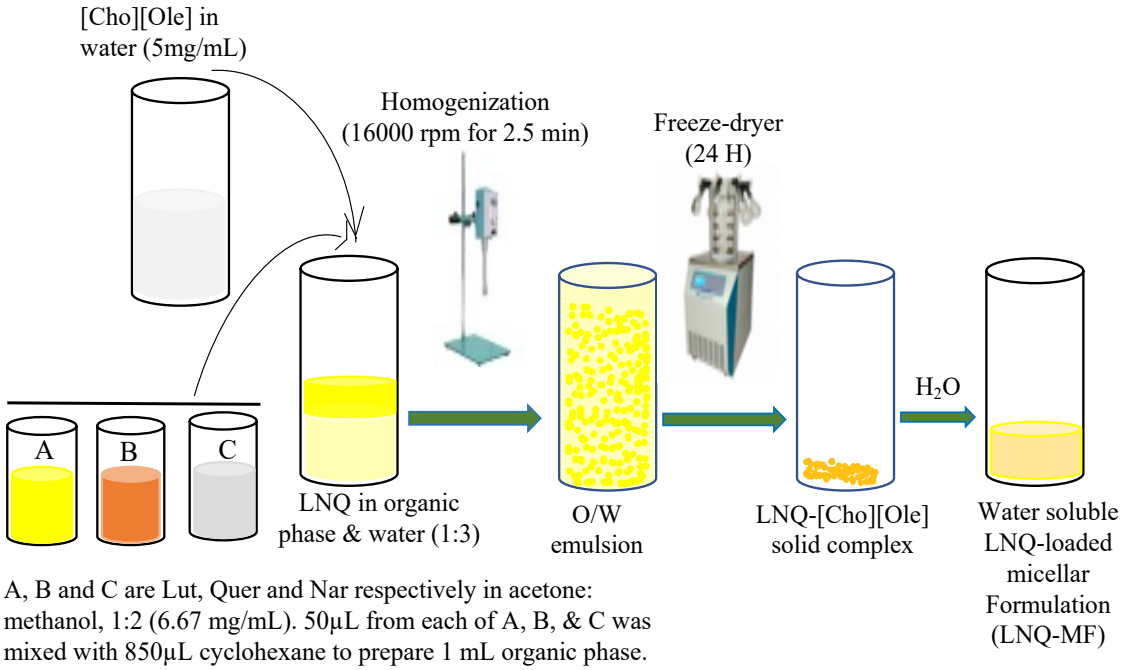

Scheme 4.1. Preparation steps of Lut, Nar and Quer loaded micellar formulation (LNQ-MF).

4.2.3 Characterizations of micellal formulations

4.2.3.1 Particle size, size distribution, and charge measurements

Dynamic light scattering (DLS) studies using a Zetasizer Nano ZS (Nano series, Malvern Instruments Ltd., USA) were conducted to determine the average particle size, the size distribution, and the zeta potential (ζ). A quartz cuvette of 1 cm path length was utilized for the measurements. Measurements were taken after 5 minutes of equilibration before each measurement and an average of 5 measurements provided the mean data. The tests were

repeated three times at 25°C. Data analysis was performed using the Zetasizer Version 7.03 software.

4.2.3.2 Transmission electron microscopy (TEM) analysis

The JEOL JEM-2010 Transmission Electron Microscope was used to examine the shape of the Nar-MF, LN-MF, and LNQ-MF. Freeze dried Nar-MF, LN-MF, and LNQ-MF were dissolved in water at a concentration of 0.5 mg/mL, and 2 μL of the samples were placed on separate copper grids coated with carbon and allowed to dry for 2 minutes. A piece of filter paper was used to remove extra sample from the copper grid, and 2.5 μL of Milli-Q water was used for a single wash. To stain the samples, 2.0 μL of uranyl acetate was applied and set aside for 2 minutes. The TEM grid was vacuum-dried in a desiccator. Finally, TEM was used to get the morphology at a 120 kV accelerating voltage.

4.2.3.3 XRD

The XRD spectra of free flavonoid (Lut, Nar and Quer), free carrier (blank MF), lyophilized micellar formulations of flavonoids, and the physical mixer (free flavonids and blank-MF) were obtained by the X-ray diffractometer (Rigaku, Smartlab, Tokyo, Japan) with the Cu-Kα radiation (λ = 1.54182 Å), operating at 40 kV and 30 mA. The spectra were acquired using the following parameters: the diffraction angle (2θ) 5°– 40°, the scanning rate 10°/min, and the scanning step 0.02°.

4.2.3.4 Fourier transform infrared analysis

The molecular interactions between [Cho][Ole] and flavonoids in the micelles were examined through FT-IR spectrometer (Perkin Elmer, Waltham, MA). FT-IR of the free Lut, Nar, and Quer as a powder form, and freeze-dried [Cho][Ole], Nar-MF, LN-MF, and LNQ-MF (without redispersing into water) were measured in the wavenumber range 500−4000 cm^{-1} with accumulation of 20 scans and resolution of 4 cm^{-1}.

4.2.4 HPLC conditions for flavonoids measurement

Utilizing an HPLC, the flavonoid contents (Lut, Nar, and Quer) of several samples were determined. The HPLC system consisted of a photo diode array (PDA) detector, an auto-sampler, pump, and a column oven controller (JASCO International Co. Ltd., HachioJi,

Tokyo, Japan). The mobile phase had a 43:57 (v/v) ratio of methanol to 0.2% phosphoric acid aqueous solution and flowed at the rate of 1.0 mL/min [8]. The chromatographic separation of flavonoids was performed on the octadecyl (C_{18}) column (GL Sciences Inc., Japan) for 85 min by isocratic elution. The absorbance of the flavonoids was detected at 230 nm for Nar and 350 nm for Lut and Quer [11]. Twenty μL of standards and samples were injected and the temperature of the column oven was set at 25 °C. The standard stock solution of Lut, Nar, and Quer was prepared at the concentration of 1 mg/mL in methanol and diluted to 2-32 g/mL with the mobile phase.

4.2.4.1 Encapsulation efficiency (EE), Loading efficiency (LE) and Loading capacity (LC)

EE is the measurement of the drug concentration encapsulated within the carrier substance. Non-encapsulated drugs are crystalline in nature and can not pass through the filter [11]. EE of optimized Nar-MF, LN-MF and LNQ-MF was evaluated by a filtration method. For EE, HPLC was used to assess concentrations in a filtered sample and unfiltered sample. Excess amount of flavonoids were added to the fixed amount of carrier materials to determine LC of prepared samples and non-encapsulated flavonoids were removed using the 0.22 μm filter. The EE (%) [33], LE (%) [23] and LC (%) [34] were estimated by the following equations-

EE (%) = Flavonoid in filtered sample/ Flavonoid in unfiltered sample × 100 …….. (1)

LE (%) = Flavonoid in filtered sample/ Total added flavonoid in sample × 100 …….. (2)

LC (%) = Flavonoid in filtered sample/ Total [Cho][Ole] added × 100 ……..... (3)

4.2.4.2 Maximum solubility

The maximum solubility of flavonoids (Lut, Nar and Quer) in the formulations was measured using an HPLC system [33]. The freeze-dried formulation was solubilized in 1 mL Milli-Q by gentle shaking and rotating. Then this dissolved formulation was transferred to another freeze-dried formulation and this process was repeated until the solution turned turbid. The insoluble flavonoids were excluded through centrifugation (10000 rpm for 10 minutes) and a syringe filter measuring 0.22 μm was used to filter the supernatant. Flavonoids that had been solubilized were diluted with the mobile phase and then measured using an HPLC instrument.

4.2.5 ^{1}H NMR

^{1}H NMR experiments were conducted to explore the interactions between free [Cho][Ole], Lut, Nar, and Quer in their LNQ-MF on a JEOL ECZ400S 400 MHz spectrometer (Tokyo, Japan). All the investigated compounds were solubilized in deuterated dimethyl sulfoxide (DMSO-d_6) solution at 25°C and tetramethylsilane (TMS) was used as internal standard. The spectra were processed in JEOL Delta Software (version 5.3.1).

4.2.6 Stability Assay

The stability of Nar-MF, LN-MF and LNQ-MF was investigated utilizing DLS measurement and visual inspection by 30 days storage at 4°C, 25°C, and 37 °C. To determine whether the formulation was stable, the particle size and PDI were examined.

4.2.7 *In vitro* release profile

The Nar and Quer were dissolved in DMSO and then they were mixed with Milli-Q water to prepare the Nar suspension and the Quer suspension in 20% DMSO solution. Nar-loaded MF, Lut-Nar loaded MF and Lut-Nar-Quer loaded MF were prepared in water. The releasing media was prepared by mixing 30% ethanol with phosphate-buffered saline (PBS) (pH 7.4) [11]. Those suspension and micellar formulations were used to explore the release pattern in 25 mL medium at 37°C using a dialysis membrane (12–14 kD, Spectrum Laboratories, Inc., USA). 0.5 mL of micellar formulations and suspensions (each containing 0.5 mg flavonoid) were added to a pre-activated membrane. The dialysis bag was submerged in the release media after being hermetically sealed on both sides using plastic clips. The releasing medium was constantly being stirred at a speed of 100 rpm. At various time intervals (0.08 to 12 hours), sampling (1 mL) was done, and the removed sample volume was refilled with the preheated fresh medium. Each sample (1 mL extracted) underwent membrane filtering before being diluted twice in methanol. The HPLC apparatus was used for simultaneous analysis for the duplicate samples of Lut, Nar, and Quer at 230 nm and 350 nm.

4.2.8 Antioxidant activity

The antioxidant potential of free Nar and Quer, and optimized Nar-MF, Quer-MF, LN-MF and LNQ-MF was evaluated by 1,1-diphenyl-2-picrylhydrazyl (DPPH) technique [8,35].

Micellar formulations and free Nar and Quer samples in the methanol solution were produced at various concentrations (25, 50, and 100 µg/mL). Twenty-five µL of samples were placed in a 96-well plate along with 175 µL of the 0.1 mM methanolic DPPH solution. Instead of adding the sample to the DPPH solution, milli-Q water was used as a control. The mixtures were kept at 25°C in complete darkness for 30 minutes. The absorbance of the samples was measured at 517 nm using the Microplate Reader. The percentage of antioxidant activity was determined as follows:

Antioxidant activity (%) = (Ac – As)/ Ac × 100 ……..…… (4)

where Ac represents the DPPH absorbance in Milli-Q water, and As represents the absorbance of the test sample.

4.2.9 Antibacterial Assays

Antibacterial activities of Nar-MF, Quer-MF, LN-MF and LNQ-MF were tested against *Staphylococcus aureus* (ATCC 6538), *Bacillus subtilis* (ATCC 6051), *Escherichia coli* (ATCC 25922), and *Salmonella enterica* (ATCC 8400). Stock cultures of bacteria were kept at -80°C in cryovials and then cultivated for 24 hours at 37°C on Mueller-Hinton (M-H) agar (Sigma-Aldrich). Before testing, a single colony from an M-H agar plate was grown for 24 hours in M-H broth and diluted in M-H broth to a McFarland turbidity of 0.5 (1 x 10^8 colony forming unit per mL).

Flat-bottom polystyrene 96-well microplates were used to test the minimum inhibitory concentration (MIC) and minimum bactericidal concentration (MBC) of the developed micellar formulations using the serial microdilution method, which has been described in the literature with some modifications [36]. After freeze drying, the solid MF was dissolved to a 4 mg/mL concentration in the M-H broth medium, filtered through a 0.2 µm membrane filter, and serially diluted in a 96-well plate. Two hundreds µL of the M-H broth with MF were placed in each well, along with 10 µL of bacteria inoculum (1 x 10^6 CFU/mL). The M-H broth without bacteria was employed as a blank, while bacterial suspensions in the M-H broth served as the control. The 96-well plate was cultured at 37°C for 24 hours and the microplate reader was used to detect absorbance at 595 nm. Incremental increase approach was used to find out the exact MIC.

For MBC estimation, the 24 h suspension was diluted, spotted, and incubated for a further 18 hours at 37°C for CFU counting on M-H agar plates. The MBC was found to be the substance at which all bacteria died (inability to reculture bacteria).

Fractional inhibitory concentration indices (FICI) was calculated by evaluating individual FIC of the tested flavonoids to check whether the increase in antibacterial activity observed with a mixture of flavonoids.

FIC of flavonoid= MIC of single flavonoid in combination/ MIC of Lut alone ……... (5)

FICI for LN-MF= FIC of Lut + FIC of Nar …….……..…... (6)

FICI for LNQ-MF= FIC of Lut + FIC of Nar + FIC of Quer ……..……..…..... (7)

The effect of flavonoids in the mixture was judged to be synergistic when the FICI value was smaller than 0.9 and addiive when it was ≥ 0.9 [37].

4.2.10 Milk preservation test

Tetra Pack UHT milk from local market was purchased and mixed with sterile water, Nar-MF, and LNQ-MF (2 mg/mL) at 1:1 ratio. *S. aureus* (10^6 CFU/mL) was inoculated and cultured at 25℃ and 37℃ for 72 hours. After 72 hours, milk was poured on the petri dish and stood for 15 minutes. Then then supernatant was removed, and the precipitation of the milk was observed [38].

4.3 Results and discussion

4.3.1 Preparation and optimization of micellar formulations

An encapsulation technique is used to cover the bioactive compounds to facilitate the poor aqueous solubility and instability. Here, we have encapsulated three flavonoids (Lut, Nar and Quer) in six different combinations, i.e., Naringenin-loaded micellar formulation (Nar-MF), Quercetin-loaded micellar formulation (Quer-MF), Luteolin and Naringenin-loaded micellar formulation (LN-MF), Luteolin and Quercetin-loaded micellar formulation (LQ-MF), Naringenin and Quercetin-loaded micellar formulation (NQ-MF), and Luteolin, Naringenin and Quercetin-loaded micellar formulation (LNQ-MF). All the MFs were prepared by the solid-in-water nanodispersion technique using a surface-active choline

oleate ([Cho][Ole]) ionic liquid. Our previous result showed that [Cho][Ole] in the presence of an organic solvent and homogenization was suitable carrier material for Lut encapsulation because of good solubility and bioactivity [8]. SAILs or surfactants reduce the interfacial tension of emulsion and thus play an important role in emulsion stability and particle size. The optimum amount of [Cho][Ole] required to form the MF was investigated by varying the [Cho][Ole] concentration. Visual observation and the particle size measurement showed that all the six MFs produced clear and transparent formulations at the different concentration of [Cho][Ole] (10 to 35 mg/mL) on 0 day. The optimum concentration of emulsifying agent is required to prevent the particle aggregation. While transparent formulations indicate the smaller particle size because of the easily transmittance of wavelength of light through small droplets [39]. Quer-MF, LQ-MF and NQ-MF became turbid after 10 days storage at room temperature (25°C) and Nar-MF, LN-MF and LNQ-MF prepared with 15 mg/mL [Cho][Ole] were transparent with monomodal particle distribution. Thus, we have selected Nar-MF, LN-MF and LNQ-MF for the further study.

4.3.2 Characterization of Nar-MF, LN-MF and LNQ-MF

To explore the particle sizes, size distributions and zeta potential of the micelles in the aqueous solution, dynamic light scattering (DLS) experiments were conducted. The average particle size of Nar-MF, LN-MF and LNQ-MF were 113.0 nm, 110.3 nm, and 150.2 nm respectively (Table 4.1). The particle sizes of Nar nanoparticle was found to be 90 nm which is quite near to our Nar-MF (113 nm) [29]. Tiny particles aggregate easily and larger particle hamper drug loading capacity [25]. Our previous study showed that the size of Lut-MF using the [Cho][Ole] was 75.43 nm [8]. Binary (LN-MF) and ternary (LNQ-MF) co-delivery of flavonoids demonstrated larger particle size which agree well with a previous study where the ternary nanoparticle demonstrated larger particle size [25]. Lower PDI denotes more homogeneity to the samples. PDI <0.2 are considered to be standard, while PDI >0.5 are suggestive of a wide size distribution [36]. The PDI of the developed MFs was less than 0.25 indicating monomodal size distribution of optimized formulation. The zeta potential is the surface charge on particles, and it could specify the stability of aqueous micelles. The repulsive forces of the zeta potential surmounted the attractive van der Waals forces and facilitate to maintain stability. The Nar-MF, LN-MF and LNQ-MF showed a zeta potential of less than -90 mV and this value indicated the possibility of a long term stability of the formulations due to their repulsive forces stabilizing the particles against agglomeration.

Changes in the zeta potential after addition of flavonoids suggest some change in interfacial composition [23]. Curcumin formulation prepared by [Cho][Ole] also displayed a high negative zeta potential (-84.1 mV) [33].

Table 4.1. Z-average size, polydispersity index and surface charge of Nar-MF, LN-MF, and LNQ-MF.

Formulations	Particle size (nm)	PDI	Zeta potential (mV)
Nar-MF	113.0	0.228	-91.5
LN-MF	110.3	0.134	-97.2
LNQ-MF	150.2	0.117	-105.5

The morphology of the Nar-MF, LN-MF, and LNQ-MF was determined by TEM (Fig. 4.1). The photographs of the Nar-MF, LN-MF, and LNQ-MF obtained by TEM clearly show the spherical shapes, which could be attributed to the encapsulated formulation. Interestingly, Nar-MF and LN-MF showed some adhesion.

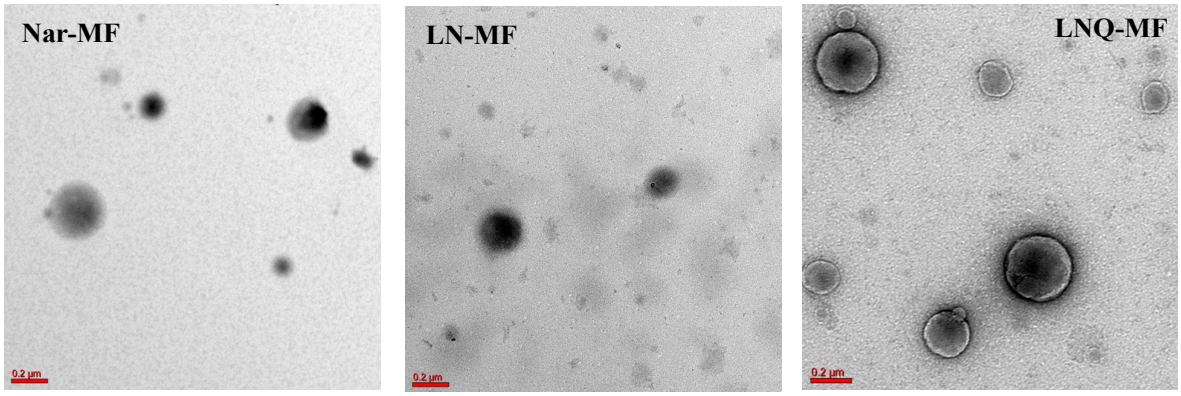

Fig. 4.1. TEM images of Nar-MF, LN-MF, and LNQ-MF at10k resolution.

The XRD diffractogram of free Lut, Nar, Quer, [Cho][Ole] alone, physical mixture of Lut, Nar, Quer and [Cho][Ole], and LNQ-MF were constructed and are shown in Fig. 4.2. Sharp peaks were visible in the free Lut at 13.9°, 15.3°, 17.1°, 26.6°, 27.4°, and 28.6°, free Nar showed sharp peaks at 10.7°, 15.7°, 18.0°, 20.3°, 22.2°, 23.7°, and 25.3° and some small peaks were observed at 12.4°, 13.1°, 14.1°, 22.2°, and 23.6° for free Quer. All these peaks showed very much resemblance with the peaks found in the previous studies [29,34]. These results indicated that free Lut, Nar and Quer were all in a crystalline state [29,34]. Similar

strong peaks with smaller intensities were also visible in the physical mixer of free Lut, Nar, and Quer with [Cho][ole]. Those visible peaks of free Lut, Nar, and Quer totally disappeared in LNQ-MF, indicating their presence in micellar formulations as the amorphous state and this result agrees well with a literature [35].

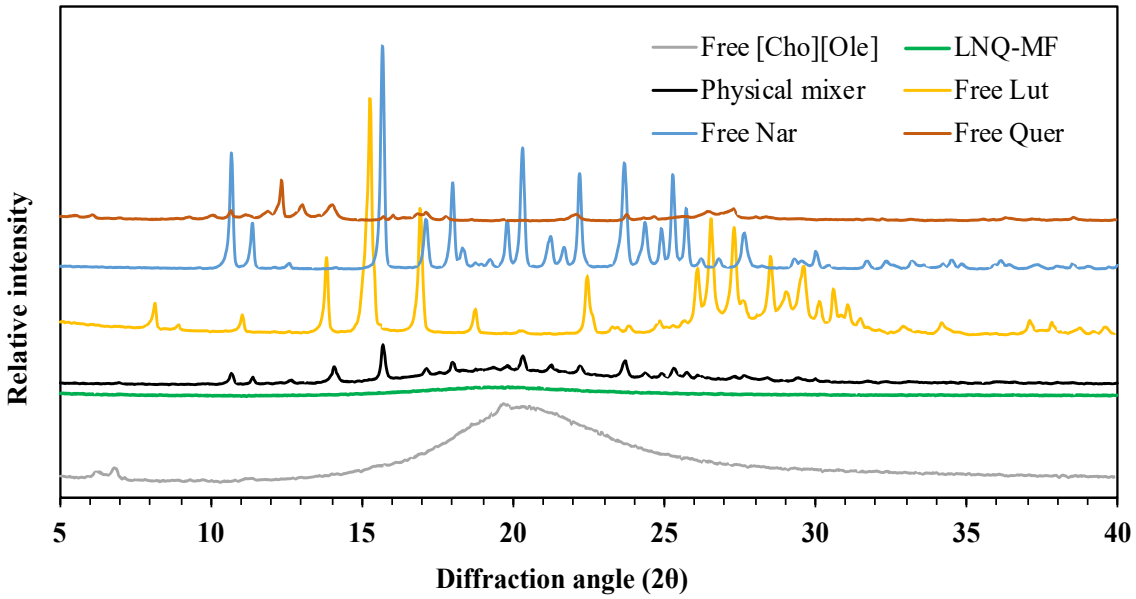

Fig. 4.2. XRD patterns of free Lut, Nar, Quer and [Cho][Ole], LNQ-MF, and a physical mixture.

FT-IR spectroscopy was utilized to find out the molecular interactions between [Cho][Ole] and flavonoids in their MF. The FT-IR results of free Lut, Nar, Quer, and freeze-dried [Cho][Ole], Nar-MF, LN-MF, and LNQ-MF are presented in Fig. 4.3. The FT-IR spectrum of free LUT showed the characteristic peaks at 1664 cm^{-1}, 1608 cm^{-1}, 1508 cm^{-1}, 1443 cm^{-1}, 1337 cm^{-1}, and 1155 cm^{-1}. Free Nar demonstrated peaks at 1607 cm^{-1}, 1584 cm^{-1}, 1308 cm^{-1}, 1248 cm^{-1}, 1155 cm^{-1}, and 831 cm^{-1}. Similarly free Quer showed their characteristic peaks at 1666 cm^{-1}, 1608 cm^{-1}, 1513 cm^{-1}, 1315 cm^{-1}, 1242 cm^{-1}, 1092 cm^{-1}, and 931 cm^{-1} for their functional groups. Besides those, free Lut, Nar and Quer depicted their vibrational stretching peaks at ~3390 to 3200 cm^{-1} for -OH groups. Free [Cho][Ole] exhibited broad and strong vibrational peaks for asymmetric and symmetric C-H stretching at 2925 cm^{-1} and 2855 cm^{-1}. Other functional groups of [Cho][Ole] also demonstrated peaks at 1572 cm^{-1}, 1390 cm^{-1}, 1090 cm^{-1}, and 955 cm^{-1}. Similar characteristic peaks of free Lut, Nar, and Quer were reported in previous reports [1,34,40]. The vibration spectrums of -OH group of free Lut, Nar, and Quer were totally absent and no new characteristic peaks were observed in their MF. All the MFs showed only the characteristic peaks of [Cho][Ole],

indicating the presence of [Cho][Ole] in all MFs. The absence of the characteristic absorption bands of free Lut, Nar, and Quer in MF spectrum suggested that they were successfully encapsulated in micelles by [Cho][Ole]. These findings are consistent with earlier investigations [34,41–43] which showed that the peaks of free flavonoids such as Lut, Quer, curcumin, and resveratrol disappeared when encapsulated by carrier materials.

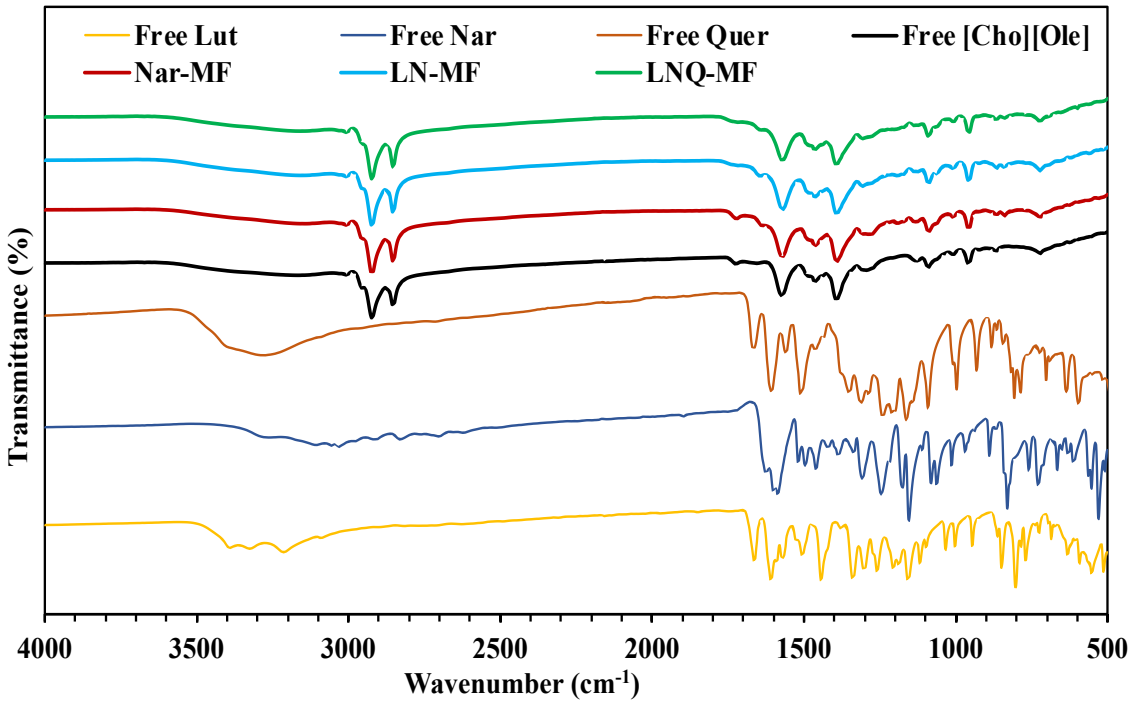

Fig. 4.3. FT-IR spectra of free Lut, Nar, Quer, [Cho][Ole], and Nar-MF, LN-MF, and LNQ-MF.

The obtained results from DLS, TEM, XRD, and FT-IR indicated that Nar-MF, LN-MF, and LNQ-MF were spherical in shape with nanometer range particle sizes and all the MFs were in amorphous state and successfully encapsulated by [Cho][Ole].

4.3.3 Encapsulation efficiency (EE), Loading efficiency (LE) & Loading capacity (LC)

One of the most important indicators for the performance of carrier materials is the encapsulation efficiency. The EE depends on the carrier material composition, which protect the compounds against adverse circumstances. The EE (%) of Nar-MF, LN-MF, and LNQ-MF was 93.7 ± 2.4, 95.2 ± 0.7 and 97.4 ± 1.6 respectively. The EE of Nar in nanoliposome formulated with 1% lecithin and Quer in nanoparticles by whey proteins were 63.89% and 51.1% respectively [12,44]. The EE of resveratrol and quercetin from their co-delivered PLGA nanoparticles was 46% and 52% respectively [45]. The entrapment efficiency of co-

delivery of quercetin and piperine in the nanostructured lipid carriers was found to be 91.95% (±4.44) and 93.72% (±1.02) for quercetin and piperine, respectively, which was in good agreement with this study [46]. It indicated the significantly increased encapsulation capacity of SAIL [Cho][Ole], indicating [Cho][Ole] as a good carrier material to deliver flavonoid.

The loading efficiency (LE) indicates the mass of flavonoids incorporated into the formulation through the preparation steps. The LE (%) of Nar-MF, LN-MF, and LNQ-MF in this study was 95.6 ± 3.3, 83.9 ± 2.8 and 95.0 ± 4.6 respectively, indicating very low loss of flavonoids in the processing steps. The LE of nanoparticles that contained either curcumin or resveratrol was approximately 63% and 78%, respectively, whereas they were approximately 71% and 85% for nanoparticles that contained both curcumin and resveratrol, which revealed the greater LE for co-delivery of flavonoids [23].

The LC (%) of [Cho][Ole]-based MF showed the highest LC for Nar-MF, and LC for LN-MF, and LNQ-MF was similar (Fig. 4.4). the LC of hydrophobic flavonoids depends on the type of carrier material. Previous studies showed the LC of Quer was 33.9% for quinoa protein, 2.5% for hydroxypropyl-β-cyclodextrin and 1.4% for compritol ATO-888 [34,44,46]. The LC results indicated that the [Cho][Ole]-based MF could be a promising co-delivery system for flavonoids.

4.3.4 Maximum solubility

The maximum solubility of Lut, Nar and Quer (together, LNQ) was 7.78 ± 1.35 mg for per mL water, and Lut-Nar from LN-MF and Nar from Nar-MF were 5.15 ± 0.38 mg/mL and 7.1 ± 0.55 mg/mL respectively through the micellar formulation development. The aqueous solubility of Lut, Nar and Quer was 1.09 ± 0.16 μg/mL, 46 ± 6 μg/mL and 2.15 μg/mL respectively [8,27,29]. The solubility of Nar was increased 154 times in micelle formulation. The MF developed using [Cho][Ole] significantly increased the solubility of Lut, Nar and Quer in water. [Cho][Ole] showed better performance to solubilize hydrophobic drugs such as acyclovir, methotrexate etc. than conventional surfactants such as Tween 80 [30].

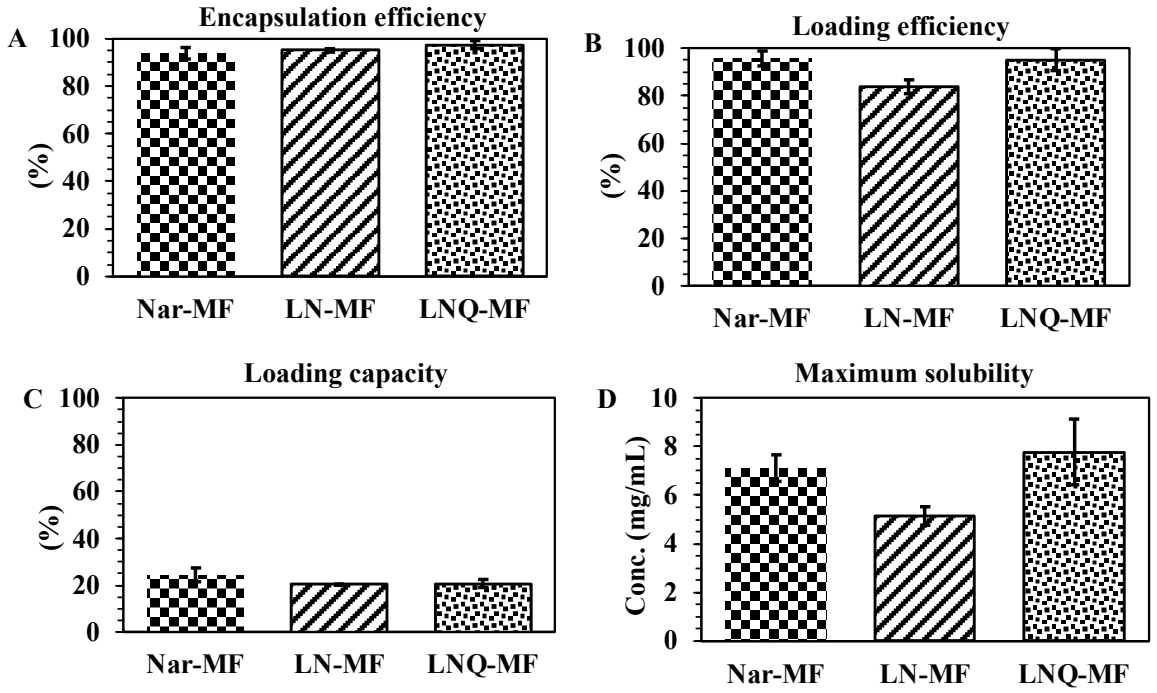

Fig. 4.4. The percentage (%) of encapsulation efficiency (A), loading efficiency (B), loading capacity (C) and concentration (mg/mL) of micellar formulations in water (D).

4.3.5 Interaction mechanism

^{1}H-NMR was used to investigate the means of dissolution and possible interactions of Lut, Nar, and Quer in MF. Two possible interaction sites were observed using spectra of free [Cho][Ole], Lut, Nar, and Quer, and LNQ-MF, as shown in Fig. 4.5. No distinctive proton peaks of the hydroxyl groups in the free Lut, Nar, and Quer (at 9.0 to 12.5 ppm) were observed in the spectrum of LNQ-MF, indicating possible hydrogen bonding interaction between the flavonoid molecules and the [Cho][Ole]. The hydroxyl groups of the free Lut, Nar, and Quer as a hydrogen bond donor interacted with the hydrogen bond acceptors of carbonyl group of [Cho][Ole] molecules. In addition, an upfield chemical shifts of aromatic protons of free Lut, Nar, and Quer were observed in LUT-loaded MF at 6.0 to 7.80 ppm (Fig. 4.5B). The upfield chemical shift of aromatic proton spectra reinforces the presence of cation-π interactions between π electrons of benzene rings of Lut, Nar, and Quer and positively charged cholinium cation of [Cho][Ole] [30]. Similarly the π-electron of oleic acid of [Cho][Ole] possibly involved in π-π interactions with the π electrons of benzene rings of flavonoids and this result agree well with other studies [47].

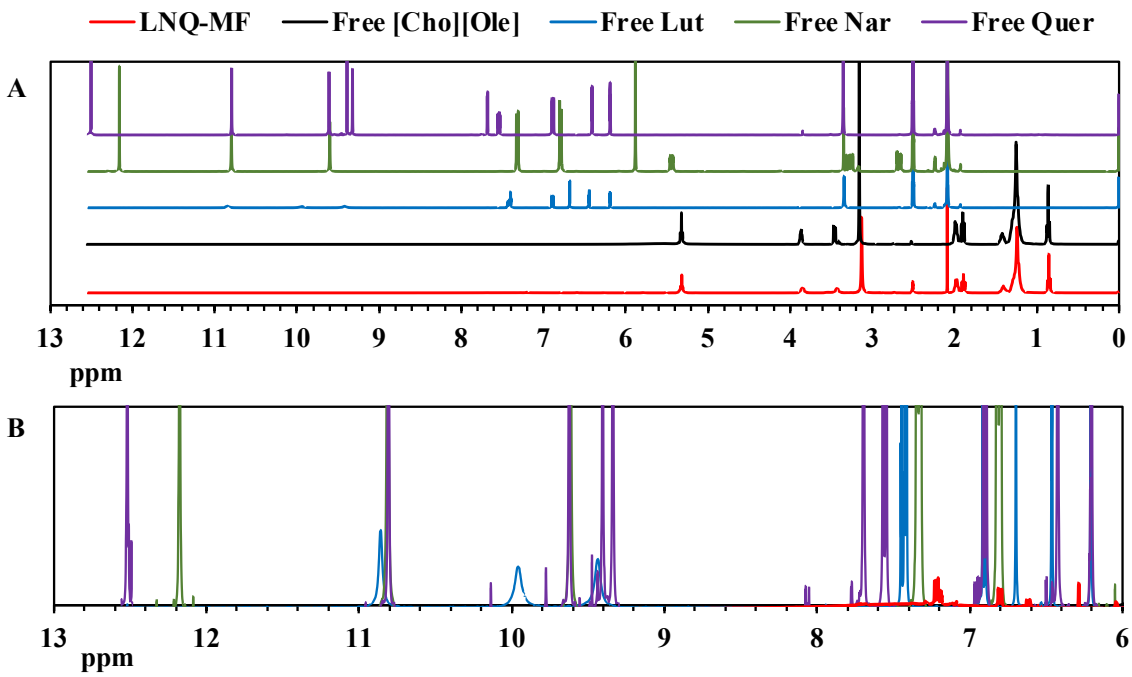

Fig. 4.5. ^{1}H NMR spectra of LNQ-MF as a representative of MFs. (A) ^{1}H NMR spectra of free Lut, Nar, Quer, [Cho][Ole] alone and LNQ-MF in DMSO-d6, (B) zoomed-in view of the overlapped ^{1}H NMR spectra between 6.0 to 13.0 ppm.

4.3.6 Stability of formulations

Stability is urgent requirement for the commercial usage of formulations and the change in particle size is an accurate measure of stability. The stability of the Nar-MF, LN-MF, and LNQ-MF was assessed through changes in the particle size and PDI during a long-term storage at various temperatures. The particle size and PDI of MFs exhibited an increasing trend with the number of storage days. After 30 days of storage, the particle size of Nar-MF rose from 113.0 nm (0 day) to 118.2 nm at 4°C and 126.1 nm at 37°C. After being stored for 30 days, the particle size of LNQ-MF changed from 150.2 nm (0 day) to 170.9 nm at 25°C and 173.5 nm at 37°C.The PDI was decreased for Nar-MF from 0.228 to 0.189 and the changes of PDI for LN-MF and LNQ-MF were very little (0.134 to 0.216 for LN-MF and 0.117 to 0.145 for LNQ-MF). It was observed from Fig. 4.6 that the changes of particle size and PDI for all the MFs were within a minimum range, which indicated the formulated MF were stable over time and temperatures tested.

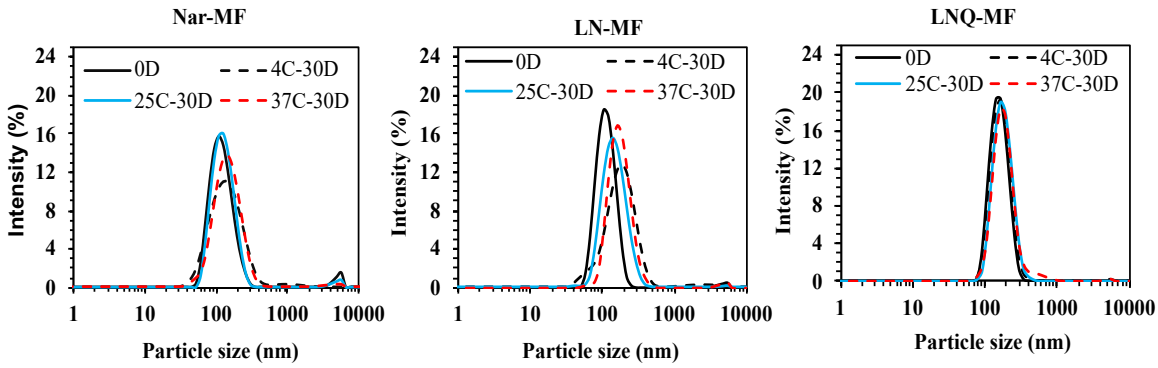

Fig. 4.6. Observation of particle size of the Nar-MF, LN-MF, and LNQ-MF over 30 days period at 4°C, 25°C and 37°C. 0D= sample on the preparation day, 4C-30D= sample kept for 30 days at 4°C, 25C-30D= sample kept for 30 days at 25°C, and 37C-30D= sample kept for 30 days at 37°C.

4.3.7 *In vitro* release profile

The *in vitro* release behaviors of Nar-MF, LN-MF, and LNQ-MF were compared with the free Nar and Quer aqueous solution into PBS containing 30% ethanol. To prevent precipitation of the flavonoids in PBS, ethanol was added. Except for Quer-DMSO, all formulations showed an initial burst within an hour and a continuous release for 12 hours. Nar dissolved in DMSO displayed higher release of Nar in compared to Quer from Quer-DMSO suspension. The mole fraction solubility of Nar and Quer in ethanol was 0.01231 and 0.00178 respectively at 308K temperature [48,49]. The higher solubility of Nar in ethanol than Quer may increase its dissolution in the ethanolic PBS solution. Nar-MF, LN-MF, and LNQ-MF released 80% of their component within 4 hours and maintained those concentration up to 12 hours.

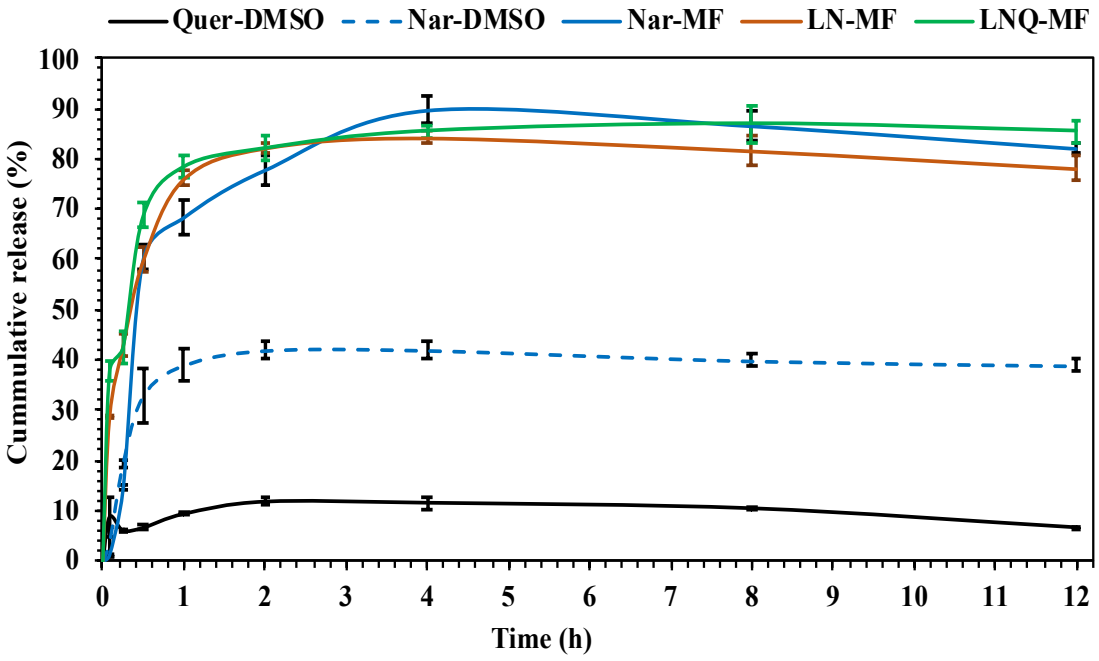

Fig. 4.7. Cumulative release of Quer suspension, Nar suspension, Nar-MF, LN-MF, and LNQ-MF into PBS medium containing 30% ethanol (v/v).

4.3.8 Antioxidant activity

The antioxidant activities of Nar-MF, LN-MF, and LNQ-MF were compared with free Nar and Quer by the DPPH method. Free Nar dissolved in methanol and Nar-MF depicted their lower antioxidant activities at all concentrations (25, 50 and 100 µg/mL), though micellar formulation of Nar and Quer demonstrated slightly higher activity than free Nar and Quer. A previous study showed that at 20 µg/mL concentration, the DPPH radical scavenging activity of Nar was 3.38% [50]. The number of hydroxyl groups in the molecule may be responsible for the difference in the radical scavenging activity of quercetin (5 hydroxyl group) and naringenin (3 hydroxyl groups). As the concentration increases from 25 to 100 µg/mL, the antioxidant activities of free Quer, Quer-MF, LN-MF and LNQ-MF also gradually increases. At 25 and 50 µg/mL concentration, the antioxidant activity of LN-MF and LNQ-MF was significantly lower than that of Quer-MF, probably due to the presence of low antioxidative Nar. Reduction of intramolecular H-bonds of Lut, Nar, or Quer in the presence of [Cho][Ole] may be stimulated their hydrogen-donating ability and demonstrated a higher antioxidant activity [8].

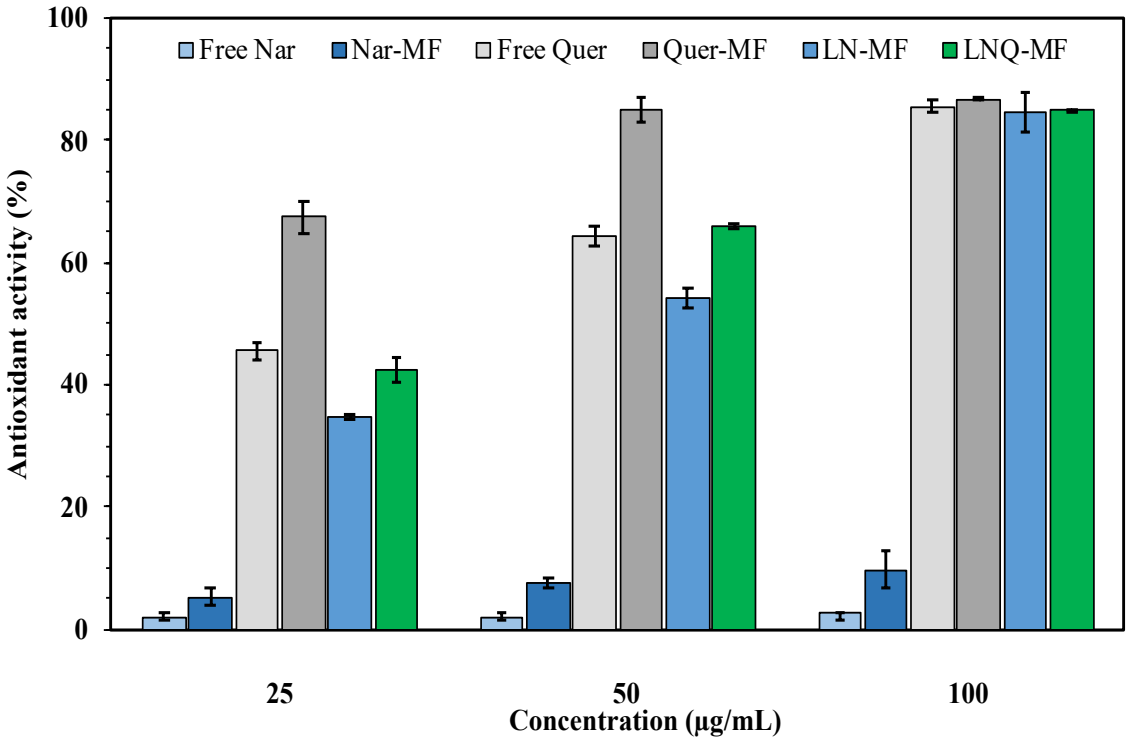

Fig. 4.8. Antioxidant activities of free Nar, Quer, Nar-MF, LN-MF, and LNQ-MF solubilized in methanol.

4.3.9 Antibacterial assay

Orally transmitted bacteria, viruses, and parasites represent the majority of foodborne pathogenic microorganisms. *Listeria monocytogenes, S. aureus*, *Salmonella*, and *E. coli* were the most significant culprits in food safety issues [25]. The MIC and MBC against two gram-positive bacteria, i.e., *S. aureus* and *B. subtilis* and two gram-negative bacteria i.e., *E. coli* and *S. enterica*, were used to assess the *in vitro* antimicrobial activity (Table 4.2). The MIC of LN-MF and LNQ-MF (≤1000 µg/mL) was lower than the MIC of Nar-MF and Quer-MF (≥1000 µg/mL). Combinations of flavonoids in LN-MF and LNQ-MF decreased the MBC value significantly. The MIC for the combination of quercetin, rutin and morin (all are flavonoids) against *S. aureus* (ATCC 43300) was estimated and it was found that the MIC for the dual combination of morin and rutin was (400+400) 800 µg/mL and for the ternary combination of morin, rutin and quercetin was (280+280+140) 700 µg/mL [51].

Lut combined with Nar and Quer in LNQ-MF had a synergistic effect on *S. aureus* and *S. enterica*, with FICIs of 0.87 and 0.71, respectively. These combinations were found to be additive against *B. subtilis* and *E. coli* with FICI of 0.93, and 1.16 respectively. Contrarily,

Lut and Nar combination in LN-MF only showed additive effects against the four bacteria investigated, with FICI ranging from 0.9 to 1.06. Combinations of flavonoids in LN-MF and LNQ-MF decreased the MBC value significantly. An increase in the inhibitory activity was observed when combining Lut, Nar, and Quer, and this findings agree well with literatures [14,37] which reported the synergistic interaction of phytochemicals in combination. Binding of one flavonoid in structural membrane proteins of bacteria enables an easier passage of another flavonoid [14]. Combinations of flavonoids function in diverse mechanism, thus destroyed the bacteria at lower concentration. This result suggest that antimicrobial properties of flavonoids were enhanced in combination and LN-MF and LNQ-MF have the potential to be used as an antimicrobial agent in food preservation.

Table 4.2. Antibacterial activity and synergism of Nar-MF, Quer-MF, LN-MF, and LNQ-MF against selected bacteria in terms of MIC and MBC.

MIC and MBC (µg/mL)								
Formulations	***S. aureus***		***B. subtilis***		***E. coli***		***S. enterica***	
	MIC	**MBC**	**MIC**	**MBC**	**MIC**	**MBC**	**MIC**	**MBC**
Lut-MF	800	1200	600	1000	600	1000	1000	1500
Nar-MF	1000	1200	1000	1200	1000	1200	1200	1600
Quer-MF	1000	>2000	1200	1600	1200	1600	1200	1600
LN-MF	800	1000	800	1200	800	1000	1000	1200
LNQ-MF	800	1000	800	1000	1000	1000	800	1000
FICI								
	FICI	Effect	FICI	Effect	FICI	Effect	FICI	Effect
LN-MF	0.90	Additive	1.06	Additive	1.06	Additive	0.91	Additive
LNQ-MF	0.87	Synergistic	0.93	Additive	1.16	Additive	0.71	Synergistic

4.3.10 Milk preservation test

Pasteurized milk has the potential to serve as a natural medium for microbial reproduction, which causes milk's proteins and lipids to aggregate as a result of microbial metabolism.

The control group had significant precipitation after 72 hours at 25°C and 37°C. Milk sample with Nar-MF treatment exhibited precipitation at 37°C, but no precipitation at 25°C. The LNQ-MF treated milk, on the other hand, showed no precipitation at 25°C and 37°C, indicating that the metabolism of *S. aureus* was reduced in the presence of LNQ-MF. This finding is consistent with earlier research [38].

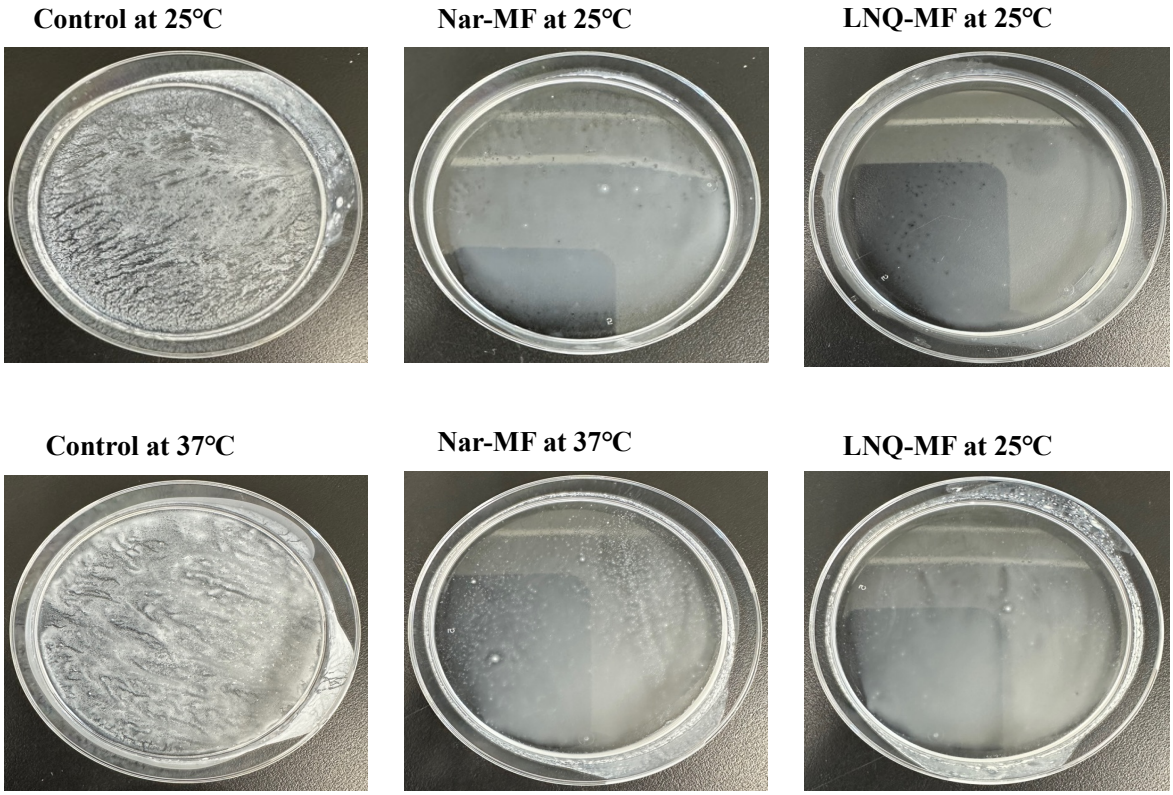

Fig. 4.9. The formation of precipitation of milk inoculated with *S. aureus* and treated with Nar-MF and LNQ-MF for 72 hours.

4.4 Conclusions

In the present study, [Cho][Ole] successfully encapsulated Lut, Nar, and Quer as nano-sized, spherical micelles with a high encapsulation efficiency and a high water solubility. The new type of dual (Lut and Nar in LN-MF) and triple (Lut, Nar, and Quer in LNQ-MG) bioactive flavonoids demonstrated good stability at 4 to 37°C over 30 days. The prolong controlled release increased their antioxidant and antibacterial properties. The micelles developed in this study could be used in food industries for the development of functional food and supplements. However, their effectiveness still needs to be investigated in food systems.

Optimization of the formulation for better performance and their safety check for animal and human will be the main objective of our upcoming work.

4.5 References

[1] G. Wang, J.J. Wang, X.L. Chen, L. Du, F. Li, Quercetin-loaded freeze-dried nanomicelles: Improving absorption and anti-glioma efficiency in vitro and in vivo, J. Control. Release. 235 (2016) 276–290. https://doi.org/10.1016/j.jconrel.2016.05.045.

[2] I. Gutiérrez-del-Río, J. Fernández, F. Lombó, Plant nutraceuticals as antimicrobial agents in food preservation: terpenoids, polyphenols and thiols, Int. J. Antimicrob. Agents. 52 (2018) 309–315. https://doi.org/10.1016/j.ijantimicag.2018.04.024.

[3] T.L.A. Nguyen, D. Bhattacharya, Antimicrobial Activity of Quercetin: An Approach to Its Mechanistic Principle, Molecules. 27 (2022) 2494. https://doi.org/10.3390/molecules27082494.

[4] A. Arafah, M.U. Rehman, T.M. Mir, A.F. Wali, R. Ali, W. Qamar, R. Khan, A. Ahmad, S.S. Aga, S. Alqahtani, N.M. Almatroudi, Multi-Therapeutic Potential of Naringenin (4′,5,7-Trihydroxyflavonone): Experimental Evidence and Mechanisms, Plants. 9 (2020) 1784. https://doi.org/10.3390/plants9121784.

[5] A. Biharee, A. Sharma, A. Kumar, V. Jaitak, Antimicrobial flavonoids as a potential substitute for overcoming antimicrobial resistance, Fitoterapia. 146 (2020) 104720. https://doi.org/10.1016/j.fitote.2020.104720.

[6] I. Górniak, R. Bartoszewski, J. Króliczewski, Comprehensive review of antimicrobial activities of plant flavonoids, Phytochem. Rev. 18 (2019) 241–272. https://doi.org/10.1007/s11101-018-9591-z.

[7] A. Adamczak, M. Ożarowski, T.M. Karpiński, Antibacterial Activity of Some Flavonoids and Organic Acids Widely Distributed in Plants, J. Clin. Med. 9 (2019) 109. https://doi.org/10.3390/jcm9010109.

[8] I.M. Shimul, R.M. Moshikur, K. Minamihata, M. Moniruzzaman, N. Kamiya, M. Goto, Choline oleate based micellar system as a new approach for Luteolin

formulation: Antioxidant, antimicrobial, and food preservation properties evaluation, J. Mol. Liq. 365 (2022) 120151. https://doi.org/10.1016/j.molliq.2022.120151.

[9] Z. Wang, M. Zeng, Z. Wang, F. Qin, J. Chen, Z. He, Dietary Luteolin: A Narrative Review Focusing on Its Pharmacokinetic Properties and Effects on Glycolipid Metabolism, J. Agric. Food Chem. 69 (2021) 1441–1454. https://doi.org/10.1021/acs.jafc.0c08085.

[10] H.-Y. Son, M.-S. Lee, E. Chang, S.-Y. Kim, B. Kang, H. Ko, I.-H. Kim, Q. Zhong, Y.-H. Jo, C.-T. Kim, Y. Kim, Formulation and Characterization of Quercetin-loaded Oil in Water Nanoemulsion and Evaluation of Hypocholesterolemic Activity in Rats, Nutrients. 11 (2019) 244. https://doi.org/10.3390/nu11020244.

[11] G. Elgin, S. Konyalioglu, E. Kilinc, Development and validation of a multidetector HPLC method for the determination of antioxidant flavonoids of some Hypericum L. species, J. Liq. Chromatogr. Relat. Technol. 32 (2009) 432–448. https://doi.org/10.1080/10826070802634638.

[12] M. Chen, R. Li, Y. Gao, Y. Zheng, L. Liao, Y. Cao, J. Li, W. Zhou, Encapsulation of Hydrophobic and Low-Soluble Polyphenols into Nanoliposomes by pH-Driven Method: Naringenin and Naringin as Model Compounds, Foods. 10 (2021) 963. https://doi.org/10.3390/foods10050963.

[13] L.H. Chin, C.M. Hon, D.K. Chellappan, J. Chellian, T. Madheswaran, F. Zeeshan, R. Awasthi, A.A. Aljabali, M.M. Tambuwala, H. Dureja, P. Negi, D.N. Kapoor, R. Goyal, K.R. Paudel, S. Satija, G. Gupta, A. Hsu, P. Wark, M. Mehta, R. Wadhwa, P.M. Hansbro, K. Dua, Molecular mechanisms of action of naringenin in chronic airway diseases, Eur. J. Pharmacol. 879 (2020) 173139. https://doi.org/10.1016/j.ejphar.2020.173139.

[14] V.G.N.V. Prasad, B.V. krishna, P.L. Swamy, T.S. Rao, G.S. Rao, Antibacterial synergy between quercetin and polyphenolic acids against bacterial pathogens of fish, Asian Pacific J. Trop. Dis. 4 (2014) 326–329. https://doi.org/10.1016/S2222-1808(14)60464-3.

[15] M.U. Amin, M. Khurram, B. Khattak, J. Khan, Antibiotic additive and synergistic

action of rutin, morin and quercetin against methicillin resistant Staphylococcus aureus, BMC Complement. Altern. Med. 15 (2015) 1–12. https://doi.org/10.1186/s12906-015-0580-0.

[16] L. Gram, L. Ravn, M. Rasch, J.B. Bruhn, A.B. Christensen, M. Givskov, Food spoilage - Interactions between food spoilage bacteria, Int. J. Food Microbiol. 78 (2002) 79–97. https://doi.org/10.1016/S0168-1605(02)00233-7.

[17] F.J. Osonga, A. Akgul, R.M. Miller, G.B. Eshun, I. Yazgan, A. Akgul, O.A. Sadik, Antimicrobial activity of a new class of phosphorylated and modified flavonoids, ACS Omega. 4 (2019) 12865–12871. https://doi.org/10.1021/acsomega.9b00077.

[18] Y. Guo, Y. Liu, Z. Zhang, M. Chen, D. Zhang, C. Tian, M. Liu, G. Jiang, The antibacterial activity and mechanism of action of luteolin against trueperella pyogenes, Infect. Drug Resist. 13 (2020) 1697–1711. https://doi.org/10.2147/IDR.S253363.

[19] M. Azeem, M. Hanif, K. Mahmood, N. Ameer, F.R.S. Chughtai, U. Abid, An insight into anticancer, antioxidant, antimicrobial, antidiabetic and anti-inflammatory effects of quercetin: a review, Polym. Bull. 80 (2023) 241–262. https://doi.org/10.1007/s00289-022-04091-8.

[20] L.H. Wang, M.S. Wang, X.A. Zeng, X.M. Xu, C.S. Brennan, Membrane and genomic DNA dual-targeting of citrus flavonoid naringenin against: Staphylococcus aureus, Integr. Biol. (United Kingdom). 9 (2017) 820–829. https://doi.org/10.1039/c7ib00095b.

[21] P. Li, Y. Peng, J. Mei, J. Xie, Effects of microencapsulated eugenol emulsions on microbiological, chemical and organoleptic qualities of farmed Japanese sea bass (Lateolabrax japonicus) during cold storage, Lwt. 118 (2020) 108831. https://doi.org/10.1016/j.lwt.2019.108831.

[22] F. Lv, H. Liang, Q. Yuan, C. Li, In vitro antimicrobial effects and mechanism of action of selected plant essential oil combinations against four food-related microorganisms, Food Res. Int. 44 (2011) 3057–3064. https://doi.org/10.1016/j.foodres.2011.07.030.

[23] R. Iqbal, Z. Mehmood, A. Baig, N. Khalid, Formulation and characterization of food grade O/W nanoemulsions encapsulating quercetin and curcumin: Insights on enhancing solubility characteristics, Food Bioprod. Process. 123 (2020) 304–311. https://doi.org/10.1016/j.fbp.2020.07.013.

[24] B.K. Tiwari, V.P. Valdramidis, C.P. O'Donnell, K. Muthukumarappan, P. Bourke, P.J. Cullen, Application of natural antimicrobials for food preservation, J. Agric. Food Chem. 57 (2009) 5987–6000. https://doi.org/10.1021/jf900668n.

[25] L. Lin, C. Luo, C. Li, X. Chen, H. Cui, A Novel Biocompatible Ternary Nanoparticle with High Antibacterial Activity: Synthesis, Characterization, and Its Application in Beef Preservation, Foods. 11 (2022) 438. https://doi.org/10.3390/foods11030438.

[26] L.C. Lin, Y.F. Pai, T.H. Tsai, Isolation of Luteolin and Luteolin-7-O-glucoside from Dendranthema morifolium Ramat Tzvel and Their Pharmacokinetics in Rats, J. Agric. Food Chem. 63 (2015) 7700–7706. https://doi.org/10.1021/jf505848z.

[27] K. Srinivas, J.W. King, L.R. Howard, J.K. Monrad, Solubility and solution thermodynamic properties of quercetin and quercetin dihydrate in subcritical water, J. Food Eng. 100 (2010) 208–218. https://doi.org/10.1016/j.jfoodeng.2010.04.001.

[28] M. Frenzel, A. Steffen-Heins, Impact of quercetin and fish oil encapsulation on bilayer membrane and oxidation stability of liposomes, Food Chem. 185 (2015) 48–57. https://doi.org/10.1016/j.foodchem.2015.03.121.

[29] N. Krishnakumar, N. Sulfikkarali, N. RajendraPrasad, S. Karthikeyan, Enhanced anticancer activity of naringenin-loaded nanoparticles in human cervical (HeLa) cancer cells, Biomed. Prev. Nutr. 1 (2011) 223–231. https://doi.org/10.1016/j.bionut.2011.09.003.

[30] M.K. Ali, R.M. Moshikur, R. Wakabayashi, M. Moniruzzaman, N. Kamiya, M. Goto, Biocompatible Ionic Liquid Surfactant-Based Microemulsion as a Potential Carrier for Sparingly Soluble Drugs, ACS Sustain. Chem. Eng. 8 (2020) 6263–6272. https://doi.org/10.1021/acssuschemeng.9b07773.

[31] A.K. Das, R.A. Sequeira, T.K. Maity, K. Prasad, Bio-ionic liquid promoted selective coagulation of κ-carrageenan from Kappaphycus alvarezii extract, Food Hydrocoll.

111 (2021) 106382. https://doi.org/10.1016/j.foodhyd.2020.106382.

[32] R. Wakabayashi, R. Ishiyama, N. Kamiya, M. Goto, A novel surface-coated nanocarrier for efficient encapsulation and delivery of camptothecin to cells, Medchemcomm. 5 (2014) 1515–1519. https://doi.org/10.1039/c4md00179f.

[33] M.R. Chowdhury, R.M. Moshikur, R. Wakabayashi, Y. Tahara, N. Kamiya, M. Moniruzzaman, M. Goto, Development of a novel ionic liquid-curcumin complex to enhance its solubility, stability, and activity, Chem. Commun. 55 (2019) 7737–7740. https://doi.org/10.1039/c9cc02812a.

[34] K. Liu, X.Q. Zha, Q.M. Li, L.H. Pan, J.P. Luo, Hydrophobic interaction and hydrogen bonding driving the self-assembling of quinoa protein and flavonoids, Food Hydrocoll. 118 (2021) 106807. https://doi.org/10.1016/j.foodhyd.2021.106807.

[35] S. Chen, Q. Li, D.J. McClements, Y. Han, L. Dai, L. Mao, Y. Gao, Co-delivery of curcumin and piperine in zein-carrageenan core-shell nanoparticles: Formation, structure, stability and in vitro gastrointestinal digestion, Food Hydrocoll. 99 (2020) 105334. https://doi.org/10.1016/j.foodhyd.2019.105334.

[36] G. Granata, S. Stracquadanio, M. Leonardi, E. Napoli, G.M.L. Consoli, V. Cafiso, S. Stefani, C. Geraci, Essential oils encapsulated in polymer-based nanocapsules as potential candidates for application in food preservation, Food Chem. 269 (2018) 286–292. https://doi.org/10.1016/j.foodchem.2018.06.140.

[37] H. Arima, H. Ashida, G. Danno, Rutin-enhanced antibacterial activities of flavonoids against bacillus cereus and salmonella enteritidis, Biosci. Biotechnol. Biochem. 66 (2002) 1009–1014. https://doi.org/10.1271/bbb.66.1009.

[38] Q. Li, S. Yu, J. Han, J. Wu, L. You, X. Shi, S. Wang, Synergistic antibacterial activity and mechanism of action of nisin/carvacrol combination against Staphylococcus aureus and their application in the infecting pasteurized milk, Food Chem. 380 (2022) 132009. https://doi.org/10.1016/j.foodchem.2021.132009.

[39] Y. Chang, L. McLandsborough, D.J. McClements, Fabrication, stability and efficacy of dual-component antimicrobial nanoemulsions: Essential oil (thyme oil) and cationic surfactant (lauric arginate), Food Chem. 172 (2015) 298–304.

https://doi.org/10.1016/j.foodchem.2014.09.081.

[40] M. Krysa, M. Szymańska-Chargot, A. Zdunek, FT-IR and FT-Raman fingerprints of flavonoids – A review, Food Chem. 393 (2022) 133530. https://doi.org/10.1016/j.foodchem.2022.133430.

[41] F. Liu, D. Ma, X. Luo, Z. Zhang, L. He, Y. Gao, D.J. McClements, Fabrication and characterization of protein-phenolic conjugate nanoparticles for co-delivery of curcumin and resveratrol, Food Hydrocoll. 79 (2018) 450–461. https://doi.org/10.1016/j.foodhyd.2018.01.017.

[42] K. Liu, H.L. Zhang, L.H. Pan, Q.M. Li, J.P. Luo, X.Q. Zha, The nanomicelles consisting of lotus root amylopectin and quinoa protein: Construction and encapsulation for quercetin, Food Chem. 387 (2022) 132924. https://doi.org/10.1016/j.foodchem.2022.132924.

[43] Y. Liang, D. Hou, Z. Ni, M. Cao, L. Cai, Preparation, characterization of naringenin, β-cyclodextrin and carbon quantum dot antioxidant nanocomposites, Food Chem. 375 (2022) 131646. https://doi.org/10.1016/j.foodchem.2021.131646.

[44] C. Chen, Q. Zhong, Z. Chen, Improved aqueous solubility, bioaccessibility and cellular uptake of quercetin following pH-driven encapsulation in whey protein isolate, Int. J. Food Sci. Technol. 57 (2022) 2747–2755. https://doi.org/10.1111/ijfs.15579.

[45] S. Kumar, V. Lather, D. Pandita, Stability indicating simplified HPLC method for simultaneous analysis of resveratrol and quercetin in nanoparticles and human plasma, Food Chem. 197 (2016) 959–964. https://doi.org/10.1016/j.foodchem.2015.11.078.

[46] V.S. Chaudhari, R.M. Borkar, U.S. Murty, S. Banerjee, Analytical method development and validation of reverse-phase high-performance liquid chromatography (RP-HPLC) method for simultaneous quantifications of quercetin and piperine in dual-drug loaded nanostructured lipid carriers, J. Pharm. Biomed. Anal. 186 (2020) 113325. https://doi.org/10.1016/j.jpba.2020.113325.

[47] L.J. Yang, S.X. Ma, S.Y. Zhou, W. Chen, M.W. Yuan, Y.Q. Yin, X.D. Yang,

Preparation and characterization of inclusion complexes of naringenin with β-cyclodextrin or its derivative, Carbohydr. Polym. 98 (2013) 861–869. https://doi.org/10.1016/j.carbpol.2013.07.010.

[48] L. Zhou, P. Zhang, G. Yang, R. Lin, W. Wang, T. Liu, L. Zhang, J. Zhang, Solubility of Naringenin in Ethanol and Water Mixtures, J. Chem. Eng. Data. 59 (2014) 2215–2220. https://doi.org/10.1021/je5001654.

[49] R.S. Razmara, A. Daneshfar, R. Sahraei, Solubility of quercetin in water + methanol and water + ethanol from (292.8 to 333.8) K, J. Chem. Eng. Data. 55 (2010) 3934–3936. https://doi.org/10.1021/je9010757.

[50] B. Tu, Z.J. Liu, Z.F. Chen, Y. Ouyang, Y.J. Hu, Understanding the structure-activity relationship between quercetin and naringenin: In vitro, RSC Adv. 5 (2015) 106171–106181. https://doi.org/10.1039/c5ra22551e.

[51] M. Güran, G. Şanlıtürk, N.R. Kerküklü, E.M. Altundağ, A. Süha Yalçın, Combined effects of quercetin and curcumin on anti-inflammatory and antimicrobial parameters in vitro, Eur. J. Pharmacol. 859 (2019) 172486. https://doi.org/10.1016/j.ejphar.2019.172486.

CHAPTER-5: SUMMARY AND FUTURE WORK

5.1 Summary

The reduction of food waste and ensuring food safety are seen as an important lever for diminishing hunger and foodborne diseases in the world. Food preservation can be achieved via chemical, physical or biological treatments or modification of foods; however, these techniques frequently have associated an adverse side effect on human and changes of organoleptic characteristics of food. Therefore, the tendency of consumers to natural additives is increasing day-by-day. Natural preservatives generally come from three sources: microorganisms, animals, and plants. Many of the plant derived compounds (flavonoids) have potential chemical and biological properties, such as antioxidant, chelating, free-radical scavenging, anti-inflammatory, anti-allergic, antimicrobial, antiviral, anticarcinogenic, chemoprevention (interfering with a disease process), and ultraviolet (UV) filtering properties. The functional applications of flavonoids are limited due to its low solubility and low bioavailability, instability, photosensitivity etc. Nanoencapsulation with a carrier material can protect them against the adverse effects of pH, oxygen, and light during processing, storage, and transport. Ionic liquids (ILs) are stable salts that are entirely consisted of organic cations and inorganic anions and have melting temperatures below 100°C. In the pharmaceutical and biomedical fields, Bio-ILs are used as stabilizer agents for biomolecules, as solvents, or as part of drug carrier systems for poorly soluble drugs, such as in API-IL systems. Surface active agents (surfactant) as carrier materials are generally used as a promising vehicle for bioactive compounds because of their long-term stability and the high drug solubilization capacity. Utilization of ILs as solubilizing agents or carrier materials for the application in food industries are scare. To explore the possibilities and challenges of ILs applications in food systems, we have designed this study.

In the **second chapter,** we have devised to screen and synthesize bio-based phenolic acids bearing amino acid ester ILs as a potent green solvent for dissolving Luteolin (Lut) for food processing applications. Twenty cations (standard amino acid ethyl esters) and nine anions (phenolic acids) were selected and combined to form 180 ILs, which were then assessed for dissolution of LUT via COSMO-RS. To address the poor aqueous solubility of flavonoids, we have synthesized four novel proline ethyl ester-based phenolic acids ILs (PEEP-ILs). The synthesized IL[ProEt][Cou], IL[ProEt][Van], and IL[ProEt][Ben] were characterized, and their aqueous solubility and biocompatibility were determined. The PEEP-ILs (60% IL

in water) increased aqueous LUT solubility by 207 to 879 folds compared with that in water, indicating the possibility of utilization of LUT in the aqueous system. COSMO-RS prediction of LUT solubility showed good agreement with experimental solubility in PEEP-ILs. ^{1}H NMR assessment confirmed that the ILs facilitated to solubilize the LUT through multiple hydrogen bonding, π–π, and cation–π interactions between the LUT and the ILs. The biocompatibility study revealed that PEEP-ILs were relatively harmless. LUT with newly synthesized PEEP-ILs retained better organoleptic properties of red apple piece. These results clearly suggest that PEEP-ILs can be potential green alternatives to conventional toxic solvents for bioactivity of poorly water-soluble natural preservatives.

Encapsulation of flavonoids can be promising delivery system in food. Formulation based delivery has become a cutting-edge method due to their capacity for self-assembly, controlled release profile, and high drug encapsulation efficiency. As the Lut is photosensitive molecule, their encapsulation by carrier materials can improve their bioactivity. In the **third chapter**, we have focused on to formulate and investigate nano-sized micellar formulation of Lut using a low carrier material concentration to enhance LUT dissolution and bioactivity. The LUT-loaded micellar formulation (LUT-MF) was prepared using the solid-in-water nanodispersion technique utilizing the biocompatible and low toxic surface-active IL choline oleate. In this study, we have developed a highly water-soluble LUT-MF with a low concentration (1.5%) of an ionic liquid surfactant, choline oleate using emulsification and lyophilization processes. Dynamic light scattering (DLS) and transmission electron microscopy (TEM) confirmed that the LUT-MF formed spherical micelles with a mean particle size of approximately 73 nm. LUT-MF showed excellent encapsulation efficiency (94.3%) and enhanced the aqueous solubility. An *in vitro* release study in PBS containing 30% ethanol demonstrated 3.94 times higher release of LUT from LUT-MF than from LUT suspension after 24 h. The developed formulation showed better antioxidant activity than both free LUT and ascorbic acid. LUT-MF demonstrated higher antibacterial activity than sodium benzoate. Food preservation studies revealed that treating strawberries with LUT-MF effectively preserved color and prevented shriveling and decay over 8 days storage at 10°C, compared with the sodium benzoate treatment. The results suggest that LUT-MF is a potential natural preservative alternative to conventional toxic chemical preservatives used in the food industry.

Synergistic potentialities of flavonoids give plants a stronger defense against different diseases and serve as potent antimicrobials or immunological boosters. Different flavonoids exhibit antimicrobial activity through various mechanisms. To utilize synergistic properties of flavonoids, we concentrated in the **fourth chapter** to develop choline oleate assisted micellar formulations for luteolin, quercetin and naringenin in combinations to increase their solubility and bioactivity. The developed micelles of Lut, Nar, and Quer were encapsulated or amorphous state and spherical in shape. Higher encapsulation efficiency (>93%), loading efficiency (>83%), and loading capacity of >20% enhanced their aqueous solubility (>5.15 mg/mL). The developed MFs were stable up to 37°C temperature for 30 days. Nar-MF, LN-MF, and LNQ-MF released 80% of their component within 4 hours and maintained those concentration up to 12 hours. [Cho][Ole] based formulations showed better antioxidant activity than that of free Nar and Quer. Combinations of Lut with Nar and Lut with Nar and Quer demonstrated higher antimicrobial properties. This study suggested that combinations of flavonoids could be delivered for their bioavailability and bioactivity. These co-delivery techniques for encapsulation might be appropriate for the use in supplements and food systems.

5.2 Future work

Biocompatible ILs, cations and anions derived from natural sources, could be an alternative to conventional solvents and/ or carrier materials for the delivery of poorly water-soluble flavonoids. The recent advances have also proven that the great potential of ILs for food and biocompound processes and the product formulation is still unexplored. Considering an infinite number of natural biocompounds potentially used as a cation−anion pair, these results should encourage the synthesis of new nontoxic and possible edible ILs. Future researches should focus on the performance of microencapsulation and the use of combined natural antimicrobial compounds under a variety of environmental conditions. Their effectiveness still needs to be investigated in food systems. Besides, studies should also be done towards the discovery of novel natural preservatives aiming to expand the range of products available for the development of mixtures with boosted preservation properties for food applications. Optimization of the formulation for better performance and their safety check for animal and human will be the main objective of our upcoming work.

ABBREVIATIONS

a_w	Water activity
Ben	4-hydroxy Benzoic acid
[Cho][Ole]	Choline Oleate
CMC	Critical Micelle Concentration
COSMO-RS	COnductor-like Screening MOdel for Real Solvents
Cou	trans p-Coumaric acid
DLS	Dynamic Light Scattering
DMSO	Dimethyl sulfoxide
DPPH	1,1-diphenyl-2-picrylhydrazyl
DSC	Differential scanning calorimetry
Fer	trans Ferulic acid
FTIR	Fourier Transform Infrared
GRAS	Generally Recognized As Safe
HPLC	High Performance Liquid Chromatography
IL	Ionic Liquid
LN-MF	Luteolin-Naringenin loaded Micellar Formulation
LNQ-MF	Luteolin-Naringenin-Quercetin loaded Micellar Formulation
Lut	Luteolin
MF	Micellar Formulation
Nar	Naringenin
NMR	Nuclear Magnetic Resonance
PBS	Phosphate Buffer Saline
PEEP	Proline Ethyl Ester Phenolate
ProEt	L-Proline ethyl ester
Quer	Quercetin
SAIL	Surface Active Ionic Liquid
SDS	Sodium Dodecyl Sulfate
TEM	Transmission Electron Microscopy
TGA	Thermogravimetric analysis
Van	Vanillic acid
XRD	X-Ray Diffraction

LIST OF SCHEMES

LIST OF FIGURES

CHAPTER-1 **Page**

CHAPTER-2

LIST OF TABLES

ACKNOWLEDGEMENTS

I would like to express my greatest gratitude to Prof. Masahiro GOTO, for his guidance and support throughout PhD course in Kyushu University. It has been a great honor for having you as my academic advisor. Your insightful ideas and creative thinking have impressed me a lot and would be of help for me to become a better researcher. I am truly thankful for placing your trust and confidence in my abilities to carry out this research project. I would also like to thank Prof. Noriho Kamiya, who served as my co-advisor, for his encouragement and continuous support throughout PhD course and for invaluable advice and suggestion during the lab meetings and on my PhD thesis. I would like to express my sincere gratitude to Prof. Hisashi Shimakoshi for agreeing to be one of my PhD thesis committee. I really appreciate for his constructive comments and invaluable advice.

I am very much thankful to Associate Prof. Muhammad Moniruzzaman, who is my co-supervisor at Universiti Teknologi PETRONAS for introducing me to the GK lab and his continuous support, suggestions, and guidance towards my academic career from abroad. I would like to thank Assistant Prof. Kosuke Minamihata and Rie Wakabayashi for helping me in many aspects of my research.

I am grateful for all past and present members of the Goto-Kamiya Lab for their help, support, and friendship. I am extremely proud and fortunate to become a member of the Goto-Kamiya Lab. I would like to appreciate Dr. Md. Moshikur Rahman, Dr. Md. Raihan Chowdhury, Dr. Md. Korban Ali, Fahmida Habib Nabila, and Md. Rashedul Islam for their useful advice and help in experiments and research. I would also like to thank Dr. Hanada Takafumi, Mr. Hiroki Obayashi, Netsuke Ide, Mr. Ayato Higuchi, and others for helping and teaching me doing some experiments. I am fortunate to be a part of such conducive and supportive research environment in the lab. I also appreciate the support from Mrs. Yasura Oiwa, Support Center and MEXT authority for financial support.

I would like to appreciate the dedication and support of my family, especially my wife Mrs. Ummay Farhana Tarin for her very hard-working, caring and supporting mentality and daughter Ms. Shariha Tasni Ichika for her unconditional love. I also want to remember the contributions and struggle of my parents to reach me here. I dedicate this thesis to my family. Thank you for bringing the joy and happiness in my life.

Md. Shimul Islam

Fukuoka, Japan 20 December 2022